Modelling Tree Height-Diameter Relationships and the Effect of Climate

by

Pembegul Nozohourmehrabad

A thesis submitted in partial fulfillment of the requirements for the degree of

Doctor of Philosophy

in

Forest Biology and Management

Department of Renewable Resources
University of Alberta

Abstract

Tree size and tree height are two essential quantities to measure structure and productivity of forest stands. As such, they encourage predictability in changes among tree growth patterns and are fundamental to developing forest management plans. Tree height and size (commonly measured as diameter at breast height, DBH) vary within and between species. Monitoring their variations is necessary to understand how forest productivity changes and how forest can be managed accordingly. Moreover, recent climate change may affect tree height and diameter and their relationship, because tree growth is subject to change in climate. This thesis contributes to improving forest harvesting and silvicultural plans and tree height-diameter modelling by analyzing variation in tree diameter and height, and climate effect on their relationships.

I first started modeling tree size distribution for a wide range of forest communities and derived a Weibull distribution from stochastic tree recruitment, growth and mortality. I tested the Weibull distribution model using tree size data collected from six continents and also from Alberta, Canada. I found that the Weibull distribution provided a good description of the curvilinear relationships of the tree size data. I further showed how to use size distribution for predicting growth with the data from a 50-ha long-term forest dynamics plot on Barro Colorado Island, Panama. The result showed that variation in recruitment time and growth is sufficient to explain the differentiation in tree size.

Second, I modeled tree size (DBH) and tree height relationship and their derivative forms. Traditional tree height-diameter equations model tree height for a given size. However, the traditional models are cumulative functions and do not provide information about incremental rate in relative to tree size. The latter is more informative about tree growth, hence useful for forest management and planning silvicultural practices. Using 57,772 individual living

trees from 575 permanent sample plots across Alberta boreal forest, I identified models (from an inclusive list of 19 candidate models) that best described tree height-DBH relationship for seven major tree species of Alberta. I then explored the derivatives of the best fitted tree height-DBH models to describe tree height increment in relative to diameter increment and associated the derivatives with life history traits of species. I found that although the cumulative height-DBH relationships all had similar shape, the derivatives of tree height-diameter relationship between early successional (deciduous) species were distinctly different from that of late successional (coniferous) species. This indicates that the derivative of height-diameter relationships is more informative then the cumulative equations in revealing tree growth patterns.

Third, I studied climate effects on tree height-DBH relationships. The need to incorporate the effects of climate into existing tree height-DBH models has become clear, as tree height and diameter growth are inevitably sensitive to climate changes, and consequently so are tree height-DBH relationships. I incorporated a climate moisture index (CMI) and maximum temperature (Tmax) into seven most common tree height-DBH models to improve the predictability of traditional height-DBH models and to reveal whether species have specific response to climate change conditions. I discovered that CMI had negative effects on height growth of some species, where Tmax had significantly positive effects on height growth of all species. All climate-based tree height-DBH models increased the predictive ability of the original models. This suggests that climate effects need to be incorporated into models to predict tree growth. Also, the climate-based models showed that tree species would become taller with increasing temperature although their responses to climate moisture index would be different.

The results of my thesis contribute to improving modelling tree diameter and tree height, understanding tree growth patterns by analyzing derivative curves, and increasing predictability

of height-DBH models by including climate effects. The models derived and parameterized from this thesis should be useful in guiding forest harvesting and silvicultural planning.

Preface

This is an original work by Pembegul Nozohourmehrabad.

Chapter 2 was conceived by Fangliang He with input from Pembegul Nozohourmehrabad. Pembegul Nozohourmehabad carried out the analysis. Pembegul Nozohourmehrabad and Fangliang He jointly wrote the manuscript.

Chapter 3 was prepared for submission as a journal article, entitled "Derivative curves of tree height-diameter models reveal different growth patterns of tree species". This chapter was conceptualized by me with guidance from Fangliang He. The data were collected by the Government of Alberta and forest industries and were compiled by Jian Zhang. I carried out statistical analysis under the supervision of Fangliang He. I wrote the chapter and Fangliang He contributed to revising the manuscript.

Chapter 4 was derived from discussions with Fangliang He. I developed and estimated the models and wrote the chapter, with inputs from Fangliang He.

Acknowledgments

I gratefully acknowledge my supervisor Fangliang He, for his excellence in guidance, great inspiration and endless support. I am honored to be a member of his lab group. I would also like to thank him for supporting an opportunity to attend a working group meeting in Guangzhou, China. I am also very grateful to my supervisory committee Andreas Hamann and Ted Hogg, for their guidance, constructive comments and insightful critiques.

Thanks also to past and current members of the He Lab, especially Dingliang Xing and David Deane for being patient and answering my endless questions, sharing their knowledge and experiences with me. Also, I would specifically like to thank two friends David and Scott Boyce, for refreshing conversations and afternoon coffee breaks.

I am grateful to government and organizations who generously shared their data. This project would have been impossible without the Environment and Parks, Natural Resources Canada and Mike Michaelian, and Alwyn H. Gentry, the Missouri Botanical Garden. Many thanks to their staff which contributed to collecting and processing the data that are used in this thesis. I also thank those who contributed to the Barro Colorado Island dataset. The BCI forest dynamics research project was founded by S.P. Hubbell and R.B. Foster and is managed by the Center for Tropical Forest Science and the Smithsonian Tropical Research in Panama. Numerous organizations have provided funding, principally the U.S. National Science Foundation, and hundreds of field workers have contributed. I would also like to acknowledge academic and technical members of University of Alberta.

Finally, I thank my partner Ashkan for continuous support, my parents Nimet and Ali Pasa for believing in me no matter what, my sister and brothers, Atoosa, Murat, Osman and Huseyin, for understanding and giving moral support, my Maman Afsaneh, for endless help, and

the rest of the family and friends for keeping me as same as possible. Also, special thanks to my son, Tigin, for his infinite love.

Table of Contents

List of Tables

List of Figures

Chapter One: Introduction

1.1 Overview of forest mensuration

Tree mensuration is the basis for forestry and forest management. It provides quantitative information about trees and forest stands required for forest management and planning. Forest management plans rely on information about growth and yield and understanding on how harvesting and silvicultural activities might affect forest stand dynamics. Measurement of tree diameter and height provides essential data for growth and yield modelling, for predicting stand dynamics and for planning forest management. Tree diameter and height were first used to calculate mean and cumulative stand volume and stand growth for long-term forest inventory plots dating back the 1860s (Pretzsch, 2009). Since then they have been commonly measured to describe forest stand characteristics, to model forest growth and yield, to assess site index, and to evaluate carbon mitigation plans. By measuring tree diameter and height, harvesting and silvicultural activities can be practiced to achieve specifically desired stand (Seely et al., 2004). To inform such activities, it is helpful to compare the effect of different management scenarios on the same type of stands, or of the same management scenarios on different type of stands. Examples of such applications include predicting timber production (Garcia-Gonzalo et al., 2007) and examining vegetation and gap dynamics (Spies and Franklin, 2014; Yamamoto, 2000).

Modelling variation in tree diameter and height, and their relationships can provide important information and understanding about the structure and dynamics of forest stands, thus the functional roles of forest, e.g., biodiversity maintenance and capacity in climate change mitigation. This thesis focuses on modelling tree size distribution and tree height-diameter

relationships. In this thesis, tree size is measured as tree trunk diameter at breast height (DBH), while tree height is measured as the height from the ground base to the top of a tree.

1.2 Tree size distribution

Trees vary considerably with their sizes, shapes, wood characteristics, and growth behaviors in forests. These variations form routes to succession, stand structure, and ecosystem functioning. Variation in tree growth and other attributes exists because of several factors, such as environmental conditions, genetics, disturbances, and competition for resources. For example, shade-intolerant tree species generally grow taller than shade-tolerant tree species prior to stand canopy closure (Archibold, 1995). Describing the variation is central to predict stand dynamics (Parker et al., 1985; Pretzsch et al., 2014) and how the dynamics may be affected by disturbances (Brando et al., 2012), competition and climate (Zhang et al., 2015). Modelling tree size distribution is a necessary for evaluating variation in tree diameter in forests.

Tree size distribution describes the number of individuals that fall within each tree size class. Tree size distribution modelling has been exercised since the early 1940s (Bailey and Dell, 1973). The probability distributions that were used to model tree size distribution in early time include gamma (Nelson, 1964), log-normal (Bliss and Reinker, 1964), beta (Li et al., 2002), Johnson's SB (Hafley and Schreuder, 1977), and the Weibull distribution (Bailey and Dell, 1973). Although many models have been used to model tree size distribution of natural forests, they share important similarities that may indicate some general mechanisms underlying tree dynamics and forest stand structure. For example, a widely observed reversed-J shaped diameter distribution suggests that there is an abundance of small sized trees and few large sized trees in forests. Uniform size distribution means that trees in a forest are approximately equally

distributed across different tree size classes. In contrast, inverse sigmoid tree size distribution suggests that it is an old-growth or disturbance regenerated forest. Although recent studies propose that tree size distribution could be generated using ecological metabolic theory (Enquist and Niklas, 2001) or the variation in species traits (Coomes and Allen, 2007), understanding of tree size distribution remains elusive.

Among the many types of probability density functions for tree size distribution, the Weibull distribution is the most widely used model. The model was first introduced by Bailey and Dell (1973) and has since been used for estimating tree size distribution in different regions such as temperate forest (Wang et al., 2009) and subtropical forest (Lai et al., 2013), in different aged forest such as uneven-aged forest (Zhang et al., 2001) and even-aged forest (Lorimer and Krug, 1983), in different staged forest such as young forest (Bullock and Burkhart, 2005), and old forest (Merganič and Sterba, 2006). Why is the Weibull distribution applicable to so many different types of forests? This is a not fully answered question. In this thesis I proposed a mechanism that leads to the Weibull distribution.

1.3 Tree height-diameter relationships

The relationship between tree height and size (tree diameter) is basic to growth yield and modelling. Tree height was used for quantifying stand index and site fertility to identify productivity of a forest stand (Assmann, 1970; Pretzsch, 2009). Since then, tree height has been commonly used to determine productivity of forest stands because tree height is known to be less affected by environmental conditions than other tree attributes. In addition to being a major component for growth and yield modelling, tree height is also an important ecological attribute to investigate forest succession. Trees allocate most of their energy to height growth for

harvesting light in secondary succession following disturbances. As such tree height is a key indicator to estimate disturbance and succession history (Loehle, 2000).

The field measurement of tree height is relatively difficult and laborious compared with the measurement of tree diameter (e.g., DBH). Because of that tree height is typically estimated from tree diameter by assuming an allometric relationship between the two. But there is a wide variety of models in the literature used for describing the relationship between tree height and tree diameter, including logistic model (Pearl and Reed, 1920), exponential model (Ratkowsky, 1990), polynomial model (Curtis, 1967) and Gompertz model (Winsor, 1932). These equations have been used to describe tree height-DBH relationships since the mid-1900s (Curtis, 1967), for different species (Rijal et al., 2012) and for different forest types (Liu et al., 2017; Peng et al., 2001). However, selection of the "best" model to describe the height-diameter relationship for each species is a challenging exercise as this could be subject to sample size, specific biology of each species and modelling methods. In this thesis, I compiled a large set of data to model tree height-diameter relationships for seven major timber species in Alberta and selected the best model for each of the seven species.

1.4 Climate change effects

Forest ecosystems and the services they provide are known to be threatened by the rapid pace of global change and the resulting biotic and abiotic stress. Climate change is often identified as one of the major factors that drives change in forest ecosystems (Allen et al., 2010; Chhin et al., 2008). Climate change has both direct and indirect effects on tree growth (Chen et al., 2016; Sette Jr et al., 2016). For example, increasing temperature directly affects tree growth by influencing growing season length (Wang et al., 2011) and indirectly affects water availability in

the soil and moisture availability in the air (Hogg et al., 2008; Kreuzwieser and Gessler, 2010). Moreover, plant species have specific response to climate change (Huang et al., 2010; Zhang et al., 2015), e.g., altering wood formation under increasing temperatures (Begum et al., 2018; Granda et al., 2018). It has been observed that trees grew shorter in dry areas (Oboite and Comeau, 2019) or wider in wet areas (Yeh and Wensel, 2000). Increased precipitation could also alter the distribution of the roots (Zhang et al., 2019).

Forest systems are characterized by their specific mixture of species that differ in their life strategies and therefore in their response to global change and induced stresses. Boreal forest is one of the main forest types in the world. They cover 33% of the world's forested areas and Canada has 21% of the boreal forests. It has become evident that boreal forests are heavily affected by recent climate change (Price et al., 2013). Because, boreal forests could become a net carbon sink or carbon source (Hadden and Grelle, 2016; Ma et al., 2012) depending on the relationship between growth and decomposition rates as a result of increased fire frequency (Bond-Lamberty et al., 2007), expansion of insect outbreaks (Hogg et al., 2002) and widespread tree mortality caused by drought (Michaelian et al., 2011). However, the effects of climate change on boreal forest structure and dynamics sometimes might not be immediately evident because of the nature of long -lifespans of trees. In this thesis, I investigated climate effect on tree height-DBH relationship of species in order to understand and assess possible impact of climate change on forest structure and dynamics.

1.5 Thesis outline

This thesis investigates the variation of tree size and tree height, their species-specific relationship, and climate effect on the relationship for boreal forest of Alberta. Having set out the importance of tree diameter and height and their relationships, each data chapter can be outlined.

In **Chapter 2**, my objectives were (1) to explain how Weibull distribution arises and how the distribution fits a wide range of forest communities, and (2) to illustrate the use of tree size distributions for predicting growth. I used three large-scale empirical data sets. The first data set is the census transects data collected from Africa, Europe, North America, Mesoamerica, South America, and tropical Asia by Gentry and colleagues. The second data set is from Alberta's permanent sample plot network. These data were used to test the model and showed how Weibull distribution fits tree size distribution. The third data set is from 50-ha forest plot on Barro Colorado Island, Panama, and was used to test the model and to predict growth. I found that tree size distributions follow a curvilinear relationship and the Weibull distribution describes it well. We also verified that Weibull distribution can be used to predict growth.

In **Chapter 3**, my objectives were (1) to model tree height-DBH relationships for seven boreal tree species of Alberta and select the best height-DBH models for each of the seven species, (2) to analyze the derivatives of the best-fitted models to reveal the difference in growth patterns of the seven study species that are otherwise not obvious in the cumulative height-DBH equations, and (3) to determine whether the growth patterns revealed by the derivatives are associated with the life history traits of species. I used Alberta permanent sample plots (PSP) tree datasets. PSPs were initially established in 1960s. On average they were remeasured every 5-

years. Nineteen non-linear tree height-DBH models and the best models derivative curves were analyzed for the seven major tree species. I respectively used nonlinear least square and nonlinear mixed-effect models to model the height-DBH relationships. I showed that nonlinear mixed effect models performed better than the traditional nonlinear models. I also showed that the derivative of the best-fitted tree height-DBH models revealed tree growth patterns that were otherwise not obvious from the traditional cumulative height-DBH relationships. The derivatives showed tree growth was strongly associated with life history traits of species.

In **Chapter 4**, my objectives were (1) to incorporate climate effects into existing tree height-DBH equations for improving the predictability of the models, and (2) to assess how climate conditions may affect tree height-DBH relationships. I modeled five major boreal timber species from Alberta PSP dataset. I used the climate moisture index (CMI) and annual mean maximum temperature (Tmax), derived from BioSIM, represent climate effects. I fitted seven most widely used tree height-DBH models from the literature to each of the five species. I integrated CMI and Tmax into these models and selected the best model for each species. I used the best selected model to assess the effect of climate (CMI and Tmax, respectively) on height-DBH relationship and showed the climate based tree height-DBH models better predicted tree height than the traditional models. The results revealed that species would grow taller with increasing temperature, while species would have specific responses to increasing climate moisture index.

1.6 References

Allen, C.D., Macalady, A.K., Chenchouni, H., Bachelet, D., McDowell, N., Vennetier, M., Kitzberger, T., Rigling, A., Breshears, D.D., Hogg, E.H. (Ted., Gonzalez, P., Fensham, R., Zhang, Z., Castro, J., Demidova, N., Lim, J.H., Allard, G., Running, S.W., Semerci, A., Cobb, N., 2010. A global overview of drought and heat-induced tree mortality reveals emerging climate change risks for forests. For. Ecol. Manage. 259, 660–684. https://doi.org/10.1016/j.foreco.2009.09.001

Archibold, O.W., 1995. Ecology of World Vegetation. Springer Netherlands.

Assmann, E., 1970. The principles of forest yield study. Pergamon, Oxford, New York.

Bailey, R., Dell, T., 1973. Quantifying Diameter Distributions with the Weibull Function. For. Sci. 19, 97–104. https://doi.org/10.1093/forestscience/19.2.97

Begum, S., Kudo, K., Rahman, M.H., Nakaba, S., Yamagishi, Y., Nabeshima, E., Nugroho, W.D., Oribe, Y., Kitin, P., Jin, H.O., Funada, R., 2018. Climate change and the regulation of wood formation in trees by temperature. Trees - Struct. Funct. 32, 3–15. https://doi.org/10.1007/s00468-017-1587-6

Bliss, C.I., Reinker, K.A., 1964. A lognormal approach to diameter distributions in even-aged stands. For. Sci. 10, 350–360.

Bond-Lamberty, B., Peckham, S.D., Ahl, D.E., Gower, S.T., 2007. Fire as the dominant driver of central Canadian boreal forest carbon balance. Nature 450, 89–92. https://doi.org/10.1038/nature06272

Brando, P.M., Nepstad, D.C., Balch, J.K., Bolker, B., Christman, M.C., Coe, M., Putz, F.E., 2012. Fire-induced tree mortality in a neotropical forest: The roles of bark traits, tree size, wood density and fire behavior. Glob. Chang. Biol. 18, 630–641.

https://doi.org/10.1111/j.1365-2486.2011.02533.x

Bullock, B.P., Burkhart, H.E., 2005. Juvenile diameter distributions of loblolly pine characterized by the two-parameter Weibull function. New For. 29, 233–244. https://doi.org/10.1007/s11056-005-5651-5

Chen, H.Y.H., Luo, Y., Reich, P.B., Searle, E.B., Biswas, S.R., 2016. Climate change-associated trends in net biomass change are age dependent in western boreal forests of Canada. Ecol. Lett. 19, 1150–1158. https://doi.org/10.1111/ele.12653

Chhin, S., Hogg, E.H. (Ted., Lieffers, V.J., Huang, S., 2008. Potential effects of climate change on the growth of lodgepole pine across diameter size classes and ecological regions. For. Ecol. Manage. 256, 1692–1703. https://doi.org/10.1016/j.foreco.2008.02.046

Coomes, D.A., Allen, R.B., 2007. Effects of size, competition and altitude on tree growth. J. Ecol. 95, 1084–1097. https://doi.org/10.1111/j.1365-2745.2007.01280.x

Curtis, R.O., 1967. Height-Diameter and Height-Diameter-Age Equations For Second-Growth Douglas-Fir. Science (80-.). 13, 365–375.

Enquist, B.J., Niklas, K.J., 2001. Invariant scaling relations across tree-dominated communities. Nature 410, 655–660. https://doi.org/10.1038/nature02023

Garcia-Gonzalo, J., Peltola, H., Zubizarreta Gerendiain, A., Kellomäki, S., 2007. Impacts of forest landscape structure and management on timber production and carbon stocks in the boreal forest ecosystem under changing climate. For. Ecol. Manage. 241, 243–257. https://doi.org/10.1016/j.foreco.2007.01.008

Granda, E., Alla, A.Q., Laskurain, N.A., Loidi, J., Sánchez-Lorenzo, A., Camarero, J.J., 2018. Coexisting oak species, including rear-edge populations, buffer climate stress through xylem adjustments. Tree Physiol. 38, 159–172. https://doi.org/10.1093/treephys/tpx157

Hadden, D., Grelle, A., 2016. Changing temperature response of respiration turns boreal forest from carbon sink into carbon source. Agric. For. Meteorol. 223, 30–38. https://doi.org/10.1016/j.agrformet.2016.03.020

Hafley, W.L., Schreuder, H.T., 1977. Statistical distributions for fitting diameter and height data in even-aged stands. Can. J. For. Res. 7, 481–487.

Hogg, E.H., Brandt, J.P., Kochtubajda, B., 2002. Growth and dieback of aspen forests in northwestern Alberta, Canada, in relation to climate and insects. Can. J. For. Res. 32, 823–832. https://doi.org/10.1139/x01-152

Hogg, E.H., Brandt, J.P., Michaelian, M., 2008. Impacts of a regional drought on the productivity, dieback, and biomass of western Canadian aspen forests. Can. J. For. Res. 38, 1373–1384. https://doi.org/10.1139/X08-001

Huang, J.A., Tardif, J.C., Bergeron, Y., Denneler, B., Berninger, F., Girardin, M.P., 2010. Radial growth response of four dominant boreal tree species to climate along a latitudinal gradient in the eastern Canadian boreal forest. Glob. Chang. Biol. 16, 711–731. https://doi.org/10.1111/j.1365-2486.2009.01990.x

Kreuzwieser, J., Gessler, A., 2010. Global climate change and tree nutrition: Influence of water availability. Tree Physiol. 30, 1221–1234. https://doi.org/10.1093/treephys/tpq055

Lai, J., Coomes, D.A., Du, X., Hsieh, C. fu, Sun, I.F., Chao, W.C., Mi, X., Ren, H., Wang, X., Hao, Z., Ma, K., 2013. A general combined model to describe tree-diameter distributions within subtropical and temperate forest communities. Oikos 122, 1636–1642. https://doi.org/10.1111/j.1600-0706.2013.00436.x

Li, F., Zhang, L., Davis, C.J., 2002. Modeling the Joint Distribution of Tree Diameters and Heights by Bivariate Generalized Beta Distribution. For. Sci. 48, 47–58.

Liu, M., Feng, Z., Zhang, Z., Ma, C., Wang, M., Lian, B. ling, Sun, R., Zhang, L., 2017. Development and evaluation of height diameter at breast models for native Chinese Metasequoia. PLoS One 12, 1–17. https://doi.org/10.1371/journal.pone.0182170

Loehle, C., 2000. Strategy space and the disturbance spectrum: A life-history model for tree species coexistence. Am. Nat. 156, 14–33. https://doi.org/10.1086/303369

Lorimer, C.G., Krug, A.G., 1983. Diameter distributions in even-aged stands of shade-tolerant and midtolerant tree species. Am. Midl. Nat. 109, 331–345. https://doi.org/10.2307/2425414

Ma, Z., Peng, C., Zhu, Q., Chen, H., Yu, G., Li, W., Zhou, X., Wang, W., Zhang, W., 2012. Regional Drought-Induced Reduction in the Biomass Carbon Sink of Canada's Boreal Forests. Proc. Natl. Acad. Sci. 109, 2423–2427. https://doi.org/10.1073/pnas.1111576109

Merganič, J., Sterba, H., 2006. Characterisation of diameter distribution using the Weibull function: Method of moments. Eur. J. For. Res. 125, 427–439. https://doi.org/10.1007/s10342-006-0138-2

Michaelian, M., Hogg, E.H., Hall, R.J., Arsenault, E., 2011. Massive mortality of aspen following severe drought along the southern edge of the Canadian boreal forest. Glob. Chang. Biol. 17, 2084–2094. https://doi.org/10.1111/j.1365-2486.2010.02357.x

Nelson, T.C., 1964. Diameter distribution and growth of Loblolly pine. For. Sci. 10, 105–114.

Oboite, F.O., Comeau, P.G., 2019. Competition and climate influence growth of black spruce in western boreal forests. For. Ecol. Manage. 443, 84–94. https://doi.org/10.1016/j.foreco.2019.04.017

Parker, G.R., Leopold, D.J., Eichenberger, J.K., 1985. Tree dynamics in an old-growth, deciduous forest. For. Ecol. Manage. 11, 31–57. https://doi.org/10.1016/0378-

1127(85)90057-X

Pearl, R., Reed, L.J., 1920. On the rate of growth of the population of the United States since 1790 and its mathematical representation. Proc. Natl. Acad. Sci. 6, 275–288.

Peng, C., Zhang, L., Liu, J., 2001. Developing and validating nonlinear height-diameter models for major tree species of Ontario's boreal forests. North. J. Appl. For. 18, 87–94. https://doi.org/10.1093/njaf/18.3.87

Pretzsch, H., 2009. Forest dynamics, growth and yield: From measurement to model, Forest Dynamics, Growth and Yield: From Measurement to Model. Springer Berlin Heidelberg. https://doi.org/10.1007/978-3-540-88307-4

Pretzsch, H., Biber, P., Schütze, G., Uhl, E., Rötzer, T., 2014. Forest stand growth dynamics in Central Europe have accelerated since 1870. Nat. Commun. 5, 1–10. https://doi.org/10.1038/ncomms5967

Price, D.T., Alfaro, R.I., Brown, K.J., Flannigan, M.D., Fleming, R.A., Hogg, E.H., Girardin, M.P., Lakusta, T., Johnston, M., McKenney, D.W., Pedlar, J.H., Stratton, T., Sturrock, R.N., Thompson, I.D., Trofymow, J.A., Venier, L.A., 2013. Anticipating the consequences of climate change for Canada's boreal forest ecosystems. Environ. Rev. 21, 322–365. https://doi.org/10.1139/er-2013-0042

Ratkowsky, D.A., 1990. Handbook of Nonlinear Regression Models. Marcel Dekker, Inc., New York. https://doi.org/10.2307/2347928

Rijal, B., Weiskittel, A.R., Kershaw, J.A., 2012. Development of regional height to diameter equations for 15 tree species in the North American Acadian Region. Forestry 85, 379–390. https://doi.org/10.1093/forestry/cps036

Seely, B., Nelson, J., Wells, R., Peter, B., Meitner, M., Anderson, A., Harshaw, H., Sheppard, S.,

Bunnell, F.L., Kimmins, H., Harrison, D., 2004. The application of a hierarchical, decision-support system to evaluate multi-objective forest management strategies: A case study in northeastern British Columbia, Canada. For. Ecol. Manage. 199, 283–305. https://doi.org/10.1016/j.foreco.2004.05.048

Sette Jr, C.R., Tomazello Fo, M., Lousada, J.L., Lopes, D., Laclau, J.P., 2016. Relationship between climate variables, trunk growth rate and wood density of Eucalyptus grandis W. Mill ex Maiden trees. Rev. Arvore 40, 337–346. https://doi.org/10.1590/0100-67622016000200016

Spies, T.A., Franklin, J.F., 2014. Gap Characteristics and Vegetation Response in Coniferous Forests of the Pacific Northwest Author (s): Thomas A . Spies and Jerry F . Franklin Published by : Ecological Society of America GAP CHARACTERISTICS AND VEGETATION RESPONSE IN. Ecol. Soc. Am. 70, 543–545.

Wang, X., Hao, Z., Zhang, J., Lian, J., Li, B., Ye, J., Yao, X., 2009. Tree size distributions in an old-growth temperate forest. Oikos 118, 25–36. https://doi.org/10.1111/j.0030-1299.2008.16598.x

Wang, X., Piao, S., Ciais, P., Li, J., Friedlingstein, P., Koven, C., Chen, A., 2011. Spring temperature change and its implication in the change of vegetation growth in North America from 1982 to 2006. Proc. Natl. Acad. Sci. U. S. A. 108, 1240–1245. https://doi.org/10.1073/pnas.1014425108

Winsor, C.P., 1932. The Gompertz Curve as a Growth Curve. Proc. Natl. Acad. Sci. 18, 1–8. https://doi.org/10.1073/pnas.18.1.1

Yamamoto, S.-I., 2000. Forest Gap Dynamics and Tree Regeneration. J. For. Res. 5, 223–229. https://doi.org/10.1007/bf02767114

Yeh, H.-Y., Wensel, L.C., 2000. The relationship between tree diameter growth and climate for coniferous species in northern California. Can. J. For. Res. 30, 1463–1471. https://doi.org/10.1139/cjfr-30-9-1463

Zhang, B., Cadotte, M.W., Chen, S., Tan, X., You, C., Ren, T., Chen, M., Wang, S., Li, W., Chu, C., Jiang, L., Bai, Y., Huang, J., Han, X., 2019. Plants alter their vertical root distribution rather than biomass allocation in response to changing precipitation. Ecology 100, 1–10. https://doi.org/10.1002/ecy.2828

Zhang, J., Huang, S., He, F., 2015. Half-century evidence from western Canada shows forest dynamics are primarily driven by competition followed by climate. Proc. Natl. Acad. Sci. U. S. A. 112, 4009–4014. https://doi.org/10.1073/pnas.1420844112

Zhang, L., Gove, J.H., Liu, C., Leak, W.B., 2001. A finite mixture of two Weibull distributions for modeling the diameter distributions of rotated-sigmoid, uneven-aged stands. Can. J. For. Res. 31, 1654–1659. https://doi.org/10.1139/cjfr-31-9-1654

Chapter two: Tree size distribution across forest communities

2.1 Abstract – The size distribution of forest trees is highly right-skewed – many trees are small, a few are large. Recent studies in macroecology predict a power-law form to the distribution, arising from the stand-level process of self-thinning. Empirical data, however, suggest that log-transformed diameter distributions are curvilinear and cannot be described by a power-law. Here I derived a Weibull tree size distribution from processes of stochastic recruitment, growth, and mortality. I tested the model with three large data sets and showed the Weibull distribution fitted the observed size distributions very well. More importantly, I showed how tree size distribution can be used to predict tree growth and age, key information about community dynamics.

2.2 Introduction

Tree size distribution — a relationship describing the number of stems that fall within tree size classes — is widely used to describe stand structure in forest and, more generally, plant communities (Bailey and Dell, 1973; Harper, 1977; Leak, 1965; Silvertown and Charlesworth, 2001; Yoda et al., 1963). Knowledge about the variation in tree size is important to understand competition and stand dynamics (Ford, 1975; Harper, 1977; Hynynen and Ojansuu, 2003; Weiner and Solbrig, 1984). Numerous factors can contribute to the variation in tree size distributions, e.g., environmental conditions, density effect, differentiation in growth and metabolic allometrics (Enquist et al., 1998; Firbank and Watkinson, 1990; Turner and Deborah, 1983; Weiner, 1986; Yoda et al., 1963). Although tree abundances are widely recognized to have a negative relationship to decline with increasing tree size, there remains substantial disagreement on questions such as how the prevalent negative relationship is produced and whether there is a universal mathematical form underlying the negative pattern (Bokma, 2004; Brown et al., 2004; Enquist et al., 1998; Reynolds and Ford, 2005). In this study, I address these questions. Here, tree size is measured by the diameter at breast height (dbh).

Recent advances in allometric theory and interest in the search for general community assembly rules have renewed interest in modeling and reinterpreting tree size distribution from the perspective of macroecology (Enquist et al., 1998; Enquist and Niklas, 2001). A significant result arising from this macroecological effort is the revision of the long-standing "-3/2 thinning law" originating from forestry and widely applied to model plant size (Enquist et al., 1998; Yoda et al., 1963). The new prediction is that the dry mass of the average plant in mature populations relates via a power-function to maximum plant density with an exponent of -4/3. If the

relationship is expressed in terms of tree diameter (rather than tree mass) and density, the scaling relationship becomes (Enquist and Niklas, 2001)

$$f(x) = cx^{-2}, \tag{2.1}$$

where $f(x)$ is the number of stems in a given area, x is stem diameter, and c is a normalization factor that may vary with the kind of organisms and communities.

This simple yet elegant scaling model is derived, as a first approximation, from the assumption that the resources (energy) consumed by all individuals in a saturated community and the resources supplied from the environment are in balance (Enquist et al., 1998). While the model is justified theoretically, the approximate nature of first principles suggests that although the model may predict size variation well over a certain range, it may not do so for a wider range of size distribution. This is indeed the case in many empirical tree size frequency distributions where the log-transformed data do not show a straight line across the range in tree size, particularly at large diameters (see Figures 2.1 and 2.2).

Here I develop a model that fits the size distribution for a wide range of tree communities. The model assumes that variation in tree size in a community is determined by stochastic recruitment, growth, and mortality. I show that the stochastic processes lead to a Weibull distribution of tree size, of which the power-law is a special case. The Weibull distribution not only describes the negative relationship between the number of trees and tree size, but also precisely captures the curvilinearity typically observed. Since the size distribution depends on growth, I show further how the static tree size distribution can be used to predict growth. Three large-scale empirical data sets are used to test the model. The first is the tree data collected worldwide in small census transects by late Alwyn H. Gentry; the second is from the

Alberta permanent sampling plot network; the third is from the 50-ha plot on Barro Colorado Island, Panama.

2.3 The model

Consider a tree community changing due to recruitment, growth, and mortality of stems. By allometric theory, stem (or body mass) growth rate is assumed to take a simple form (Calder, 1984; Enquist et al., 1998)

$$\frac{dx}{dt} = rx^{\alpha}, \tag{2.2}$$

where r and α are constants and x is body size.

Imagine an even-aged community where all trees have the same growth rate. Model (2.2) would predict that every stem in the community has the same size if they are observed at the same time. Such a community rarely exists in nature. Instead, recruitment and mortality occur continuously, and young trees colonize the space freed up by the death of old trees. Given uneven ages in the community, model (2.2) predicts that trees will vary in size, because they vary in age. I relax the even-age condition by considering tree age as a random variable following an exponential distribution:

$$g(t) = \lambda e^{-\lambda t}, \tag{2.3}$$

where λ is a parameter and $1/\lambda$ is the mean age of the trees in the community. This exponential distribution is justified if mortality-colonization is a random process, independent of size and age. This is equivalent to a classic queue model: if customers randomly arrive at a service counter, customer waiting time follows an exponential distribution.

Models (2.2) and (2.3) together describe a community in which trees colonize the community at different times but grow at the same rate. If all the trees are measured (harvested) at the same time, then tree size will vary according to a Weibull distribution (shown below). Similarly, I can imagine a situation where all trees colonize the community at the same time and grow at the same rate as defined by model (2.2) but each is observed (harvested) at different times with the observation time following exponential model (2.3). This will result in the same Weibull distribution for the tree size.

Individual tree size *x* in model (2.2) is a deterministic variable. But it varies from one tree to another because of variation in age (or harvesting time). It is straightforward to derive the probability density function (pdf) for size variation by the transformation technique for a random variable, $f(x) = g(t)\left|\frac{dt}{dx}\right|_{t=w(x)}$, where $t = w(x)$ is a function solved from model (2.2). This leads to tree size model: $f(x) = cx^{-\alpha} \exp(-\beta x^{1-\alpha})$. Normalizing this equation we arrive at a Weibull probability distribution:

$$f(x) = \beta(1-\alpha)x^{-\alpha} \exp(-\beta x^{1-\alpha}), \tag{2.4}$$

where $\beta = \frac{\lambda}{r(1-\alpha)}$ and $\alpha \neq 1$. α is often called shape parameter and β is scale parameter.

When α in model (2.2) equals 1, it is easy to show that tree size distribution *f*(*x*) becomes a power-law distribution (also called a Pareto or Zipf distribution):

$$f(x) = cx^{-\xi}, \tag{2.5}$$

where $\xi = \lambda / r$. Model (2.1) is a special case of model (2.5) with $\xi = 2$. See Reed and Hughes (2002) and Solow (2005) for the derivation of the power-law model from the consideration of statistical processes.

2.4 Model test

2.4.1 Data

I tested the model using three large sets of tree data. The first is the forest transect data collected over 22 years from six continents by Gentry and colleagues (Gentry, 1993, 1988; see http://www.mobot.org/MOBOT/Research/gentry/transect.shtml). Gentry's data contain 226 2×50 m transects located in six major forests from Africa, Europe, North America, Mesoamerica, South America, and tropical Asia. The forests range from near-monospecific to highly diverse rain forest stands, the latitude spans 40.43° S to 60.48° N, and the elevation varies from 20 to 3,050 m. Mesoamerica includes all the Central American countries (Panama, Costa Rica, Nicaragua, El Salvador, Honduras, Guatemala, Belize) and five Mexican States east of the Isthmus of Tehuantepec (Chiapas, Tabasco, Campeche, Yucatan, and Quitana Roo). In each transect, all stems, including lianas, with diameter (dbh) larger than a certain size (the low diameter cutoff is unknown for Gentry's data) were measured. All the trees are grouped into dbh classes at 2.5, 3, 4, 5, … cm. It is unclear whether the 2.5 cm dbh class includes stems from 1, 1.5 or 2 cm. To avoid ambiguity and sampling bias, our analysis only included stems with dbh ≥ 3 cm (i.e., the regularly spaced dbh classes). The final data includes 55,747 stems with maximum dbh ranging between 76 and 412 cm. The European dataset has 892 stems, North American 3,761, African 5,564, Asian 5,582, Mesoamerican, 7,849, and South American 32,099 stems. The Weibull distribution model (2.4) was fitted to each of the six regions separately.

The second data set is permanent sampling plots (PSPs) from Alberta Environments and Parks, which were established by the Government of Alberta and forest industries starting in the 1960s (Forest Management Branch, 2005). The plot sizes vary from 400 to 8,000 m^2. All standing trees > 9 cm dbh were mapped, measured, and identified to species. PSPs remeasured

periodically. The final data have 96,417 stems with maximum dbh = 80.8 cm. The Weibull distribution model was fitted to the PSP data.

The third data set is from the 50-ha long-term forest dynamics plot on Barro Colorado Island (BCI), Panama (Condit et al., 1996; Hubbell and Foster, 1983). The plot is 1000×500 m and was established in 1981. All free-standing trees and shrubs ≥ 1 cm dbh have been enumerated, mapped, and identified to species (Condit, 1998). Six censuses (1982, 1985, 1990, 1995, 2000 and 2005) have been completed. The 1990 and 1995 censuses were used in this study. There were 229,049 stems belonging to 301 species in the 1995 census. Two analyses were conducted. (i) The Weibull distribution model (2.4) was fitted to the 1995 census diameter data. (ii) Diameter increments between 1990 and 1995 censuses were used to fit tree growth model (2.2). The growth model allows two independent calculations of the growth exponent α, one directly from observed growth, and one from the Weibull fitted to the diameter distribution.

2.4.2 Parameter estimation

Least-squares regression of log-transformed data is commonly used to fit allometric scaling exponents. However, this method is inappropriate for frequency data such as tree abundance in diameter categories. Maximum likelihood estimation is preferred. Because each dataset has a minimum dbh, $x_{\min}$, (3 cm in Gentry's data, 9 cm in Alberta data, 1 cm in the BCI data), the truncated Weibull distribution was used. The truncation form is:

$f(x) = \frac{\beta(1-\alpha)x^{-\alpha}\exp(-\beta x^{1-\alpha})}{\exp(-\beta x_{\min}^{1-\alpha})}$. The maximum likelihood method was applied to this model to estimate parameters α and β. The goodness-of-fit of the model was assessed using R^2 (e.g., Enquist and Niklas, 2001).

The allometric growth model (2.2) was fitted to the BCI data using linear regression with log-transformed data: $\log(\, dx/dt\,) = \log(\, r\,) + \alpha \log(\, x\,)$. The growth data were the mean by dbh size classes. The growth rate *dx*/*dt* was approximated by the dbh increment between the 1990 and 1995 censuses.

2.5. Results

The tree size distributions of the Gentry tree communities, Alberta permanent sample plots and the BCI permanent plot are shown in figures 2.1, 2.2 and 2.3. A notable feature common to all the distributions is the curvilinearity on a log-log graph. The Weibull distribution describes this curvilinearity well and explains a large proportion of the variation in the tree abundance, with $R^2 \geq 0.95$ (Table 2.1).

The Weibull fit is also confirmed independently by fitting the growth model (2.2) for BCI data. The fit of model (2.2) to the growth data (i.e., the increment in dbh between 1990 and 1995) led to the growth exponent $\alpha = 0.6435$ with standard error of 0.0354 (Figure 2.3, right panel). This is remarkably close to α estimated from the Weibull distribution to the 1995 dbh (= 0.6856, with standard error = 0.0005; Table 2.1, bottom row).

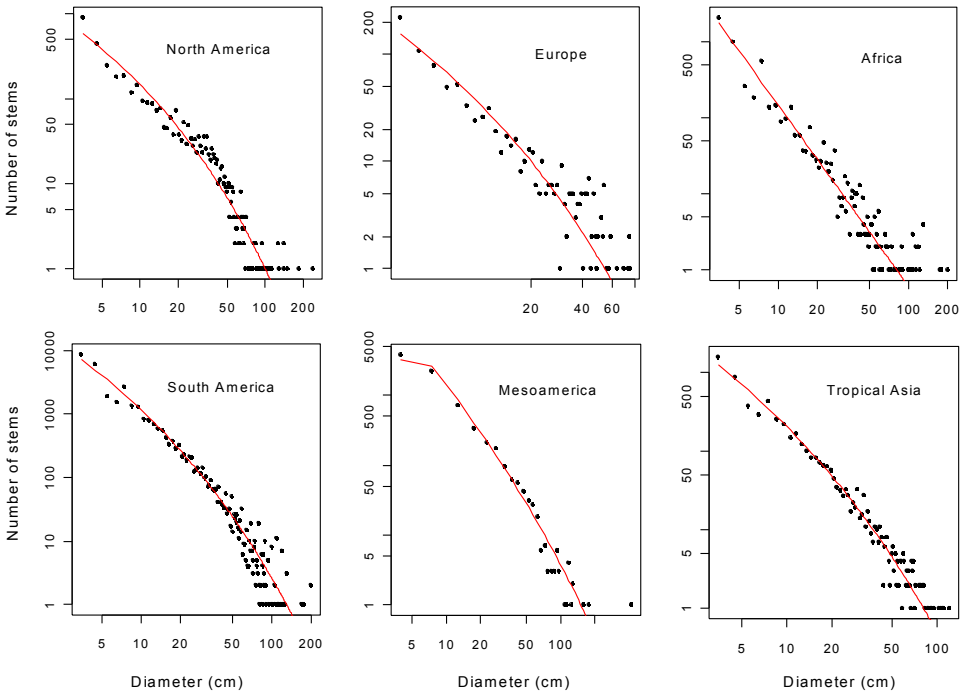

Figure 2.1 Tree size distributions of the six global tree communities of Gentry and the fit of model (2.4).

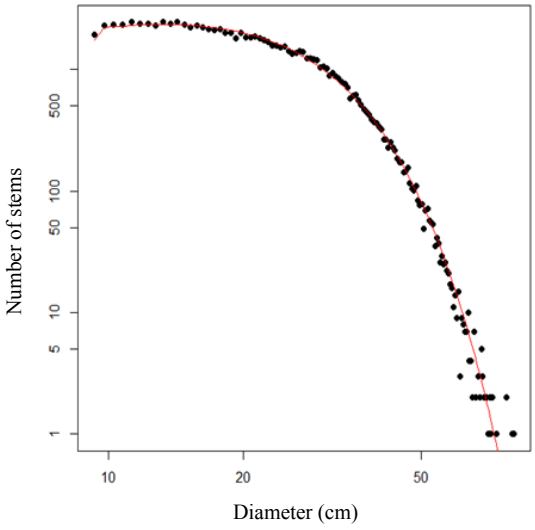

Figure 2.2 Tree size distributions of the Alberta PSP data set and the fit of model (2.4).

I can also estimate the average age of trees for the BCI forest as $1/\lambda$ of model (2.3), where λ can be calculated from the relationship given by model (4): $\beta = \frac{\lambda}{r(1-\alpha)}$. Using β estimated from the tree size distribution (Table 2.1, bottom row) and the intercept and slope of the growth model (2.3) (Figure 2.3, right panel), λ is: $\lambda = \beta r(1-\alpha) = 2.2136 \times \exp(-3.4254) \times (1-0.6435) = 0.02568$. The average age of the BCI trees is thus estimated to be 38.9 years (=1/0.02568). This age is consisted with the average age that is estimated to be between 30 and 50 (Stephen Hubbell, pers. comm., unpublished data).

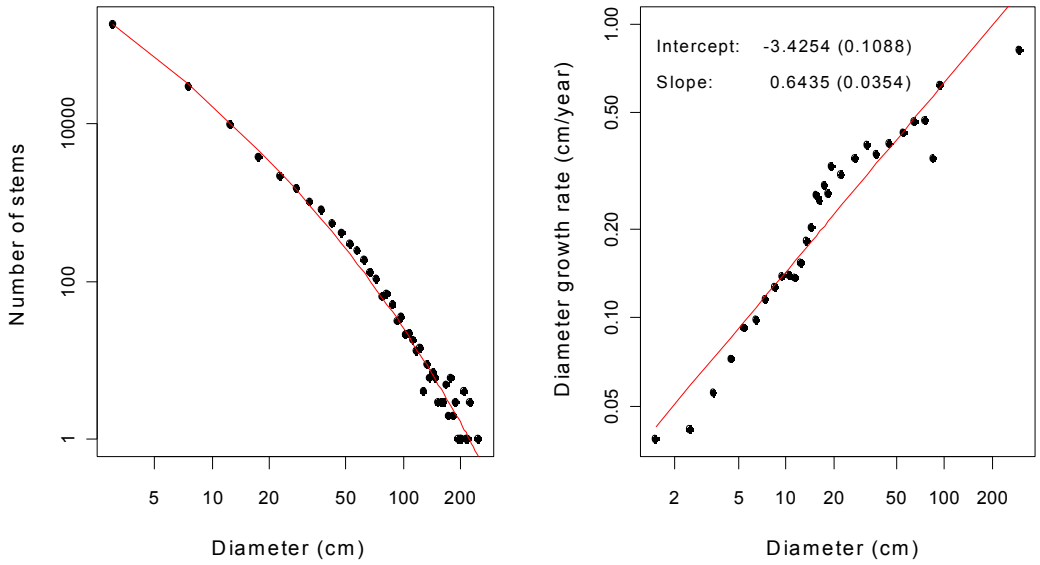

Figure 2.3 Left panel: Tree size distribution for the 1995 census of the 50 ha forest on Barro Colorado Island, Panama and the fit of the Weibull distribution model (2.4). Right panel: Diameter growth of trees on BCI between 1990 and 1995 and the fit of growth model (2.2). The slope (i.e., α) of growth model (2.2) is 0.6435 with standard error = 0.0354. It is a good match to the slope of 0.6856 estimated from tree size data using the Weibull distribution (see Table 2.1).

The average age can also be estimated from model (2.2) using the form integrated from the model: $t = t_0 + \frac{\alpha}{r}\left(\frac{1}{x_0^{\alpha+1}} - \frac{1}{x^{\alpha+1}}\right)$, where x_0 is the minimum diameter cutoff (= 1 cm in the case of BCI), t_0 is the age at x_0. The average age for trees of 1 cm is estimated to be 17.7 years (Hubbell, pers. comm.). This leads to t = 17.7 + 19.6 = 37.3 years. (19.6 is the average age of trees grow from 1 cm to x cm, calculated from the above formula.) This is almost identical to the age estimated from $1/\lambda$.

Table 2.1 Estimates of the shape and scale parameters (α and β) of the Weibull distribution model (4) and R^2 of the fit to the tree size data from the global tree communities of Gentry (the first six regions), Alberta PSP data and the 50 ha forest on Barro Colorado Island (BCI), Panama. The small standard errors (SE) are the result of the large sample sizes.

Region	No of trees	α (SE)	β (SE)	R^2
Europe	892	0.5692 (0.0073)	0.9032 (0.0302)	0.9623
Africa	5564	0.9824 (0.0002)	75.3401 (1.0100)	0.9830
Temperate North America	3761	0.5669 (0.0035)	0.7950 (0.0130)	0.9488
South America	32099	0.6510 (0.0011)	1.6706 (0.0095)	0.9718
Meso America	7849	0.7468 (0.0019)	2.9280 (0.0330)	0.9894
Tropical Asia	5582	0.6454 (0.0028)	1.5958 (0.0214)	0.9743
Alberta	96417	-0.8010 (0.0058)	0.0042 (0.0341)	0.9979
BCI	229049	0.6856 (0.0005)	2.2136 (0.0046)	0.9998

2.6 Discussion

Trees within a forest differ in size. The variation is characterized by right-skewed distributions – many trees are small, a few are large (Figures 2.1, 2.2 and 2.3). Although a multitude of processes may cause this negative pattern (Enquist et al., 1998; Harper, 1977; Reynolds and David Ford, 2005; Silvertown and Charlesworth, 2001; Weiner and Solbrig, 1984; Yoda et al., 1963), e.g., variation in recruitment, differentiation in growth rates, competition, disturbances and metabolic allometrics, my study showed that variation in recruitment time and growth is sufficient to explain the differentiation in tree size of a stand. This simple hypothesis can be understood in two ways. One is to consider an even-age stand where all the trees have the same growth rate as defined by model (2.1) but each tree is observed at different time and this time is an exponential distribution. Equivalently, we can consider an uneven-aged forest with the age following an exponential distribution and all the trees are observed at the same time. In this latter case, according to model (2.2) tree growth will vary because of the difference in age. Both scenarios give rise to the Weibull distribution (2.4).

While the negative tree size distribution is widely observed, there is little consensus on which is the best model describing the pattern. Power laws such as model (2.5) are commonly observed in nature (Mandelbrot, 1990). The current debate on the power-law model centers on questions such as what exponent the machinery of nature produces and how it is produced (Enquist et al., 1998; Enquist and Niklas, 2001; Glazier, 2005). Previous studies show that tree size distribution often follows a thinning power-law with exponent of -3/2 or -4/3 (Enquist et al., 1998; Yoda et al., 1963). My study suggests that the real question is perhaps not whether there is a universal exponent but whether the power-law as a whole is general enough for describing the entire range of tree size distribution across different communities. Although the power-law is

shown to be able to describe size distribution at some range (Enquist and Niklas, 2001), it apparently fails to capture the curvilinearity across the tree size distributions as shown in figures 2.1 and 2.2 (Coomes et al., 2003). The arrival of the Weibull distribution and the fact that the power-law is its special case suggests that the power-law is just a first approximation to tree size distribution; trees in a community do probably not partition space in the manner of power-law.

My derivation of the Weibull is consistent with the approach of Reed and Hughes (2002) and Solow (2005), showing that regularity in size distribution can simply arise from statistical processes. It is worth to note that mathematically the Weibull is no more complex than the power-law model (2.5) as both have two parameters although the latter is a special form of the former. The Weibull is well known in forestry for modeling tree size distribution (Bailey and Dell, 1973; Clutter et al., 1983; Gove, 2003). Beyond its popularity, however, there have not been any serious theories proposed to explain its genesis and thus the application of the Weibull distribution in forestry has remained a purely phenomenological exercise. The model in this study provides a mechanistic foundation for interpreting the Weibull distribution.

In addition to the allometric growth model (2.2), other models can also be used to model tree growth. The logistic and Gompertz models are the two most commonly used. The logistic growth model is written as $\frac{dx}{dt} = rx(1 - \frac{x}{k})$, and the Gompertz model as $x(t) = \beta e^{-\beta_1 e^{-\beta_2 t}}$, where r, k, β, β_1, and β_2 are parameters. The logistic model under exponential harvesting, i.e., model (2.2), leads to a tree size distribution taking the form

$$f(x) = c\frac{(k - x)^{\alpha - 1}}{x^{\alpha + 1}}, \quad 0 < x \le k, \tag{2.6}$$

where c is a normalization constant and $\alpha = r / \lambda$ is a ratio of growth rate over harvesting (mortality) rate. Obviously, model (2.6) is entirely determined by this ratio. It is interesting to

observe that when the growth rate equals the harvesting rate, model (2.1) results. If the growth rate is larger than the harvesting rate, the curvilinear shape in the tree size distribution such as those observed in figures 2.1 and 2.2 will arise. If the growth rate is smaller than the harvesting rate, the system cannot be sustained at steady state.

Similarly, it is easy to derive tree size distribution for the Gompertz growth under exponential harvesting:

$$f(x) = c\,\frac{(\log\ \beta - \log\ x)^{\alpha-1}}{x}, \quad 0 < x \le \beta, \tag{2.7}$$

where $c = \alpha\beta_1^{-\alpha}$ and $\alpha = \dfrac{\lambda}{\beta_2}$.

It is worthwhile to note that both models (2.6) and (2.7) can also be used to describe the tree size distribution data studied in this paper, all resulting in high R^2 comparable to that of the Weibull distribution. There are three reasons for this study to focus on the Weibull distribution. (i) The Weibull is a model of wide application in forestry, (ii) Equations (2.6) and (2.7) are three-parameter models. (iii) It is often difficult to make the maximum likelihood estimation of models (2.6) and (2.7) converge; the maximization is sensitive to the initial values required for the iteration. In this case, least squares regression method has to be used to parameterize models (2.6) and (2.7).

What is interesting is that the Weibull distribution very accurately reflects two important dynamic parameters for the BCI trees, and thus can potentially be used to predict these parameters. The first one is the growth exponent α of model (2.2), which is 0.686 estimated from the Weibull distribution to the dbh data (Table 2.1, bottom row) and 0.644 estimated from growth model (2.2) fitted to the independent growth data for BCI (Figure 2.2, right panel). The second parameter is the average age ($\approx$ 38 years) estimated for the BCI trees. The prediction of

the growth rate and tree age in this study are very significant results. Tree size distribution is a major stand structure that is a static pattern, while growth rate is a time-dependent process. It is a big challenge in ecology how patterns may be used to infer community dynamics because theories to predict dynamics from patterns have simply not been developed yet. I believe this study represents a promising step toward this direction. It shows that linking patterns with dynamics may not be as difficult as it appears. The success in predicting growth rate and tree age lies in the fact that the tree size (Weibull) distribution is derived from a simple dynamic process as defined by model (2.2) and (2.3). This dynamic assumption makes a lot of sense because tree size is the outcome of many years' growth, it ought to carry information on dynamics.

2.7 References

Bailey, R., Dell, T., 1973. Quantifying Diameter Distributions with the Weibull Function. For. Sci. 19, 97–104. https://doi.org/10.1093/forestscience/19.2.97

Bokma, F., 2004. Evidence against universal metabolic allometry. Funct. Ecol. 18, 184–187. https://doi.org/10.1111/j.0269-8463.2004.00817.x

Brown, J.H., Gillooly, J.F., Allen, A.P., Savage, V.M., West, G.B., 2004. Toward a metabolic theory of ecology. Ecology 85, 1771–1789.

Calder, W.A., 1984. Size, function and life history. Harvard University Press, Cambridge, Massachusetts.

Clutter, J.L., Fortson, J.C., Pienaar, L.V., Brister, G.H., Bailey, R.L., 1983. Timber management: a quantitative approach. John Wiley & Sons, New York.

Condit, R., 1998. Tropical Forest Census Plots. Springer-Verlag and R. G. Landes Company, Berlin, Germany, and Georgetown, Texas.

Condit, R., Hubbell, S.P., Foster, R.B., 1996. Changes in Tree Species Abundance in a Neotropical Forest: Impact of Climate Change. J. Trop. Ecol. 12, 231–256.

Coomes, D.A., Duncan, R.P., Allen, R.B., Truscott, J., 2003. Disturbances prevent stem size-density distributions in natural forests from following scaling relationships. Ecol. Lett. 6, 980–989. https://doi.org/10.1046/j.1461-0248.2003.00520.x

Enquist, B.J., Brown, J.H., West, G.B., 1998. Allometric scaling of plant energetics and population density. Nature 395, 163–165.

Enquist, B.J., Niklas, K.J., 2001. Invariant scaling relations across tree-dominated communities. Nature 410, 655–660. https://doi.org/10.1038/nature02023

Firbank, L.G., Watkinson, A.R., 1990. On the effects of competition: from monocultures to mixtures, in: Grace, J.B., Tilman, D. (Eds.), Perspectives on Plant Competition. Academic Press, San Diego, California, USA, pp. 165–192.

Ford, E.D., 1975. Competition and Stand Structure in Some Even-Aged Plant Monocultures. J. Ecol. 63, 311–333. https://doi.org/10.2307/2258857

Forest Management Branch, 2005. Permanent sample plot (PSP) field procedures manual. Public Lands and Forests Division, Alberta Sustainable Resource Development.

Gentry, A.H., 1993. In Biodiversity and Conservation of Neotropical and Montane Forests, in: Churchill, S.P. et al. (Ed.), . New York Botanical Garden, New York, pp. 103–126.

Gentry, A.H., 1988. Changes in plant community diversity and floristic composition on environmental and geographical gradients. Ann. Missouri Bot. Gard. 75, 1–34.

Glazier, D.S., 2005. Beyond the'3/4-power law':variation in the intra-and interspecific scaling of metabolic rate in animals. Biol. Rev. 80, 611–662.

Gove, J.H., 2003. Estimation and applications of size-biased distributions in forestry., in: Amaro, D.R., Soares, P. (Eds.), Modelling Forest Systems. CAB International, Oxford, UK, pp. 201–212. https://doi.org/10.1079/9780851996936.0201

Harper, J.L., 1977. Population biology of plants. Academic Press, London, UK.

Hubbell, S.P., Foster, R.B., 1983. Diversity of canopy trees in a neotropical forest and implications for conservation., in: Whitmore, T.C., Chadwick, A.C., Sutton, S.L. (Eds.), Tropical Rain Forest: Ecology and Management. Blackwell Scientific Publications, Oxford., pp. 24–41.

Hynynen, J., Ojansuu, R., 2003. Impact of plot size on individual-tree competition measures for growth and yield simulators. Can. J. For. Res. 33, 455–465. https://doi.org/10.1139/x02-173

Leak, B., 1965. The J-shaped Probability Distribution. For. Sci. 11, 405–409.

Mandelbrot, B.B., 1990. The fractal geometry of nature. W.H. Freeman, New York.

Reed, W.J., Hughes, B.D., 2002. From gene families and genera to incomes and internet file sizes: Why power laws are so common in nature. Phys. Rev. E 66, 4. https://doi.org/10.1103/PhysRevE.66.067103

Reynolds, J.H., David Ford, E., 2005. Improving competition representation in theoretical models of self-thinning: A critical review. J. Ecol. 93, 362–372. https://doi.org/10.1111/j.1365-2745.2005.00976.x

Reynolds, J.H., Ford, E.D., 2005. Improving competition representation in theoretical models of self-thinning : a critical review. J. Ecol. 93, 362–372. https://doi.org/10.1111/j.1365-2745.2005.00976.x

Silvertown, J., Charlesworth, D., 2001. Introduction to plant population biology, 4th editio. ed. Blackwell Science, Oxford, UK.

Solow, A.R., 2005. Power law without complexity. Ecol. l 8, 361–363.

Turner, M.D., Deborah, R., 1983. Factors Affecting Frequency Distributions of Plant Mass : The Absence of Dominance and Suppression in Competing Monocultures of Festuca Paradoxa. Ecology 64, 469–475.

Weiner, J., 1986. How Competition for Light and Nutrients Affects Size Variability in Ipomoea Tricolor Populations. Ecology 67, 1425–1427.

Weiner, J., Solbrig, O.T., 1984. The meaning and measurement of size hierarchies in plant populations. Oecologia 61, 334–336. https://doi.org/10.1007/BF00379630

Yoda, K., Kira, T., Ogawa, H., Hozumi, K., 1963. Self-thinning in overcrowded pure stands under cultivated and natural conditions. J. Biol. Osaka City Univ. 14, 107–129.

Chapter three: Derivative curves of tree height-diameter models reveal different growth patterns of tree species

3.1 Abstract - Models describing the relationship between tree height and tree diameter are fundamental to forest management. They answer the question of what the height is for given a tree size. However, the accumulative form does not answer the question of what the height incremental rate is relative to tree size. This rate is more informative for describing the trajectory of tree growth and is critical for silvicultural practices and forest management planning. To address this question, I modeled height-diameter relationships for seven major forest tree species of Alberta, Canada. I then analyzed and compared the accumulative models and their derivatives of the best fitted height-diameter models for each of the seven species. The results showed that the best-fitting models for each of the seven species are of the same form: $ht = 1.3 + e^{a+bx^c}$. Although this model showed similar height-diameter shapes across species, their derivatives revealed drastically different growth patterns of species. Species with different life-histories (e.g. shade-tolerant versus shade-intolerant species or coniferous species versus deciduous species) had very different growth patterns. This study suggests that it is necessary to examine the derivative form of the tree height-diameter models for better understanding growth patterns and the biology responsible for the patterns.

3.2 Introduction

Tree size (typically measured by tree diameter at the breast height, DBH) and tree height are two basic quantities in forestry. Because tree diameter is easier to measure than tree height in the field, the latter is commonly predicted from allometric relationships between the two (Assmann 1970, Pretzsch 2009). These relationships are essential for assessing stand structure and productivity (Homeier et al. 2010), estimating volume, biomass (Segura & Kanninen 2005, Colgan et al. 2013) and carbon (Chave et al. 2005), predicting stand growth dynamics (Pretzsch et al. 2014), and calibrating remote sensing data (Tomppo et al. 2008, Kunneke et al. 2014). Inaccurate estimation of height will bias timber volume prediction, biomass, and carbon estimation, thus potentially compromising forest management planning. It is therefore important to select adequate height-diameter models for species of different growth patterns.

Many tree height-size equations have been proposed in the literature (Curtis 1967, Wykoff et al. 1982, Farr et al. 1989, Peng et al. 2001, Calama & Montero 2004). Most of them are statistical models selected from goodness-of-fit to field measurements of height and diameter. For example, in boreal forest of Alberta, Canada, height-DBH models have been developed and applied to guide silvicultural practice and estimate forest biomass (Huang et al. 1992, Huang & Titus 1999, Huang et al. 2000). Although these models have very different mathematical forms and species are different in their strategies of growth (e.g., deciduous species such as aspen and coniferous species such as white spruce) (Huang et al. 1992, Sharma & Parton 2007, Rijal et al. 2012), their height-DBH relationships appear to be similar (Figure 3.1a). However, the derivatives of their statistical models could have starkly different shapes (Figure 3.1b). This raises questions why the derivative curves are so different among species, what they may reveal about tree growth patterns of different species, and can the cumulative height-DBH

relationships and their derivatives be related to species' biology and ecology? For example, early successional species are intolerance to shade (Henry & Aarssen 1997). The optimal early growth strategy is therefore to allocate more energy to attain their maximum height to overcome shade (Boojh & Ramakrishnan 1982). Thus, early successional species should grow fast initially and invest to height growth at the expense of girth growth, resulting in slim, tall trees. In contrast, late successional tree species are shade-tolerant, and could sustain slow growth when young and grow chunky. Although height-DBH models all have similar shapes, these differences in growth between shade-intolerant and tolerant species could be reveal by derivative curves, as illustrated in Figure 3.1.

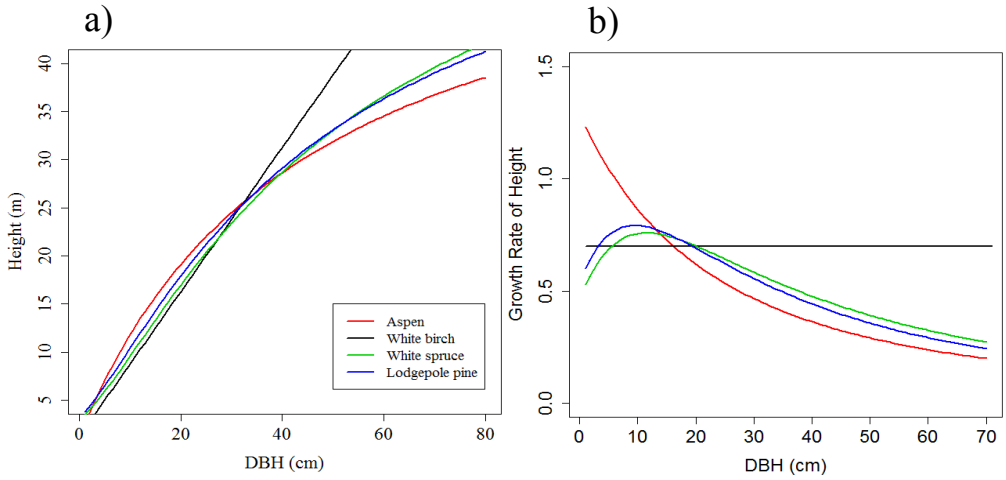

Figure 3.1 (a) The height-DBH models for species aspen (*Populus tremuloides*), white birch (*Betula papyrifera*), white spruce (*Picea glauca*), and lodgepole pine (*Pinus contorta*) and they all have very similar shapes from this study. The black linear line is for hypothetical species. (b) The derivative curves of the height-DBH models. The derivatives of height-DBH models could produce very different curves, varying from a constant (in black for a hypothetical species), decreasing (red) or even symmetrical (blue and green) height incremental rates with respective to DBH.

In this study, I analyzed tree height-DBH mathematical models by asking: what is the increment in height growth given one unit of diameter increment at a given size? To answer this question, I take derivative of the height-DBH models. The derivatives of the best fitting height-DBH models allow for the comparison in the rate of height change as a function of diameter among species. The derivative curves could be informative of understanding the difference in height growth pattern among species that would otherwise be very similar in their cumulative height-DBH mathematical models. I am particularly interested in knowing whether species of similar life history strategies (e.g., shade-tolerant species vs shade-intolerant species or coniferous species vs broadleaved deciduous species) may share similar growth patterns.

I compiled a large set of tree height and DBH data from forest inventory plots in Alberta, Canada to model and compare height-DBH models and their derivative forms for seven major tree species (aspen, white spruce, lodgepole pine, balsam poplar, black spruce, balsam fir and white birch). My objectives were to: (1) select the best height-DBH models for each of the seven tree species, (2) analyze the derivatives of the best-fitted models to reveal the difference in growth patterns of the seven study species that are otherwise not obvious in the cumulative height-DBH equations, and (3) determine whether the growth patterns revealed by the derivatives are associated with the life history traits of species.

3.3 Materials and methods

3.3.1 Study area and data

The study was conducted in boreal forests of Alberta, Canada, with latitude ranging from 49.00-° N to 59.70-°N and longitude from -119.65-°W to -115.05-°W (Appendix A). The study area contains three major natural regions of Alberta (Boreal Forest Natural Region, Rocky Mountain

Natural Region, and Foothills Natural Region). The climate in the study area is cold in the winter following with short summer. Mean annual temperature ranges from +0.5°C to -0.5°C, and average annual precipitation ranges from 480 mm to 800 mm (Natural Regions Committee 2006).

Data used in this study were based on permanent (inventory) sampling plots (PSPs) from Alberta Environments and Parks, which are established by the Government of Alberta and forest industries starting in the 1960s to monitor stand dynamics and effect of different management practices on growth and yield (Forest Management Branch 2005). The spatial location, elevation, slope, aspect and other attributes of plots were recorded at the time of establishment of each PSP. The plot size varies from 400 to 8,000 m^2 and elevation of the PSPs ranges from 245 to 2,065 m. Trees with DBH $\geq$ 9cm within each plot were tagged, identified to species, recorded at the time of establishment and remeasured at average 5 years interval (ranges from 2 years to 15 years). The earliest plots were established in 1960. In this study, I included PSPs up to 2009. I excluded PSPs and trees from analysis that met the following conditions: (1) PSPs that had major disturbances, e.g., fires and mistletoe infestation, (2) trees that had dead top or dieback, multiple leaders, broken top, standing dead, pronounced crook. A total of 57,772 individual living trees belonging to seven major tree species (Table 3.1) were finally compiled from 572 PSPs for this study.

Table 3.1 Seven of Alberta's major tree species name, code and number of individual trees.

Common name	Scientific name	Code	Individual #trees	Total #of measures
Aspen	*Populus tremuloides*	AW	6233	9408
White birch	*Betula papyrifera*	BW	489	652
Balsam poplar	*Populus balsamifera*	PB	1746	2669
White spruce	*Picea glauca*	SW	19225	31356
Black spruce	*Picea mariana*	SB	6313	9549
Lodgepole pine	*Pinus contorta*	PL	20082	32014
Balsam fir	*Abies balsamea*	FB	3684	5449

3.3.2 Fitting the best height-DBH models

A large number of mathematical models have been proposed to model tree height-DBH relationships. Specifically, Huang et al. (1992) compared 20 nonlinear height-DBH models for tree species in Alberta (Table 3.2; only 19 models are included in Table 3.2 because two of the models in Huang et al. 1992 are basically the same model with a slightly different mathematical expression). It is a very complete list of tree height-DBH models, including power type, exponential type, and quadratic type. Although Huang et al.'s (1992) data and ours cover similar study areas, many more data have been collected since 1992. As such, my data set is about for times larger than the data used in Huang et al. (1992) and has a much higher spatial coverage density of plots. With this larger data, there is no guarantee that the best models selected in Huang et al. (1992) remain the best. I therefore remodeled the height-DBH equations shown in Table 3.2 to test if the "best" models in Huang et al. (1992) would change for the larger data for each of the seven species. I followed Huang et al.'s (1992) approach of non-linear least square to

fit each of the models listed in Table 3.2. Because the data I complied include trees within a same plot and measured multiple times (repeated measurements), I thus also used mixed-effect models to control clustering effects of the remeasurement over the years and the similar growth condition within a plot. I treated "plot"/"tree" as a random effect and estimated each height-DBH model using nonlinear mixed effect models. There are several ways to incorporate the random effects by considering one or more of the parameters in each model shown in Table 3.2 as a random term. I tried all of the possible ways of setting up the random effect term (by adding random effect to each parameter each time) and selected the best model for each species. Pseudo-R^2, root mean square error (RMSE) and Akaike's information criterion (AIC) were used to compare the performance of the non-linear least square height-DBH models and non-linear mixed-effect height-DBH models for each species. I used the reported model parameters of Huang et al. (1992) as my initial parameter values. I then plotted the derivative curves of the best selected models to compare the growth pattern of the seven species and attempted to associate the different growth patterns with known ecology of the species.

R statistical computing and graphics language (https://www.r-project.org/) and R package "nls" and "nlme" programs (Bates & Watts 1988, Pinheiro et al. 2020) were used for modelling analyses in this study.

Table 3.2 19 height-DBH mathematical models from Huang et al. (1992). These models are used in this study to fit height-DBH data for the 7 tree species to select the best model for each of them. *a, b* and *c* are model parameters, 1.3 is tree girth height at which tree diameter was measured. *x* represents DBH.

Model number	DBH-height models	Derivative equations
1	$ht = 1.3 + ax^b$	abx^{b-1}
2	$ht = 1.3 + e^{a+b/(x+1)}$	$-be^{a+b/(x+1)}/(x+1)^2$
3	$ht = 1.3 + ax/(b+x)$	$ab/(b+x)^2$
4	$ht = 1.3 + a(1-e^{-bx})$	abe^{-bx}
5	$ht = 1.3 + x^2/(a+bx)^2$	$2ax/(a+bx)^3$
6	$ht = 1.3 + ae^{b/x}$	$-abe^{b/x}/x^2$
7	$ht = 1.3 + ax/(x+1) + bx$	$a/(x+1)^2 + b$
8	$ht = 1.3 + a(x/(1+x))^b$	$abx^{b-1}/(1+x)^2$
9	$ht = 1.3 + e^{a+bx^c}$	$bcx^{c-1}e^{a+bx^c}$
10	$ht = 1.3 + a/(1+be^{-cx})$	$abce^{-cx}/(b+e^{-cx})^2$
11	$ht = 1.3 + a(1-e^{-bx})^c$	$abce^{-bx}(1-e^{-bx})^{c-1}$
12	$ht = 1.3 + a(1-e^{-bx^c})$	$abcx^{c-1}e^{-bx^{c-1}}$
13	$ht = 1.3 + ae^{-be^{-cx}}$	$-abce^{-be^{-cx}-cx}$
14	$ht = \{1.3^b + (c^b - 1.3^b)[1 - e^{-ax}]/[1-e^{-100a}]\}^{1/b}$	$a/b[1.3^b + (c^b - 1.3^b)(1-e^{-ax})/(1-e^{-100a})]^{1/b}(c^b - 1.3^b)e^{-ax}/(1-e^{-100a})$
15	$ht = 1.3 + x^2/(a+bx+cx^2)$	$x(2a+bx)/(a+bx+cx^2)^2$
16	$ht = 1.3 + ax^{bx^{-c}}$	$ax^{(bx^{-c}-c-1)}(1-c\log(x))$
17	$ht = 1.3 + ae^{b/(x+c)}$	$-abe^{b/(x+c)}/(x+c)^2$
18	$ht = 1.3 + a/(1+x^{-c}/b)$	$abcx^{c-1}/(1+bx^c)^2$
19	$ht = 1.3 + a(1-be^{-cx})^d$	$abcde^{-cx}(1-be^{-cx})^{d-1}$

3.4 Results

Each of the 19 height-DBH models listed in Table 3.2 was fitted to each of the seven study species using nonlinear and nonlinear-mixed modelling approaches, respectively. The results show that nonlinear mixed models outperformed the nonlinear models (Appendix B), and the best models selected in this study are different from those of Huang et al. (1992) (Table 3.3). Model 5 (Loetsch et al. 1973), model 9 (Curtis et al. 1981), model 17 (Ratkowsky 1990) and model 18 (Ratkowsky & Reedy 1986) listed in Table 3.2 were selected as the best models for the seven species. Model 9 is the best fit for deciduous species, aspen and white birch. Model 17 is the best fit for conifer species lodgepole pine and black spruce (Table 3.4, Appendix B). The coefficient of determination (R^2) for Huang et al.'s models ranged from 0.55 to 0.97 with average being 0.76 for my data, while the R^2 of the best models selected from this study ranged from 0.83 to 0.98 with average being 0.93. Also, RMSE of my best models were smaller then RMSE of Huang et al.'s best models (Table 3.3). Figure 3.2 shows my models fit the data better than the Huang et al. best models, particularly for species white spruce, lodgepole pine and balsam fir.

For comparison, I plotted the best fitted height-DBH models in Figure 3.2 together in Figure 3.3a, and they all show similar shapes across species, with little chance to distinguish them. However, the derivative of the models shows very different shapes across species. In particular, the derivatives show deciduous and coniferous species have different growth patterns (Figure 3.3b). The height growth with respective to DBH growth for deciduous species is the highest at smaller DBH than that for conifers (Figure 3.4, Table 3.5). Deciduous species have higher maximum height growth with respective to DBH than conifers but that trend reverses at large DBH (Figure 3.3b, Table 3.5).

Table 3.3. The best fit height-DBH models of this study and Huang et al. (1992), Coefficient of determination of the best models of this study and Huang et al. (1992), Root mean square error of the best fitted models of this study and Huang et al. (1992). *a*, *b* and *c* are model parameters, 1.3 is tree girth height at which tree diameter was measured.

Species	Best models of this study	Best models of Huang et al. (1992)	R^2 of best models	R^2 of Huang et al. (1992) best models	RMSE of best models	RMSE of Huang et al. (1992) best models
Aspen	$ht = 1.3 + e^{a+bx^c}$	$ht = 1.3 + a(1 - e^{-bx^c})$	0.96	0.76	0.95	2.44
White birch	$ht = 1.3 + e^{a+bx^c}$	$ht = 1.3 + ax/(b + x)$	0.91	0.55	0.96	2.13
Balsam poplar	$ht = 1.3 + x^2/(a + bx)^2$	$ht = 1.3 + a(1 - e^{-bx})$	0.97	0.77	0.89	2.38
White spruce	$ht = 1.3 + a/(1 + (x^{-c}/b)$	$ht = 1.3 + a(1 - e^{-bx})^c$	0.90	0.78	2.03	3.02
Black spruce	$ht = 1.3 + ae^{b/(x+c)}$	$ht = 1.3 + e^{a+bx^c}$	0.83	0.97	1.43	2.03
Lodgepole pine	$ht = 1.3 + ae^{b/(x+c)}$	$ht = 1.3 + x^2/(a + bx + cx^2)$	0.98	0.69	0.64	2.58
Balsam fir	$ht = 1.3 + x^2/(a + bx)^2$	$ht = 1.3 + a/(1 + (x^{-c}/b)$	0.98	0.79	0.62	2.30

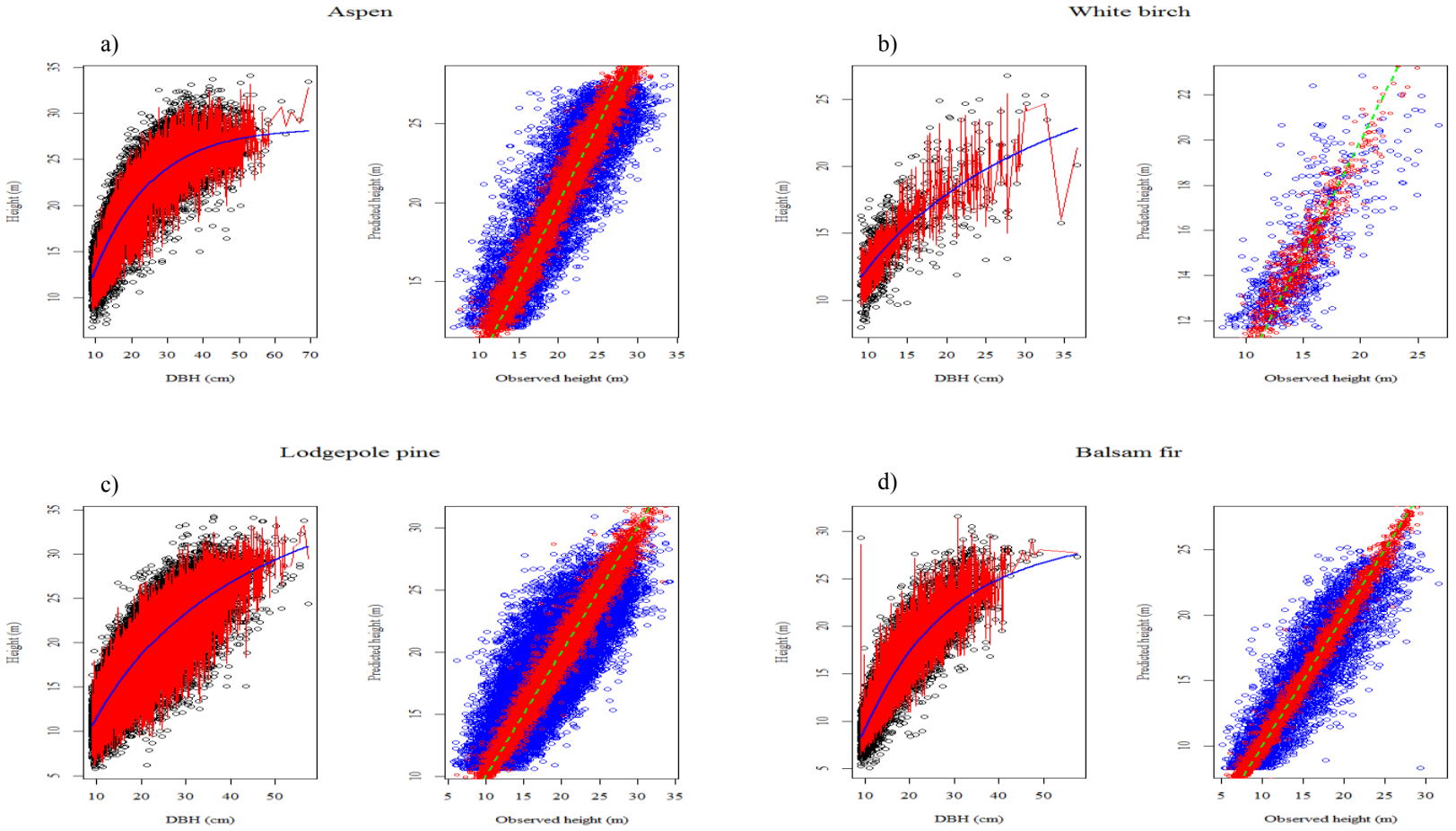

Figure 3.2 Graphs on the left panels show how well selected best model of our (red line) and Huang et al. (1992) (blue line) fits the observed data for species: (a) aspen, (b) white birch, (c) lodgepole pine, (d) balsam fir. Graphs on the right panels show observed versus predicted height for our best models (red points) and Huang et al best models (blue points) for species: (a) aspen, (b) white birch, (c) lodgepole pine, (d) balsam fir.

Table 3.4 The best fit height-DBH models, their derivative equations and estimated parameters for equations. *a*, *b* and *c* are model parameters, 1.3 is tree girth height at which tree diameter was measured.

Species common name	Best fit model	Derivative equation	*a*	*b*	*c*
Aspen	$ht = 1.3 + e^{a+bx^c}$	$bcx^{c-1}e^{a+bx^c}$	3.603	-5.778	-0.710
White birch	$ht = 1.3 + e^{a+bx^c}$	$bcx^{c-1}e^{a+bx^c}$	3.364	-5.587	-0.757
Balsam poplar	$ht = 1.3 + x^2/(a+bx)^2$	$2ax/(a+bx)^3$	1.388	0.169	
White spruce	$ht = 1.3 + a/(1+x^{-c}/b)$	$abcx^{c-1}/(1+bx^c)^2$	41.176	0.013	1.334
Black spruce	$ht = 1.3 + ae^{b/(x+c)}$	$abe^{b/(x+c)}/(x+c)^2$	63.028	-49.978	14.887
Lodgepole pine	$ht = 1.3 + ae^{b/(x+c)}$	$abe^{b/(x+c)}/(x+c)^2$	64.136	-43.823	12.484
Balsam fir	$ht = 1.3 + x^2/(a+bx)^2$	$2ax/(a+bx)^3$	2.116	0.146	

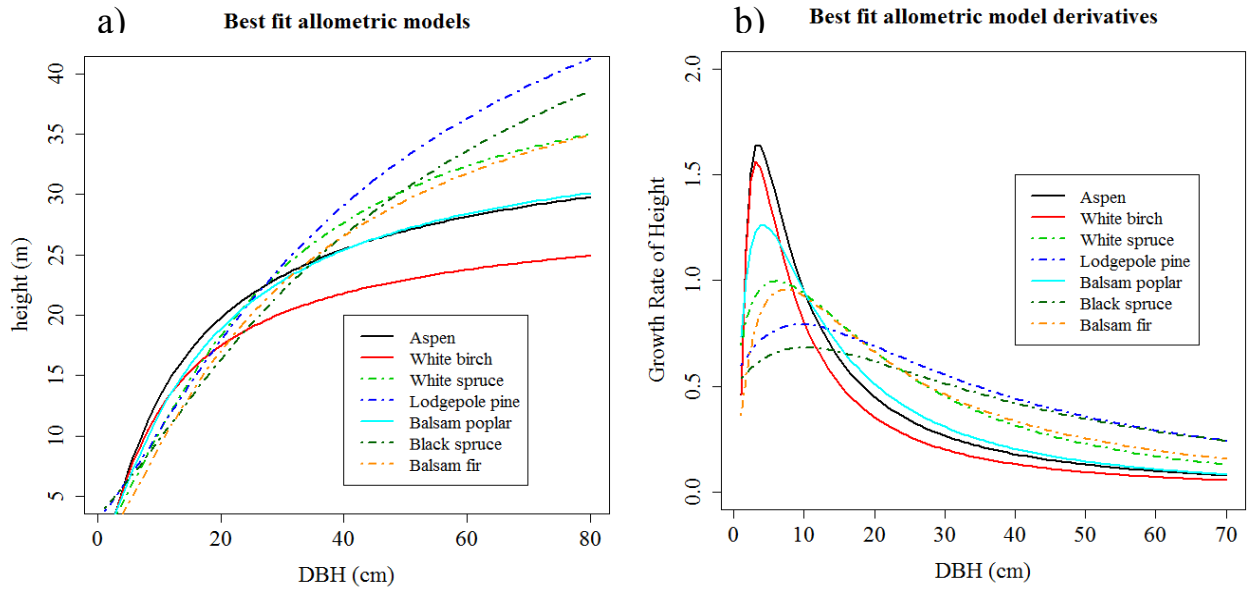

Figure 3.3 (a) Graphs on the left panel are the selected best fit model shapes for seven major tree species of Alberta. (b) Graphs on the right panel are derivative curves of selected best fit models.

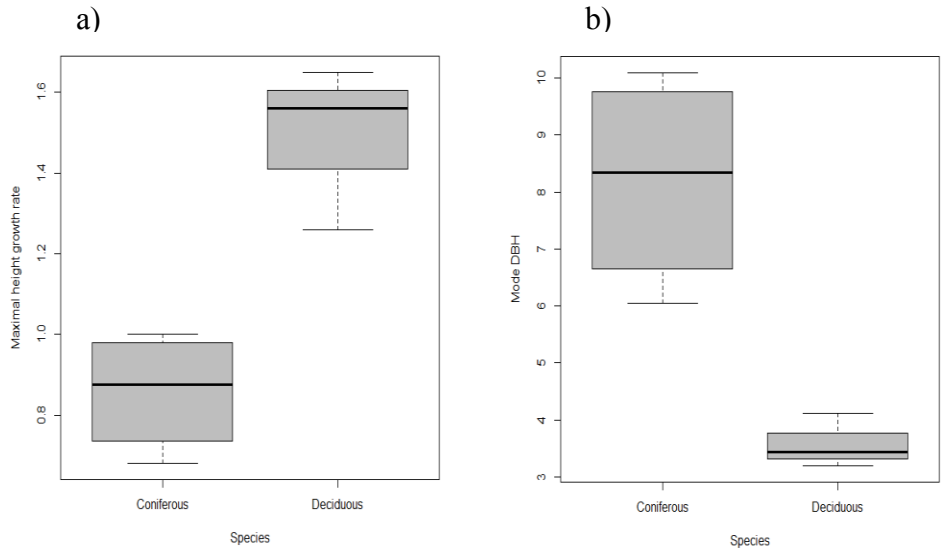

Figure 3.4 (a) Boxplot showing the difference in the maximal derivative rates between deciduous and coniferous species as shown in Table 5, and (b) the mode DBH at which the maximal derivative is obtained.

Table 3.5 Maximum height growth rate at a given DBH and diameter at which have maximum derivative.

Species	Max. derivative	dbh at max. derivative
Aspen	1.65	3.43
White birch	1.56	3.19
Balsam poplar	1.26	4.11
White spruce	1.00	6.04
Black spruce	0.68	10.10
Lodgepole pine	0.79	9.43
Balsam fir	0.96	7.25

3.5 Discussion

Tree height is important for growth and yield modelling, estimating biomass and carbon, quantifying site index and describing structure of forest stands. In this study, over 500 plots of boreal mixed forest were used to evaluate and validate height-DBH models for seven major forest tree species of Alberta. The best height-DBH models selected from this study performed very well (Table 3.3; Figure 3.2) and improved those models developed in previous study (Huang et al. 1992). These improvements are likely due to that much larger dataset and the nonlinear mixed-effect modeling were used in this study. The later controlled the variation in tree height-DBH relationships within sampling plots and also took account the repeated measurements. The mixed-effect modeling is a necessary approach to handle the influence of habitat conditions on tree size and height growth within each plot and the variation in individual growth.

This study shows that, if height-DBH models were modeled by non-linear least squares approach, Chapman-Richard (model 11) and modified Chapman-Richard (model 19) models overall described height-DBH relationship better than other models (Appendix B). These findings were consistent with previous studies (Chai et al. 2018, Kalbi et al. 2018, and Tsega et al. 2018). If non-linear mixed-effects were considered, model 15 (known as Curtis or Prodan model in the literature) stood out as a strong candidate for all species (Appendix B). I therefore recommend that three-parameter nonlinear mixed effect models should be used for modeling height-diameter data for tree species of Alberta.

The derivatives of the height-DBH models describe height growth increment given one unit increment in diameter at a given diameter. These derivative curves reveal the growth patterns of tree height-DBH relationships that are otherwise not obvious with the height-DBH models. These patterns are more informative for understanding the height-DBH relationship and for making silvicultural planning. In this study, the derivatives of the best tree height-DBH models showed deciduous and coniferous species had very different growth patterns, with deciduous having higher height incremental rate at small diameter but lower at large diameter than coniferous (Figure 3.4). It is interesting to observe that the deciduous in this study (aspen, white birch and balsam poplar) are early successional species and intolerant to shading. The growth patterns revealed by the derivatives reflect the nature of shade-intolerant pioneering species that generally grow fast before the closure of stand canopy (Archibold 1995). In contrast, the conifers (black spruce, white spruce, lodgepole pine and balsam fir) are shade-tolerant late successional species. They showed lower height incremental rate at smaller diameter but higher incremental rate at large diameter than deciduous (Fig. 3 and 4). This association of growth patterns with species' life history traits was only obvious with the derivative curves of the

height-DBH relationships. As far as I am aware, there have been no studies to associate height-DBH relationships with the biology of study species (e.g. conifers vs deciduous) for the saplings and mature trees. I suggest it be necessary to analyze derivative of height-diameter models for better understanding tree growth patterns and their association with the life history traits of species in future.

3.6 References

Archibold OW (1995). Ecology of World Vegetation. Springer Netherlands, pp. 510 pp.

Assmann E (1970). Section D - Structure, Increment and Yield of Stands in Relation To Silvicultural Treatment. The Principles of Forest Yield Study. 207–433. - doi: 10.1016/b978-0-08-006658-5.50008-x

Bates DM, Watts DG (1988). Nonlinear regression analysis and its applications. Wiley.

Boojh R, Ramakrishnan PS (1982). Growth strategy of trees related to successional status II. Leaf dynamics. Forest Ecology and Management. 4: 375–386. - doi: 10.1016/0378-1127(82)90036-6

Calama R, Montero G (2004). Interregional nonlinear height-diameter model with random coefficients for stone pine in Spain. Canadian Journal of Forest Research. 34: 150–163. - doi: 10.1139/x03-199

Chai Z, Tan W, Li Y, Yan L, Yuan H, Li Z (2018). Generalized nonlinear height-diameter models for a Cryptomeria fortunei plantation in the Pingba region of Guizhou Province, China. Web Ecology. 18: 29–35. - doi: 10.5194/we-18-29-2018

Chave J, Andalo C, Brown S, Cairns MA, Chambers JQ, Eamus D, Fölster H, Fromard F, Higuchi N, Kira T, Lescure JP, Nelson BW, Ogawa H, Puig H, Riéra B, Yamakura T (2005). Tree allometry and improved estimation of carbon stocks and balance in tropical forests. Oecologia. 145: 87–99. - doi: 10.1007/s00442-005-0100-x

Colgan MS, Asner GP, Swemmer T (2013). Harvesting tree biomass at the stand level to assess the accuracy of field and airborne biomass estimation in savannas. Ecological Applications. 23: 1170–1184. - doi: 10.1890/12-0922.1

Curtis RO (1967). Height-Diameter and Height-Diameter-Age Equations For Second-Growth

Douglas-Fir. Science. 13: 365–375.

Curtis RO, Clendenen GW, DeMars DJ (1981). A new stand simulator for coast Douglas-fir: DFSIM user's guide. US Department of Agriculture, Forest Service, General Technical Report, pp. 79.

Farr WA, DeMars DJ, Dealy JE (1989). Height and crown width related to diameter for open-grown western hemlock and Sitka spruce. Canadian Journal of Forest Research. 19: 1203–1207. - doi: 10.1139/x89-181

Forest Management Branch (2005). Permanent sample plot (PSP) field procedures manual. Public Lands and Forests Division, Alberta Sustainable Resource Development. Retrieved from https://open.alberta.ca/dataset/ef9eee08-d868-4444-8851-9dab36631a75/resource/5eff457b-330e-40e5-8825-9ed0e8820958/download/2005-permanent-sample-plot-psp-field-procedure-manual-march-2005.pdf

Henry HAL, Aarssen LW (1997). On the Relationship between Shade Tolerance and Shade Avoidance Strategies in Woodland Plants. Oikos. 80: 575–582.

Homeier J, Siegmar WB, Sven G, Rütger TR, Christoph L (2010). Tree diversity, forest structure and productivity along altitudinal and topographical gradients in a species-rich ecuadorian montane rain forest. Biotropica. 42: 140–148. Retrieved from http://dx.doi.org/10.1111/j.1744-7429.2009.00547.x

Huang S, Price D, Titus SJ (2000). Development of ecoregion-based height-diameter models for white spruce in boreal forests. Forest Ecology and Management. 129: 125–141. - doi: 10.1016/S0378-1127(99)00151-6

Huang S, Titus SJ (1999). An individual tree height increment model for mixed white spruce–aspen stands in Alberta, Canada. Forest Ecology and Management. 123: 41–53. - doi:

10.1016/S0378-1127(99)00015-8

Huang S, Titus SJ, Wiens DP (1992). Comparison of nonlinear height-diameter functions for major Alberta tree species. Canadian Journal of Forest Research. 22: 1297–1304.

Kalbi S, Fallah A, Bettinger P, Shataee S, Yousefpour R (2018). Mixed-effects modeling for tree height prediction models of Oriental beech in the Hyrcanian forests. Journal of Forestry Research. 29: 1195–1204. - doi: 10.1007/s11676-017-0551-z

Kunneke A, Aardt J van, Roberts W, Seifert T (2014). Bioenergy from Wood. (T. Seifert, Ed.). Springer Netherlands, Dordrecht, Vol. 26, pp. 11–41. - doi: 10.1007/978-94-007-7448-3

Loetsch F, Zöhrer F, Haller KE (1973). Forest inventory. BLV, Verlagsgesellschaft mbH, München, Germany, pp. Vol II.

Natural Regions Committee (2006). Natural regions and subregions of Alberta. Natural regions and subregions of Alberta : Natural Regions Committee /. https://doi.org/10.5962/bhl.title.115367

Peng C, Zhang L, Liu J (2001). Developing and validating nonlinear height-diameter models for major tree species of Ontario's boreal forests. Northern Journal of Applied Forestry. 18: 87–94. - doi: 10.1093/njaf/18.3.87

Pinheiro J, Bates D, DebRoy S, Sarkar D, R Core Team (2020). nlme: Linear and Nonlinear Mixed Effects Models. R package version 3.1-147. Retrieved from https://cran.r-project.org/package=nlme

Pretzsch H (2009). Forest dynamics, growth and yield: Chapter 6 standard analysis of long-term experimental plots. Forest Dynamics, Growth and Yield. Springer Berlin Heidelberg, pp. 423–491. - doi: 10.1007/978-3-540-88307-4

Pretzsch H, Biber P, Schütze G, Uhl E, Rötzer T (2014). Forest stand growth dynamics in

Central Europe have accelerated since 1870. Nature Communications. 5: 1–10. - doi: 10.1038/ncomms5967

Ratkowsky DA (1990). Handbook of Nonlinear Regression Models. Marcel Dekker, Inc., New York. - doi: 10.2307/2347928

Ratkowsky DA, Reedy TJ (1986). Choosing Near-Linear Parameters in the Four-Parameter Logistic Model for Radioligand and Related Assays. International Biometric Society. 42: 575–582.

Rijal B, Weiskittel AR, Kershaw JA (2012). Development of regional height to diameter equations for 15 tree species in the North American Acadian Region. Forestry. 85: 379–390. - doi: 10.1093/forestry/cps036

Segura M, Kanninen M (2005). Allometric Models for Tree Volume and Total Aboveground Biomass in a Tropical Humid Forest in Costa Rica. Biotropica. 37: 2–8. - doi: 10.1111/j.1744-7429.2005.02027.x

Sharma M, Parton J (2007). Height-diameter equations for boreal tree species in Ontario using a mixed-effects modeling approach. Forest Ecology and Management. 249: 187–198. - doi: 10.1016/j.foreco.2007.05.006

Tomppo E, Olsson H, Ståhl G, Nilsson M, Hagner O, Katila M (2008). Combining national forest inventory field plots and remote sensing data for forest databases. Remote Sensing of Environment. 112: 1982–1999. - doi: 10.1016/j.rse.2007.03.032

Tsega M, Guadie A, Teffera ZL, Belayneh Y, Niu D (2018). Development and Validation of Height-Diameter Models for Cupressus lusitanica in Gergeda Forest, Ethiopia. Forest Science and Technology. 14: 138–144. - doi: 10.1080/21580103.2018.1482794

Wykoff WR, Crookston NL, Stage AR (1982). User's guide to the stand prognosis model. US

Department of Agriculture, Forest Service, General Technical Report. Ogden, Utah.

Chapter four: Climate-based height-diameter models for major tree species of Alberta, Canada

4.1 Abstract – Tree height-diameter relationships are central to tree growth and yield modelling. They help understand and predict changes in tree growth. However, height-diameter relationships may be subject to climate effects as tree height and diameter growth could be differentially sensitive to change in climate. As such, it is necessary to incorporate climate to model height-diameter relationship. To address this problem, I included a climate moisture index and annual mean daily maximum temperature into the height-diameter models. I found that climate altered tree height growth, e.g. tree grow taller under increasing temperature. I analyzed and compared 400 climate-based height-diameter models for five major forest tree species of Alberta. The result showed that the incorporation of climate moisture index and mean annual temperature increased the accuracy of the height-diameter models by 3% to 7%. My study suggests that including climate factors into the height-DBH models is necessary for better prediction of tree growth.

4.2 Introduction

Boreal forests provide valuable ecological (e.g., habitat for wildlife), economical (e.g., timber and its products), and sociological (e.g., recreational areas) services, and also have an important role in the global carbon cycle and maintaining biodiversity. These systems and the services they provide are threatened by climate change (Price et al., 2013). Thus, it is necessary to project and understand the effects of the climate if forests are to be managed sustainably.

Growth and yield models (GYMs) inform sustainable forest management and are relied on the accurate measurement of tree height and diameter. However, the accurate measure of tree height is often not feasible and is typically estimated from height-diameter relationships (Calama and Montero, 2004; Huang et al., 1992; Peng et al., 2001). The traditional height-DBH models assume tree height is entirely dependent on tree size, or diameter at breast height (DBH). However, it has been found that although tree height is closely related to DBH, other factors such as climate can directly and indirectly affect tree growth (Chen et al., 2016; Sette Jr et al., 2016). These exogenous effects could alter the tree height-DBH relationships. For example, increased temperature can both increase the length of the growing season and decrease water availability and transpiration (Allen et al., 2010; Chen et al., 2005). This will have an effect on tree growth because height is mostly affected by the availability of light (Moles et al., 2009; Pacala et al., 1994) and availability of moisture (Hogg et al., 2005). It is also found that DBH is closely related to water availability (Bullock, 2000; Butt et al., 2014). These climatic effects on tree height and DBH could be species specific (Chhin et al., 2008; Huang et al., 2010; Zhang et al., 2015) as the response of xylem and wood formations to climate could be different for different species (Begum et al., 2018; Granda et al., 2018; Olson et al., 2018). These suggest the necessity to

extend the traditional height-DBH models to consider the effects of climate so that to improve the predictability of height-DBH models and hence the GYM models.

Climate impacts on the height-DBH relationship depend not only on species but also on the severity of the change in climate, which differs in different climate zones. It is known that climates at high latitudes will change most (IPCC, 2001; Pepin et al., 2015), suggesting that boreal forest could be heavily affected by climate change (Kramer et al., 2000). This will have serious consequence on 35 million hectares of natural forest in Alberta (https://www.alberta.ca/sustainable-forest-management-statistics.aspx). For example, boreal forests can function as a net carbon source or sink depending on the balance between growth and decomposition rates of the trees. As such, the projected change in climate in the boreal zone can change boreal carbon sink to carbon source (Hadden and Grelle, 2016; Lindroth et al., 1998).

Several height-DBH models have been developed for forest tree species of Alberta (Cortini et al., 2011; Huang et al., 2009, 2000; Huang and Titus, 1994) but these models do not account for the effect of climate change. There is a need to develop practical and reliable tree climate-based height-diameter models for the major tree species of Alberta for quantifying the impact of climate change, thus to improve growth-yield modeling.

In this study, I modeled and compared climate-based height-DBH models for five major tree species of Alberta. My objectives were to: (1) develop climate-based height-DBH models, (2) select the best climate-based height-DBH model for each species, and (3) use the best model to assess the effect of climate on height-DBH relationship for each species.

4.3 Methods

4.3.1 Study area

The study was conducted in the boreal forest of Alberta, Canada (49°-59.7 °N, 119.65-115.05 °W) (Appendix A). The study area included three major natural regions of Alberta, Canada: Boreal Forest Natural Region, Rocky Mountain Natural Region and Foothills Natural Region. The regions have cold winters with following short warm or cool summer. Mean annual temperature varies from +0.5°C in the Boreal and Foothills region to -0.5°C in the Rocky Mountain region (Natural Regions Committee, 2006). Average mean annual precipitation ranges from 480 mm in the Boreal region to 800 mm in the Rocky Mountain region. The Foothills region has moderate annual precipitation that increases with elevation (Natural Regions Committee, 2006).

4.3.2 Data

Permanent sampling plots (PSPs)

The data of the Alberta PSP network were used in this study. The network was established by the government and forestry industries (Forest Management Branch, 2005). They were recensused at average 5-year intervals (varying from 2 to 15 years) by the government and forest industry companies starting the 1960s. More than 2000 PSPs were established throughout the high productive mixedwood forest in Alberta. The spatial location, elevation, slope, aspect, and other attributes of plots were recorded at the time of establishment for each PSP. The plot size varies from 400 to 8,000 m^2 and the elevation of the PSPs ranges from 245 to 2,065 m. All trees within each plot were tagged, identified to species, recorded at the time of establishment. The earliest plots were established in 1960. In this study, I included PSPs up to 2009. I excluded PSPs and

trees from the analyses that met the following conditions: (1) PSPs that had major disturbances, e.g., fires and mistletoe infestation, (2) PSPs that only had one census because data of multiple censes are needed to model the effect of climate, (3) trees that had dead top or dieback, multiple leaders, broken top, standing dead, fork, pronounced crook, severe leaning to eliminate miscalculation of growth, (4) trees with DBH ≤ 9 cm so that to eliminate saplings (9 cm is the DBH cutoff of PSPs but some plot did include smaller stems) effect on growth, and (5) trees that do not have measurement of both diameter and height in all census years. I used the field measurement of diameter and height. A total of 53,599 living stems belonging to five major tree species were compiled and modeled from 554 PSPs (Table 4.1).

Table 4.1 Sample size and the total number of measure records of height and DBH for each of the five study species.

Common name	Scientific name	Code	Number of stems	Total number of measures
Aspen	*Populus tremuloides*	AW	6233	9408
Balsam poplar	*Populus balsamifera*	PB	1746	2669
Lodgepole pine	*Pinus contorta*	PL	20082	32014
Black spruce	*Picea mariana*	SB	6313	9549
White spruce	*Picea glauca*	SW	19225	31356

Climate variables

Climate data for the study region were obtained from the BioSIM software tool (https://cfs.nrcan.gc.ca/projects/133). This tool generates data by simulation models. Simulation models are based on regional air temperature and precipitation, which are interpolated from the nearby weather stations, and adjusted for elevation and location differentials with regional gradients. Based on the latitude and longitude location of PSPs, two climatic variables were obtained: CMI (annual climate moisture index) following the calculation from Hogg (1994) and

Tmax (mean annual daily maximum temperature) for the period of 1959-2010. Appendix D shows minimum and maximum values of CMI and Tmax for the period of 1959-2010 obtained for the PSPs used in this study. There was not significant correlation between CMI and Tmax. CMI and Tmax were derived annually. Since PSPs were measured on average 5 yearly intervals, I recalculated CMI and Tmax for PSP measurement intervals as mean CMI and mean Tmax.

4.3.3 Modelling climate-based height- DBH relationships

To develop climate-based tree height-DBH models, I selected the most widely used tree height-DBH models from the literature (Table 4.2). I added climate factors into these base models in two different ways. First, I added CMI and Tmax into the base models as linear term one at a time to represent the direct effect of climate on tree height. Second, I added CMI and Tmax into the models one at a time as a linear term of model parameters to show climate effects on height growth. Table 4.2 shows the base model and climate-based model forms.

To estimate the models, I fit all the candidate models for each of the five species using nonlinear modelling algorithm. I then used nonlinear mixed-effect models to cope with clustering effect from similar growing environment and repeated measurement of trees. I treated "plot"/"tree" as a random effect. I tried all of the possible ways of setting up the random effect term and selected the best models from all the models for each species. Overall, I tested 184 height-DBH and climate-based height-DBH models for each species. Model comparison and selection criteria were based on Akaike's information criterion (AIC) and mean squared error (MSE). I used the reported model parameters of Huang et al. (1992) or reported model parameters of Chapter 3 as the initial parameter values. I then plotted the derivative curves of the

best fitted models while keeping the diameter at a mean value to see how species react to climate specifically.

All calculations were done with R statistical computing and graphics language (R Core Team, 2019) and model fitting was done with R package “nls” and “nlme” programs (Bates and Watts, 1988; Pinheiro et al., 2020).

Table 4.2 Seven height-DBH and fifty-six climate-based height-DBH candidate models. These models are used in this study to fit height-DBH data of 5 tree species in Alberta to select the best model for each species. *mcmi* is the mean annual climate moisture index, *mtmax* is the mean annual maximum temperature, *a, b, c* and *d* are model parameters, 1.3 is tree girth height at which tree diameter was measured.

Model number	Model form	References	
1	$ht = 1.3 + adbh^b$	(Huang et al., 1992)	
2	$ht = 1.3 + e^{a+b/(dbh+1)}$	(Huang et al., 1992; Kalbi et al., 2018)	
3	$ht = 1.3 + dbh^2/(a + bdbh)^2$	(Huang et al., 1992; Kalbi et al., 2018)	
4	$ht = 1.3 + a(dbh/(1 + dbh))^b$	(Kalbi et al., 2018)	
5	$ht = 1.3 + a(1 - e^{-bdbh})^c$	(Peng et al., 2001; Sharma and Parton, 2007)	
6	$ht = 1.3 + a(1 - e^{-bdbh^c})$	(Huang et al., 1992; Peng et al., 2001; Tsega et al., 2018)	
7	$ht = 1.3 + ae^{-b*e^{-cdbh}}$	(Huang et al., 1992; Hulshof et al., 2015)	
Height-DBH models that incorporate climatic factors			
Model number	Model form	Model number	Model form
8	$ht = 1.3 + adbh^b + dmcmi$	19	$ht = 1.3 + (a + dmcmi) * (1 - e^{-bdbh})^c$
9	$ht = 1.3 + e^{a+b/(dbh+1)} + dmcmi$	20	$ht = 1.3 + (a + dmcmi) * (1 - e^{-bdbh^c})$
10	$ht = 1.3 + dbh^2/(a + bdbh)^2 + dmcmi$	21	$ht = 1.3 + (a + dmcmi) * e^{-b*e^{-cdbh}}$
11	$ht = 1.3 + a(dbh/(1 + dbh))^b + dmcmi$	22	$ht = 1.3 + adbh^{(b+dmcmi)}$
12	$ht = 1.3 + a(1 - e^{-bdbh})^c + dmcmi$	23	$ht = 1.3 + e^{a+(b+dmcmi)/(dbh+1)}$
13	$ht = 1.3 + a(1 - e^{-bdbh^c}) + dmcmi$	24	$ht = 1.3 + dbh^2/(a + (b + dmcmi) * dbh)^2$
14	$ht = 1.3 + ae^{-b*e^{-cdbh}} + dmcmi$	25	$ht = 1.3 + a(dbh/(1 + dbh))^{(b+dmcmi)}$
15	$ht = 1.3 + (a + dmcmi) * dbh^b$	26	$ht = 1.3 + a(1 - e^{-(b+dmcmi)*dbh})^c$
16	$ht = 1.3 + e^{(a+dmcmi)+b/(dbh+1)}$	27	$ht = 1.3 + a(1 - e^{-(b+dmcmi)*dbh^c})$
17	$ht = 1.3 + dbh^2/((a + dmcmi) + bdbh)^2$	28	$ht = 1.3 + ae^{-(b+dmcmi)*e^{-cdbh}}$
18	$ht = 1.3 + (a + dmcmi) * (dbh/(1 + dbh))^b$	29	$ht = 1.3 + a(1 - e^{-bdbh})^{(c+dmcmi)}$

Model number	Model form	Model number	Model form
30	$ht = 1.3 + a(1 - e^{-bdbh^{(c+dmcmi)}})$	44	$ht = 1.3 + (a + dmtmax) * (1 - e^{-bdbh})^c$
31	$ht = 1.3 + ae^{-b*e^{-(c+dmcmi)*dbh}}$	45	$ht = 1.3 + (a + dmtmax) * (1 - e^{-bdbh^c})$
32	$ht = 1.3 + adbh^b + dmtmax$	46	$ht = 1.3 + (a + dmtmax) * e^{-b*e^{-cdbh}}$
33	$ht = 1.3 + e^{a+b/(dbh+1)} + dmtmax$	47	$ht = 1.3 + adbh^{(b+dmtmax)}$
34	$ht = 1.3 + dbh^2/(a + bdbh)^2 + dmtmax$	48	$ht = 1.3 + e^{a+(b+dmtmax)/(dbh+1)}$
35	$ht = 1.3 + a(dbh/(1 + dbh))^b + dmtmax$	49	$ht = 1.3 + dbh^2/(a + (b + dmtmax) * dbh)^2$
36	$ht = 1.3 + a(1 - e^{-bdbh})^c + dmtmax$	50	$ht = 1.3 + a(dbh/(1 + dbh))^{(b+dmtmax)}$
37	$ht = 1.3 + a(1 - e^{-bdbh^c}) + dmtmax$	51	$ht = 1.3 + a(1 - e^{-(b+dmtmax)*dbh})^c$
38	$ht = 1.3 + ae^{-b*e^{-cdbh}} + dmtmax$	52	$ht = 1.3 + a(1 - e^{-(b+dmtmax)*dbh^c})$
39	$ht = 1.3 + (a + dmtmax) * dbh^b$	53	$ht = 1.3 + ae^{-(b+dmtmax)*e^{-cdbh}}$
40	$ht = 1.3 + e^{(a+dmtmax)+b/(dbh+1)}$	54	$ht = 1.3 + a(1 - e^{-bdbh})^{(c+dmtmax)}$
41	$ht = 1.3 + dbh^2/((a + dmtmax) + bdbh)^2$	55	$ht = 1.3 + a(1 - e^{-bdbh^{(c+dmtmax)}})$
42	$ht = 1.3 + 10^{(a+dmtmax)} * dbh^b$	56	$ht = 1.3 + ae^{-b*e^{-(c+dmtmax)*dbh}}$
43	$ht = 1.3 + (a + dmtmax) * (dbh/(1 + dbh))^b$		

4.4 Results

Each of the 56 height-DBH models listed in Table 4.2 was fitted to each of the five study species using non-linear least square and non-linear mixed effect models, respectively. The results show that models performed better after a climate variable was added into the models (Appendix C). Climate based model (4) (known as the Curtis model in the literature) and model (7) (known as the Gompertz model in the literature) were the most general models. They both were either the best or the second best model. Climate-based model (7) was the best fit for aspen and white spruce, and climate-based model (4) was the best fit for balsam poplar and black spruce (Table 4.3). For lodgepole pine, the climate-based model (1) was the best fit (Table 4.3). Explained variation differed widely among species (pseudo R^2 ranges for top-ranked models 0.58-0.80) and within species across all candidate models (Appendix C).

The CMI added models increased explained variation by 3% for aspen, balsam poplar, and white spruce, and 7% for lodgepole pine. However, the explained variation was decreased for black spruce when CMI was added into the height-DBH models (Table 4.4, Appendix C). Three of the five species (balsam poplar, lodgepole pine, and white spruce) improved the explained variation (as measured by R^2) by 3%, 7% and 1%, respectively, when annual maximum temperature was added into the models (Table 4.4, Appendix C). However, the explained variation did not change for species aspen and black spruce when Tmax was added into the models. Tmax added model parameters were significant for all species except white spruce, while CMI added model parameters were significant for species aspen, black spruce and white spruce (Table 4.5). All species, except lodgepole pine, showed a similar pattern when fitting the best fit models (Figure 4.1).

Table 4.3 The best fit climate sensitive height-DBH models. *mcmi* is mean climate moisture index for measurement intervals, *mtmax* is mean annual maximum temperature for measurement intervals, *a,b,c* and *d* are model parameters, 1.3 is tree girth height at which tree diameter was measured. Derivative forms represent height growth respect to climate variable change at a given DBH.

Species name		Climate-based height-DBH models	Derivative forms
Aspen	CMI	$ht = 1.3 + ae^{-b*e^{-(c+dmcmi)*dbh}}$	$abddbhe^{b-e^{-dbh(c+dmcmi)}-dbh(c+dmcmi)}$
	Tmax	$ht = 1.3 + ae^{-(b+dmtmax)*e^{-cdbh}}$	$-ade^{-e^{-cdbh}(b+dmtmax)-cdbh}$
Balsam poplar	CMI	$ht = 1.3 + a(dbh/(1+dbh))^{b} + dmcmi$	d
	Tmax	$ht = 1.3 + a(dbh/(1+dbh))^{(b+dmtmax)}$	$a(\frac{dbh}{1+dbh})^{dmtmax+b}\ln(dbh/(1+dbh))d$
Lodgepole pine	CMI	$ht = 1.3 + adbh^{(b+dmcmi)}$	$adlog(dbh)dbh^{b+dmcmi}$
	Tmax	$ht = 1.3 + adbh^{(b+dmtmax)}$	$adlog(dbh)dbh^{b+dmtmax}$
Black spruce	Tmax	$ht = 1.3 + a(dbh/(1+dbh))^{(b+dmtmax)}$	$a(\frac{dbh}{1+dbh})^{dmtmax+b}\ln(dbh/(1+dbh))d$
White spruce	CMI	$ht = 1.3 + a(1-e^{-(b+dmcmi)*dbh^{c}})$	$addbh^{c}e^{-dbh^{c}(b+dmcmi)}$
	Tmax	$ht = 1.3 + ae^{-(b+dmtmax)*e^{-cdbh}}$	$-ade^{-e^{-cdbh}(b+dmtmax)-cdbh}$

Table 4.4 The best fit climate-based models code, their R^2 and their base models R^2.

Species name	The best model		The best model R^2	Models without climate variable	Models without climate variable R^2
Aspen	CMI added	aw7nlscmic	0.70	aw7nls	0.67
	Tmax added	awnlstmaxb	0.67	aw7nls	
Balsam poplar	CMI added	pb4nlmecmirandomb	0.80	pb4nls	0.77
	Tmax added	pb4nlstmaxb	0.80	pb4nls	
Lodgepole pine	CMI added	pl1nlmecmibrandomb	0.59	pl1nls	0.53
	Tmax added	pl1nlstmaxb	0.60	pl1nls	
Black spruce	CMI added	-	-	-	-
	Tmax added	sb4nlstmax	0.69	sb4nls	0.69
White spruce	CMI added	sw6nlscmib	0.77	sw6nls	0.74
	Tmax added	sw7nlstmaxb	0.76	sw7nls	0.75

Table 4.5 Estimated model parameters for climate-based height-DBH models. * indicates significance at confidence level p-value<0.05.

Species Code		*a*	*b*	*c*	*d*
AW	CMI model	26.440*	1.978*	0.095*	-0.0004*
	Tmax model	26.481*	1.724*	0.088*	0.024*
PB	CMI model	32.811	11.067		-0.081
	Tmax model	32.493*	11.173*		0.139*
PL	CMI model	4.049	0.499		-0.001
	Tmax model	2.645*	0.552*		0.009*
SB	CMI model	29.840*	12.830*		
	Tmax model	29.951*	13.599*		-0.085*
SW	CMI model	30.590*	0.016*	1.357*	-0.0002*
	Tmax model	30.240	1.796	0.079	0.012

All species showed higher height growth for given DBH in the initial or middle-range phase when having Tmax in the model (Figures 4.1, 4.2 and 4.3). Lodgepole pine and white spruce would grow taller with higher maximum annual temperature. CMI did not affect height growth of balsam poplar. White spruce and aspen would grow shorter with higher climate moisture index, while lodgepole pine would become somewhat taller (Figures 4.2 and 4.3). There is no association between life histories, e.g., conifer vs deciduous or early successional vs late successional species, and the effect of the climate. Instead, growth rates of all species were affected by climate variables, positively or negatively.

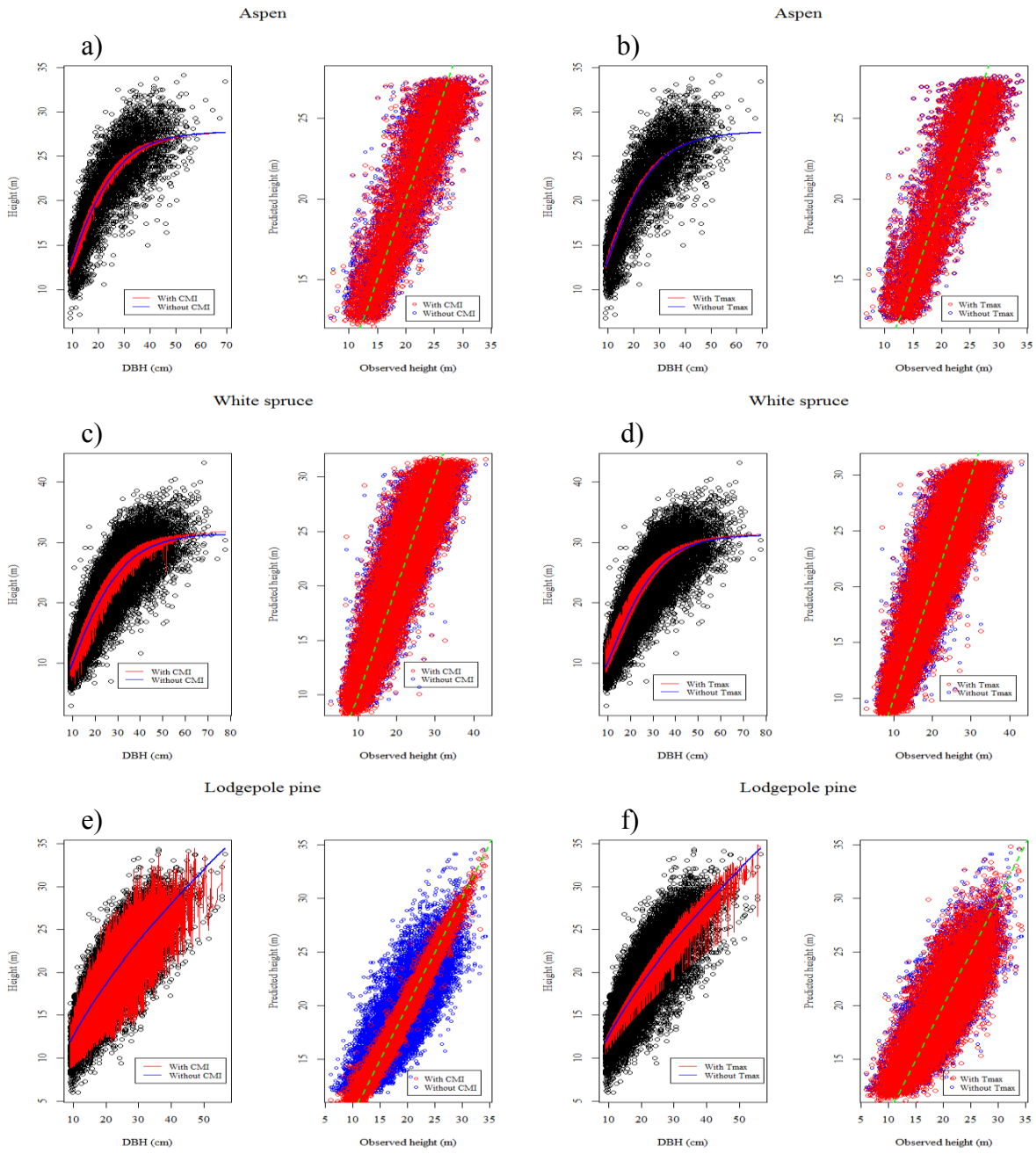

Figure 4.1 The left panel of each graph shows how well the selected best models fit the observed data with climate (red lines) and without climate (blue lines) data into the model for species: (a, b) aspen, (c, d) white spruce, (e, f) lodgepole pine. The right panel of each graph shows observed versus predicted height with climate (red points) and without climate (blue points) for species: (a, b) aspen, (c, d) white spruce, (e, f) lodgepole pine.

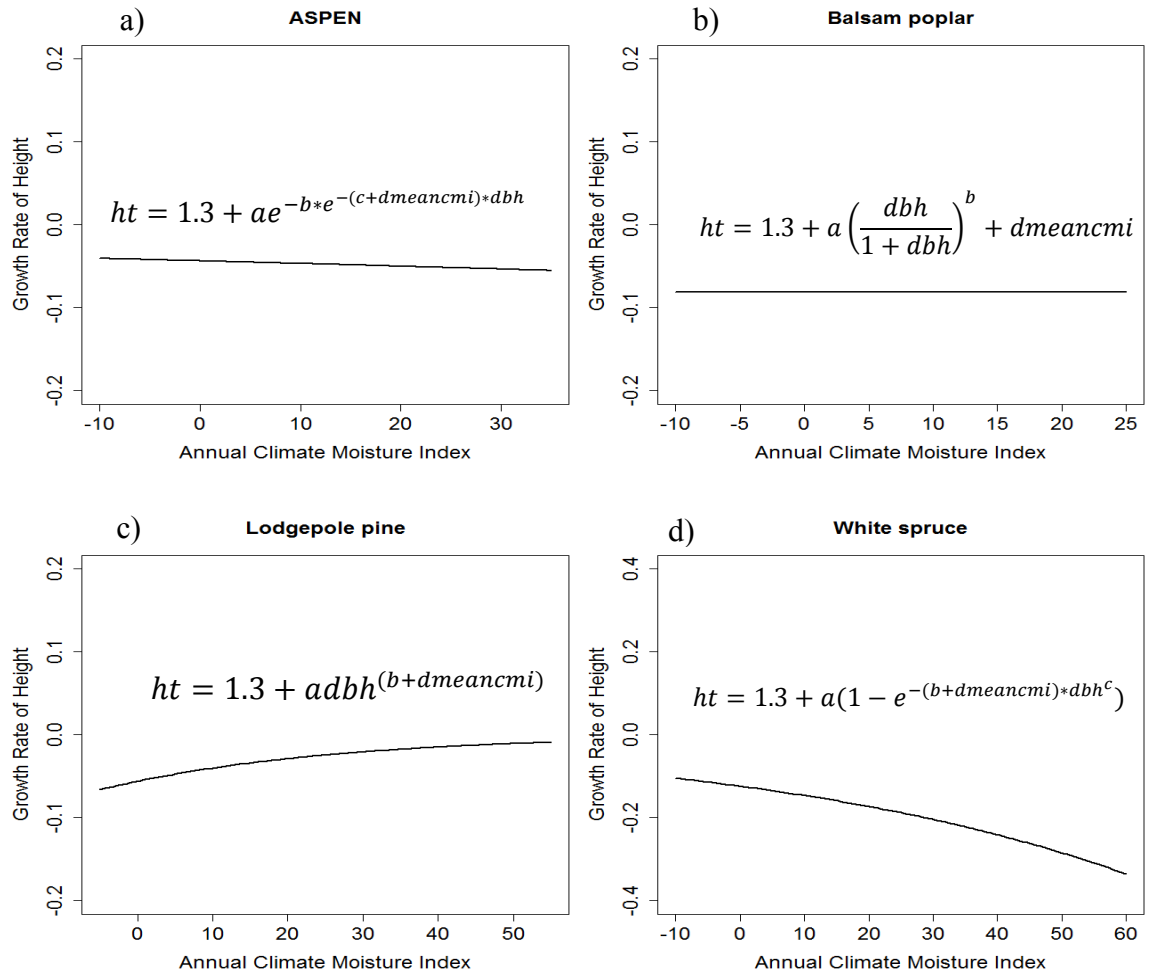

Figure 4.2 Graphs show how the height incremental rate changes with respect to annual climate moisture index at a given DBH for species: (a) aspen, (b) balsam poplar, (c) lodgepole pine, (d) white spruce.

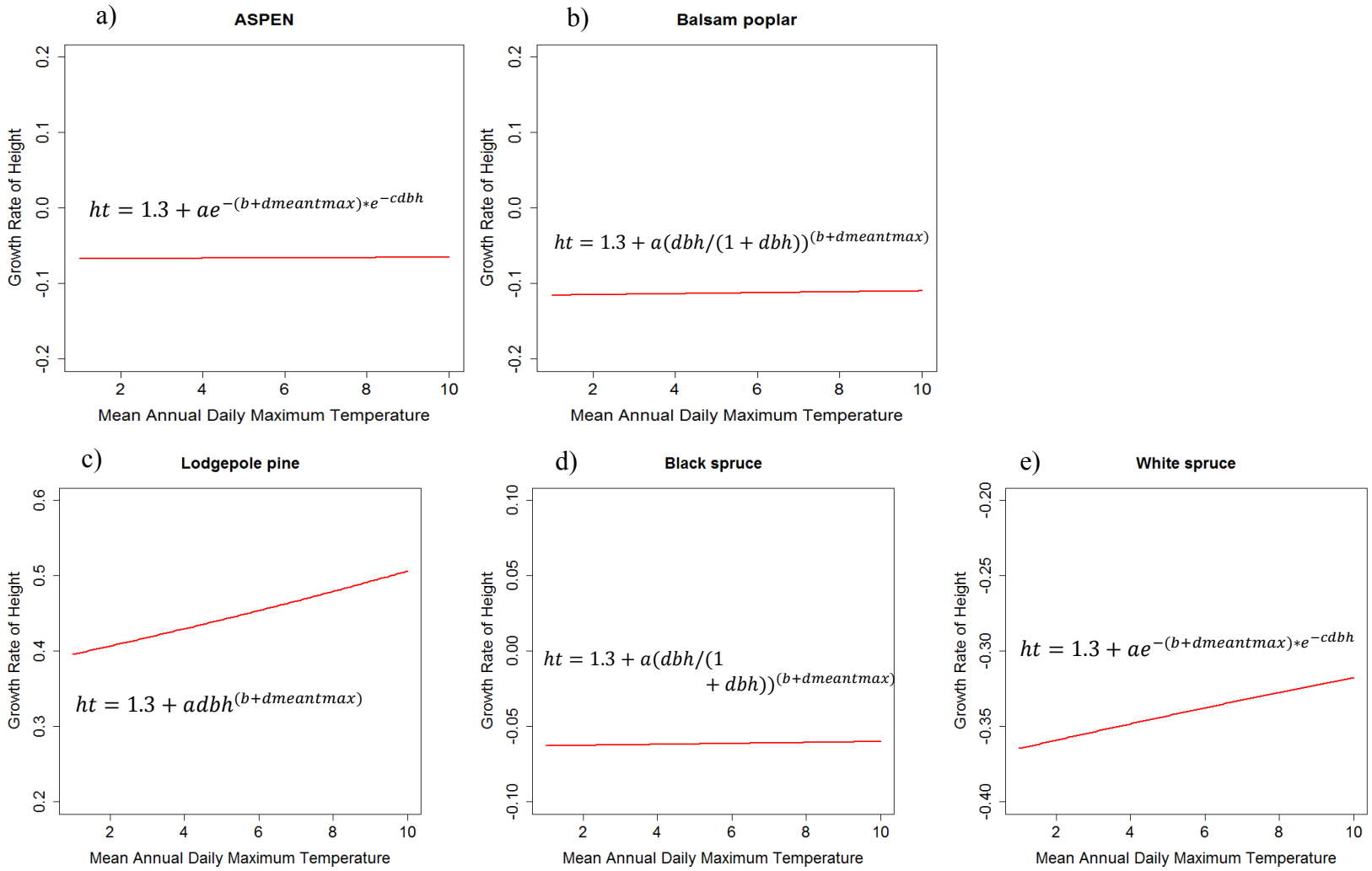

Figure 4.3 Graphs show how the height incremental rate changes with respect to mean annual daily maximum temperature at a given DBH for species: (a) aspen, (b) balsam poplar, (c) lodgepole pine, (d) black spruce, (e) white spruce.

4.5 Discussion

It is necessary to quantify the effect of climate on tree height and size and their relationships for understanding the impact of climate change on forest structure and management. In this study, I analyzed data from over 500 permanent sample plots of Alberta that were established and remeasured over the past 60 years. I examined around 800 climate-based models based on seven non-linear height-DBH models for each of the five major timber species of Alberta. All seven base models have been commonly used to model tree height-DBH relationships (Chai et al., 2018; Huang et al., 1992; Sharma and Parton, 2007). Most of the proposed climate-based models outperformed those traditional height-DBH models in this study as measured by R^2, MSE, and AIC criteria's.

Climate variables were added in the base models linearly or to the parameters of the base models to reflect the direct and indirect impact of climate on tree height (Begum et al., 2018; Yeh and Wensel, 2000). Climate moisture index and mean temperature were used as indicators of climate conditions. These two factors are important to plant growth. For example, dry and cold weather conditions limit height growth (Hogg et al., 2002; Huang et al., 2013), and trees compensate it by adjusting their xylem and wood formation (Breda et al., 2006; Zhai et al., 2012). Also, recent studies have shown that drought is an important factor influencing tree growth (Hogg et al., 2008; Zhang et al., 2015). The results of this study are also showed that climate effects tree height growth and the proposed climate-based height-DBH models improved predictions on height.

Mean annual maximum temperature has a positive effect on height growth for aspen, balsam poplar, lodgepole pine, black spruce, and white spruce. My results are consistent with Lines et al. (2012) and Messaoud and Chen (2011) that temperature is positively related to height

growth. The results also suggest that temperature affects the height growth rate as trees reduce height growth in colder areas by adjusting their xylem vessels (Breda et al., 2006; Tyree and Dixon, 1986). Climate moisture index had a negative impact on the height growth of aspen and white spruce. Results in this study are consistent with the finding of Zhou et al. (2019) that trees grow shorter with increased water content in air; however, our result showed an opposite trend from Lines et al. (2012). A positive value of CMI means higher precipitation than potential evapotranspiration, which means moist weather conditions. A negative relationship between tree height growth and climate moisture index might be because of higher diameter growth with increasing nutrition and water availability in soil.

This study showed that CMI and Tmax significantly affected growth of aspen, balsam poplar, lodgepole pine, and white spruce. Overall CMI was negatively correlated while Tmax was positively correlated with tree growth. Climatic factors overall improved the predictability of the height-DBH models. Therefore, the climate-based height-DBH models developed in this study can be used to better predict height of a given diameter for the five tree species studied here.

4.6 References

Allen, C.D., Macalady, A.K., Chenchouni, H., Bachelet, D., McDowell, N., Vennetier, M., Kitzberger, T., Rigling, A., Breshears, D.D., Hogg, E.H. (Ted., Gonzalez, P., Fensham, R., Zhang, Z., Castro, J., Demidova, N., Lim, J.H., Allard, G., Running, S.W., Semerci, A., Cobb, N., 2010. A global overview of drought and heat-induced tree mortality reveals emerging climate change risks for forests. For. Ecol. Manage. 259, 660–684. https://doi.org/10.1016/j.foreco.2009.09.001

Bates, D.M., Watts, D.G., 1988. Nonlinear regression analysis and its applications.

Begum, S., Kudo, K., Rahman, M.H., Nakaba, S., Yamagishi, Y., Nabeshima, E., Nugroho, W.D., Oribe, Y., Kitin, P., Jin, H.O., Funada, R., 2018. Climate change and the regulation of wood formation in trees by temperature. Trees - Struct. Funct. 32, 3–15. https://doi.org/10.1007/s00468-017-1587-6

Breda, N., Huc, R., Granier, A., Dreyer, E., 2006. Temperate forest trees and stands under severe drought: a review of ecophysiological responses, adaptation processes and long-term consequences. Ann. For. Sci. 63, 625–644. https://doi.org/10.1051/forest

Bullock, S.H., 2000. Developmental Patterns of Tree Dimensions in a Neotropical Deciduous Forest. Biotropica 32, 42–52.

Butt, N., Bebber, D.P., Riutta, T., Crockatt, M., Morecroft, M.D., Malhi, Y., 2014. Relationships between tree growth and weather extremes: Spatial and interspecific comparisons in a temperate broadleaf forest. For. Ecol. Manage. 334, 209–216. https://doi.org/10.1016/j.foreco.2014.09.006

Calama, R., Montero, G., 2004. Interregional nonlinear height-diameter model with random coefficients for stone pine in Spain. Can. J. For. Res. 34, 150–163.

https://doi.org/10.1139/x03-199

Chai, Z., Tan, W., Li, Y., Yan, L., Yuan, H., Li, Z., 2018. Generalized nonlinear height-diameter models for a Cryptomeria fortunei plantation in the Pingba region of Guizhou Province, China. Web Ecol. 18, 29–35. https://doi.org/10.5194/we-18-29-2018

Chen, H.Y.H., Luo, Y., Reich, P.B., Searle, E.B., Biswas, S.R., 2016. Climate change-associated trends in net biomass change are age dependent in western boreal forests of Canada. Ecol. Lett. 19, 1150–1158. https://doi.org/10.1111/ele.12653

Chen, X., Hu, B., Yu, R., 2005. Spatial and temporal variation of phenological growing season and climate change impacts in temperate eastern China. Glob. Chang. Biol. 11, 1118–1130. https://doi.org/10.1111/j.1365-2486.2005.00974.x

Chhin, S., Hogg, E.H. (Ted., Lieffers, V.J., Huang, S., 2008. Potential effects of climate change on the growth of lodgepole pine across diameter size classes and ecological regions. For. Ecol. Manage. 256, 1692–1703. https://doi.org/10.1016/j.foreco.2008.02.046

Cortini, F., Filipescu, C.N., Groot, A., MacIsaac, D.A., Nunifu, T., 2011. Regional models of diameter as a function of individual tree attributes, climate and site characteristics for six major tree species in Alberta, Canada. Forests 2, 814–831. https://doi.org/10.3390/f2040814

Forest Management Branch, 2005. Permanent sample plot (PSP) field procedures manual. Public Lands and Forests Division, Alberta Sustainable Resource Development.

Granda, E., Alla, A.Q., Laskurain, N.A., Loidi, J., Sánchez-Lorenzo, A., Camarero, J.J., 2018. Coexisting oak species, including rear-edge populations, buffer climate stress through xylem adjustments. Tree Physiol. 38, 159–172. https://doi.org/10.1093/treephys/tpx157

Hadden, D., Grelle, A., 2016. Changing temperature response of respiration turns boreal forest from carbon sink into carbon source. Agric. For. Meteorol. 223, 30–38.

https://doi.org/10.1016/j.agrformet.2016.03.020

Hogg, E.H. (Ted., 1994. Climate and the southern limit of the western Canadian boreal forest. Can. J. For. Res. 24, 1835–1845.

Hogg, E.H., Brandt, J.P., Kochtubajda, B., 2005. Factors affecting interannual variation in growth of western Canadian aspen forests during 1951-2000. Can. J. For. Res. 35, 610–622. https://doi.org/10.1139/x04-211

Hogg, E.H., Brandt, J.P., Kochtubajda, B., 2002. Growth and dieback of aspen forests in northwestern Alberta, Canada, in relation to climate and insects. Can. J. For. Res. 32, 823–832. https://doi.org/10.1139/x01-152

Hogg, E.H., Brandt, J.P., Michaelian, M., 2008. Impacts of a regional drought on the productivity, dieback, and biomass of western Canadian aspen forests. Can. J. For. Res. 38, 1373–1384. https://doi.org/10.1139/X08-001

Huang, J.A., Tardif, J.C., Bergeron, Y., Denneler, B., Berninger, F., Girardin, M.P., 2010. Radial growth response of four dominant boreal tree species to climate along a latitudinal gradient in the eastern Canadian boreal forest. Glob. Chang. Biol. 16, 711–731. https://doi.org/10.1111/j.1365-2486.2009.01990.x

Huang, J.G., Bergeron, Y., Berninger, F., Zhai, L., Tardif, J.C., Denneler, B., 2013. Impact of Future Climate on Radial Growth of Four Major Boreal Tree Species in the Eastern Canadian Boreal Forest. PLoS One 8. https://doi.org/10.1371/journal.pone.0056758

Huang, S., Price, D., Titus, S.J., 2000. Development of ecoregion-based height-diameter models for white spruce in boreal forests. For. Ecol. Manage. 129, 125–141. https://doi.org/10.1016/S0378-1127(99)00151-6

Huang, S., Titus, S.J., 1994. An age-independent individual tree height prediction model for

boreal spruce–aspen stands in Alberta. Can. J. For. Res. 24, 1295–1301. https://doi.org/10.1139/x94-169

Huang, S., Titus, S.J., Wiens, D.P., 1992. Comparison of nonlinear height-diameter functions for major Alberta tree species. Can. J. For. Res. 22, 1297–1304.

Huang, S., Wiens, D.P., Yang, Y., Meng, S.X., Vanderschaaf, C.L., 2009. Assessing the impacts of species composition, top height and density on individual tree height prediction of quaking aspen in boreal mixedwoods. For. Ecol. Manage. 258, 1235–1247. https://doi.org/10.1016/j.foreco.2009.06.017

Hulshof, C.M., Swenson, N.G., Weiser, M.D., 2015. Tree height-diameter allometry across the United States. Ecol. Evol. 5, 1193–1204. https://doi.org/10.1002/ece3.1328

IPCC, 2001. Climate Change 2001: The Scientific Basis, in: Contribution of Working Group I to the Third Assessment Report of the Intergovernmental Panel on Climate Change. Cambridge University Press, New York, USA, p. 881.

Kalbi, S., Fallah, A., Bettinger, P., Shataee, S., Yousefpour, R., 2018. Mixed-effects modeling for tree height prediction models of Oriental beech in the Hyrcanian forests. J. For. Res. 29, 1195–1204. https://doi.org/10.1007/s11676-017-0551-z

Kramer, K., Leinonen, I., Loustau, D., 2000. The importance of phenology for the evaluation of impact of climate change on growth of boreal, temperate and Mediterranean forests ecosystems: An overview. Int. J. Biometeorol. 44, 67–75. https://doi.org/10.1007/s004840000066

Lindroth, A., Grelle, A., Morén, A.S., 1998. Long-term measurements of boreal forest carbon balance reveal large temperature sensitivity. Glob. Chang. Biol. 4, 443–450. https://doi.org/10.1046/j.1365-2486.1998.00165.x

Lines, E.R., Zavala, M.A., Purves, D.W., Coomes, D.A., 2012. Predictable changes in aboveground allometry of trees along gradients of temperature, aridity and competition. Glob. Ecol. Biogeogr. 21, 1017–1028. https://doi.org/10.1111/j

Messaoud, Y., Chen, H.Y.H., 2011. The influence of recent climate change on tree height growth differs with species and spatial environment. PLoS One 6. https://doi.org/10.1371/journal.pone.0014691

Moles, A.T., Warton, D.I., Warman, L., Swenson, N.G., Laffan, S.W., Zanne, A.E., Pitman, A., Hemmings, F.A., Leishman, M.R., 2009. Global patterns in plant height. J. Ecol. 97, 923–932. https://doi.org/10.1111/j.1365-2745.2009.01526.x

Natural Regions Committee, 2006. Natural regions and subregions of Alberta, Natural regions and subregions of Alberta : Natural Regions Committee /. https://doi.org/10.5962/bhl.title.115367

Olson, M.E., Soriano, D., Rosell, J.A., Anfodillo, T., Donoghue, M.J., Edwards, E.J., León-Gómez, C., Dawson, T., Julio Camarero Martínez, J., Castorena, M., Echeverría, A., Espinosa, C.I., Fajardo, A., Gazol, A., Isnard, S., Lima, R.S., Marcati, C.R., Méndez-Alonzo, R., 2018. Plant height and hydraulic vulnerability to drought and cold. Proc. Natl. Acad. Sci. U. S. A. 115, 7551–7556. https://doi.org/10.1073/pnas.1721728115

Pacala, S.W., Canham, C.D., Silander, J.A., JR., Kobe, R.K., 1994. Sapling growth as a function of resources in a north temperate forest. Can. J. For. Res. 24, 2172–2183.

Peng, C., Zhang, L., Liu, J., 2001. Developing and validating nonlinear height-diameter models for major tree species of Ontario's boreal forests. North. J. Appl. For. 18, 87–94. https://doi.org/10.1093/njaf/18.3.87

Pepin, N., Bradley, R.S., Diaz, H.F., Baraer, M., Caceres, E.B., Forsythe, N., Fowler, H.,

Greenwood, G., Hashmi, M.Z., Liu, X.D., Miller, J.R., Ning, L., Ohmura, A., Palazzi, E., Rangwala, I., Schöner, W., Severskiy, I., Shahgedanova, M., Wang, M.B., Williamson, S.N., Yang, D.Q., 2015. Elevation-dependent warming in mountain regions of the world. Nat. Clim. Chang. 5, 424–430. https://doi.org/10.1038/nclimate2563

Pinheiro, J., Bates, D., DebRoy, S., Sarkar, D., R Core Team, 2020. nlme: Linear and Nonlinear Mixed Effects Models.

Price, D.T., Alfaro, R.I., Brown, K.J., Flannigan, M.D., Fleming, R.A., Hogg, E.H., Girardin, M.P., Lakusta, T., Johnston, M., McKenney, D.W., Pedlar, J.H., Stratton, T., Sturrock, R.N., Thompson, I.D., Trofymow, J.A., Venier, L.A., 2013. Anticipating the consequences of climate change for Canada's boreal forest ecosystems. Environ. Rev. 21, 322–365. https://doi.org/10.1139/er-2013-0042

R Core Team, 2019. R: A language and environment for statistical computing.

Sette Jr, C.R., Tomazello Fo, M., Lousada, J.L., Lopes, D., Laclau, J.P., 2016. Relationship between climate variables, trunk growth rate and wood density of Eucalyptus grandis W. Mill ex Maiden trees. Rev. Arvore 40, 337–346. https://doi.org/10.1590/0100-67622016000200016

Sharma, M., Parton, J., 2007. Height-diameter equations for boreal tree species in Ontario using a mixed-effects modeling approach. For. Ecol. Manage. 249, 187–198. https://doi.org/10.1016/j.foreco.2007.05.006

Tsega, M., Guadie, A., Teffera, Z.L., Belayneh, Y., Niu, D., 2018. Development and Validation of Height-Diameter Models for Cupressus lusitanica in Gergeda Forest, Ethiopia. Forest Sci. Technol. 14, 138–144. https://doi.org/10.1080/21580103.2018.1482794

Tyree, M.T., Dixon, M.A., 1986. Water stress induced cavitation and embolism in some woody

plants. Physiol. Plant. 66, 397–405. https://doi.org/10.1111/j.1399-3054.1986.tb05941.x

Yeh, H.-Y., Wensel, L.C., 2000. The relationship between tree diameter growth and climate for coniferous species in northern California. Can. J. For. Res. 30, 1463–1471. https://doi.org/10.1139/cjfr-30-9-1463

Zhai, L., Bergeron, Y., Huang, J.G., Berninger, F., 2012. Variation in intra-annual wood formation, foliage and shoot development of three major Canadian boreal tree species. Am. J. Bot. 99, 827–837. https://doi.org/10.3732/ajb.1100235

Zhang, J., Huang, S., He, F., 2015. Half-century evidence from western Canada shows forest dynamics are primarily driven by competition followed by climate. Proc. Natl. Acad. Sci. U. S. A. 112, 4009–4014. https://doi.org/10.1073/pnas.1420844112

Zhou, Y., Lei, Z., Zhou, F., Han, Y., Yu, D., Zhang, Y., 2019. Impact of climate factors on height growth of pinus sylvestris var. Mongolica. PLoS One 14, 1–15. https://doi.org/10.1371/journal.pone.0213509

Chapter five: Conclusions

Modelling variation in tree size, height and their relationship is important for quantifying structure and function of forest ecosystems, and for predicting growth and yield of forests. In this thesis, I have focused on studying two main tree attributes, their relationship and effect of climate on this relationship by modelling: (*i*) tree size distribution, *(ii*) tree height-DBH relationships and their derivative patterns, and (*iii*) climate effects on tree height-DBH relationships. I used long-term empirical datasets, and came to few common and several key conclusions.

In Chapter 2, I provided an explanation as to why Weibull distribution is so widely used in forestry to model tree size distribution and showed that by using three large-scale empirical datasets. I also showed how to use tree size distribution for calculating growth rates. This is a particularly interesting contribution because the derivation of the Weibull distribution links stand structure (tree size distribution) with processes (growth rate). All the three datasets used in the chapter reveal that log-transformed curvilinearity is the common feature for tree size distribution. The Weibull distribution describes this feature well.

In Chapter 3, I analyzed height-DBH relationships for seven major tree species of Alberta, including aspen, white birch, balsam poplar, lodgepole pine, white spruce, black spruce and balsam fir. I also assessed whether the derivative curves of height-DBH models reveal any tree growth pattern that is related to life-history traits of species. Tree height-DBH models have been the subject of intensive research in forestry, but little to no attention has been ever paid to the derivative of height-DBH models. I showed that derivative curves are more informative in

revealing tree growth pattern than the cumulative height-DBH models, and the derivatives showed that the species with different life history strategies, e.g., coniferous vs deciduous, had very different height growth patterns with respect to tree diameter.

In Chapter 4, I developed climate-based height-DBH models for five major tree species of Alberta's boreal forests (aspen, balsam poplar, lodgepole pine, white spruce and black spruce) by using long term permanent sampling plots and two climate variables. I found that both annual climate moisture index (CMI) and mean annual daily maximum temperature (Tmax) increased predictability of height-DBH models. CMI had varied effect on height growth, while Tmax had positive effect on height growth of species. Species would grow taller with increased temperature while they had different responses to increased climate moisture index.

5.1 Major contributions to sustainable forest management

My thesis focused on two main tree attributes, height and diameter. It should deliver important contributions to modelling tree-height relationships, hence growth and yield modelling.

Predicting growth: I showed that using the derivative of height-DBH models provide more informative then their cumulative forms when predicting height (Chapter 3). I also showed that climate has an impact on tree height-diameter relationships (Chapter 4). Moreover, I showed how to use tree size distribution for calculating growth rates (Chapter 2), and how to use height-DBH models to determine the maximum tree height growth with respect to tree DBH. Chapters 2, 3 & 4 should provide better understanding for predicting tree height and growth, hence be a good guidance when planning harvesting and silvicultural activities.

Understanding climate change effect: My result showed that climate affects tree height and diameter relationships (Chapter 4). Under current and future climate change, climate-based models will provide more accurate predictions than traditional height-DBH models. The models show whether trees grow taller or shorter under different climate conditions, contributing to understanding the possible effect of changing climates on forest stand structure.

Accuracy of height-DBH models: Height-DBH relationships for a given tree species could change across regions if the growth of tree height and diameter is subject to the effect of climate change. In current practice, a single height-DBH model is used to predict growth of each tree species across the entire province of Alberta (Huang et al., 2013). However, Alberta has 6 natural regions characterized by differences in vegetation and climate. Hence, it is necessary to develop models that take account of the variation in climate across these different regions. The model developed in Chapter 4 should provide more accurate height-DBH relationships and thus should improve growth-yield modelling.

Biomass assessment: Biomass is mostly calculated from field measurement of tree size and/or height. Measurement of tree height is relatively laborious and less accurate. Height-DBH models are typically used to estimate height and contribute to estimating forest biomass. Hence, accuracy and reliability of height-DBH models is important for improving the reliability of these biomass estimations. Climate-based height-DBH models developed in Chapter 4 should further improve the accuracy of biomass estimates.

5.2 Limitations and future work

I would like to note some limitations of my study despite its major contributions to modelling tree size and height, and their relationships. Overall, my thesis only focuses on tree height and size, ignoring other tree attributes important to forest stands, e.g., canopy size, crown height. It would be interesting to also analyze those attributes to see which of them are most likely to improve growth and yield modelling.

The dynamics of forest stands is ultimately determined by growth, mortality and recruitment. Although the measures of tree size and height are necessary for describing stand structure and dynamics, growth, mortality and recruitment are essential for understanding stand dynamics and the change of stand structure (Parker et al., 1985; Pretzsch et al., 2014). Cortini et al. (2017) showed that climate has a major effect on tree survival, and Kueppers et al. (2017) found that recruitment is affected by recent climate changes. To truly understand stand dynamics, there is a need to link the distributions of tree size and height with growth, mortality and recruitment.

Also, in the third and fourth chapters I only used trees with DBH larger than 9 cm because data on smaller trees are not available. Pacala and his callegues (1994) analyzed diameter and height growth for saplings (DBH $\leq$ 10 cm) of 10 dominant tree species in a north temperate forest, and found strong relationships with growth and light availability. The exclusion of small trees in my thesis could potentially bias the results of height-DBH relationship and climate effects on this relationship.

In the fourth chapter about incorporating climate change effect into height-DBH models, one possible limitation could be the number of climate variables. I only used CMI and Tmax measure to model climate change effects. Jiang et al. (2016) found that there is a strong

relationship between precipitation and growth but not significant relationship between growth and degree days for western Canada boreal mixedwood forest. Also, Liu and El-Kassaby (2018) found that evapotranspiration and growing degree days have an effect on tree height growth in Pacific Northwest. Hence, it would be interesting to see whether other climate variables have any significant effect on growth of Alberta boreal forest tree species. Clearly, further studies should be done to look at this issue.

Another possible limitation could be that I only considered climate effects on tree height-DBH relationships. Zhang et al. (2015) found that competition could also be important in driving stand dynamics in the same region of my study. Hogg et al. (2002) found that insects could be another component affecting growth of aspen in northwestern Alberta. Further studies can be done with addition of other environmental, disturbance and climate effects on height-DBH relationships so that to improve tree height-DBH modelling.

5.3 References

Cortini, F., Comeau, P.G., Strimbu, V.C., Hogg, E.H. (Ted., Bokalo, M., Huang, S., 2017. Survival functions for boreal tree species in northwestern North America. For. Ecol. Manage. 402, 177–185. https://doi.org/10.1016/j.foreco.2017.06.036

Hogg, E.H., Brandt, J.P., Kochtubajda, B., 2002. Growth and dieback of aspen forests in northwestern Alberta, Canada, in relation to climate and insects. Can. J. For. Res. 32, 823–832. https://doi.org/10.1139/x01-152

Huang, S., Yang, Y., Aitkin, D., 2013. Population and plot-specific individual tree height-diameter models for major Alberta tree species.

Jiang, X., Huang, J.G., Stadt, K.J., Comeau, P.G., Chen, H.Y.H., 2016. Spatial climate-dependent growth response of boreal mixedwood forest in western Canada. Glob. Planet. Change 139, 141–150. https://doi.org/10.1016/j.gloplacha.2016.02.002

Kueppers, L.M., Conlisk, E., Castanha, C., Moyes, A.B., Germino, M.J., de Valpine, P., Torn, M.S., Mitton, J.B., 2017. Warming and provenance limit tree recruitment across and beyond the elevation range of subalpine forest. Glob. Chang. Biol. 23, 2383–2395. https://doi.org/10.1111/gcb.13561

Liu, Y., El-Kassaby, Y.A., 2018. Evapotranspiration and favorable growing degree-days are key to tree height growth and ecosystem functioning: Meta-Analyses of Pacific Northwest historical data. Sci. Rep. 8, 1–12. https://doi.org/10.1038/s41598-018-26681-1

Pacala, S.W., Canham, C.D., Silander, J.A., JR., Kobe, R.K., 1994. Sapling growth as a function of resources in a north temperate forest. Can. J. For. Res. 24, 2172–2183.

Parker, G.R., Leopold, D.J., Eichenberger, J.K., 1985. Tree dynamics in an old-growth, deciduous forest. For. Ecol. Manage. 11, 31–57. https://doi.org/10.1016/0378-

1127(85)90057-X

Pretzsch, H., Biber, P., Schütze, G., Uhl, E., Rötzer, T., 2014. Forest stand growth dynamics in Central Europe have accelerated since 1870. Nat. Commun. 5, 1–10. https://doi.org/10.1038/ncomms5967

Zhang, J., Huang, S., He, F., 2015. Half-century evidence from western Canada shows forest dynamics are primarily driven by competition followed by climate. Proc. Natl. Acad. Sci. USA. 112, 4009–4014. https://doi.org/10.1073/pnas.1420844112

Bibliography

Allen, C.D., Macalady, A.K., Chenchouni, H., Bachelet, D., McDowell, N., Vennetier, M., Kitzberger, T., Rigling, A., Breshears, D.D., Hogg, E.H. (Ted., Gonzalez, P., Fensham, R., Zhang, Z., Castro, J., Demidova, N., Lim, J.H., Allard, G., Running, S.W., Semerci, A., Cobb, N., 2010. A global overview of drought and heat-induced tree mortality reveals emerging climate change risks for forests. For. Ecol. Manage. 259, 660–684. https://doi.org/10.1016/j.foreco.2009.09.001

Archibold, O.W., 1995. Ecology of World Vegetation. Springer Netherlands.

Assmann, E., 1970a. The principles of forest yield study. Pergamon, Oxford, New York.

Assmann, E., 1970b. Section D - Structure, Increment and Yield of Stands in Relation To Silvicultural Treatment. Princ. For. Yield Study 207–433. https://doi.org/10.1016/b978-0-08-006658-5.50008-x

Bailey, R., Dell, T., 1973. Quantifying Diameter Distributions with the Weibull Function. For. Sci. 19, 97–104. https://doi.org/10.1093/forestscience/19.2.97

Bates, D.M., Watts, D.G., 1988. Nonlinear regression analysis and its applications.

Begum, S., Kudo, K., Rahman, M.H., Nakaba, S., Yamagishi, Y., Nabeshima, E., Nugroho, W.D., Oribe, Y., Kitin, P., Jin, H.O., Funada, R., 2018. Climate change and the regulation of wood formation in trees by temperature. Trees - Struct. Funct. 32, 3–15. https://doi.org/10.1007/s00468-017-1587-6

Bliss, C.I., Reinker, K.A., 1964. A lognormal approach to diameter distributions in even-aged stands. For. Sci. 10, 350–360.

Bokma, F., 2004. Evidence against universal metabolic allometry. Funct. Ecol. 18, 184–187. https://doi.org/10.1111/j.0269-8463.2004.00817.x

Bond-Lamberty, B., Peckham, S.D., Ahl, D.E., Gower, S.T., 2007. Fire as the dominant driver of central Canadian boreal forest carbon balance. Nature 450, 89–92. https://doi.org/10.1038/nature06272

Boojh, R., Ramakrishnan, P.S., 1982. Growth strategy of trees related to successional status II. Leaf dynamics. For. Ecol. Manage. 4, 375–386. https://doi.org/10.1016/0378-1127(82)90036-6

Brando, P.M., Nepstad, D.C., Balch, J.K., Bolker, B., Christman, M.C., Coe, M., Putz, F.E., 2012. Fire-induced tree mortality in a neotropical forest: The roles of bark traits, tree size, wood density and fire behavior. Glob. Chang. Biol. 18, 630–641. https://doi.org/10.1111/j.1365-2486.2011.02533.x

Breda, N., Huc, R., Granier, A., Dreyer, E., 2006. Temperate forest trees and stands under severe drought: a review of ecophysiological responses, adaptation processes and long-term consequences. Ann. For. Sci. 63, 625–644. https://doi.org/10.1051/forest

Brown, J.H., Gillooly, J.F., Allen, A.P., Savage, V.M., West, G.B., 2004. Toward a metabolic theory of ecology. Ecology 85, 1771–1789.

Bullock, B.P., Burkhart, H.E., 2005. Juvenile diameter distributions of loblolly pine characterized by the two-parameter Weibull function. New For. 29, 233–244. https://doi.org/10.1007/s11056-005-5651-5

Bullock, S.H., 2000. Developmental Patterns of Tree Dimensions in a Neotropical Deciduous Forest. Biotropica 32, 42–52.

Butt, N., Bebber, D.P., Riutta, T., Crockatt, M., Morecroft, M.D., Malhi, Y., 2014. Relationships between tree growth and weather extremes: Spatial and interspecific comparisons in a temperate broadleaf forest. For. Ecol. Manage. 334, 209–216.

https://doi.org/10.1016/j.foreco.2014.09.006

Calama, R., Montero, G., 2004. Interregional nonlinear height-diameter model with random coefficients for stone pine in Spain. Can. J. For. Res. 34, 150–163. https://doi.org/10.1139/x03-199

Calder, W.A., 1984. Size, function and life history. Harvard University Press, Cambridge, Massachusetts.

Chai, Z., Tan, W., Li, Y., Yan, L., Yuan, H., Li, Z., 2018. Generalized nonlinear height-diameter models for a Cryptomeria fortunei plantation in the Pingba region of Guizhou Province, China. Web Ecol. 18, 29–35. https://doi.org/10.5194/we-18-29-2018

Chave, J., Andalo, C., Brown, S., Cairns, M.A., Chambers, J.Q., Eamus, D., Fölster, H., Fromard, F., Higuchi, N., Kira, T., Lescure, J.P., Nelson, B.W., Ogawa, H., Puig, H., Riéra, B., Yamakura, T., 2005. Tree allometry and improved estimation of carbon stocks and balance in tropical forests. Oecologia 145, 87–99. https://doi.org/10.1007/s00442-005-0100-x

Chen, H.Y.H., Luo, Y., Reich, P.B., Searle, E.B., Biswas, S.R., 2016. Climate change-associated trends in net biomass change are age dependent in western boreal forests of Canada. Ecol. Lett. 19, 1150–1158. https://doi.org/10.1111/ele.12653

Chen, X., Hu, B., Yu, R., 2005. Spatial and temporal variation of phenological growing season and climate change impacts in temperate eastern China. Glob. Chang. Biol. 11, 1118–1130. https://doi.org/10.1111/j.1365-2486.2005.00974.x

Chhin, S., Hogg, E.H. (Ted., Lieffers, V.J., Huang, S., 2008. Potential effects of climate change on the growth of lodgepole pine across diameter size classes and ecological regions. For. Ecol. Manage. 256, 1692–1703. https://doi.org/10.1016/j.foreco.2008.02.046

Clutter, J.L., Fortson, J.C., Pienaar, L.V., Brister, G.H., Bailey, R.L., 1983. Timber management: a quantitative approach. John Wiley & Sons, New York.

Colgan, M.S., Asner, G.P., Swemmer, T., 2013. Harvesting tree biomass at the stand level to assess the accuracy of field and airborne biomass estimation in savannas. Ecol. Appl. 23, 1170–1184. https://doi.org/10.1890/12-0922.1

Condit, R., 1998. Tropical Forest Census Plots. Springer-Verlag and R. G. Landes Company, Berlin, Germany, and Georgetown, Texas.

Condit, R., Hubbell, S.P., Foster, R.B., 1996. Changes in Tree Species Abundance in a Neotropical Forest: Impact of Climate Change. J. Trop. Ecol. 12, 231–256.

Coomes, D.A., Allen, R.B., 2007. Effects of size, competition and altitude on tree growth. J. Ecol. 95, 1084–1097. https://doi.org/10.1111/j.1365-2745.2007.01280.x

Coomes, D.A., Duncan, R.P., Allen, R.B., Truscott, J., 2003. Disturbances prevent stem size-density distributions in natural forests from following scaling relationships. Ecol. Lett. 6, 980–989. https://doi.org/10.1046/j.1461-0248.2003.00520.x

Cortini, F., Comeau, P.G., Strimbu, V.C., Hogg, E.H. (Ted., Bokalo, M., Huang, S., 2017. Survival functions for boreal tree species in northwestern North America. For. Ecol. Manage. 402, 177–185. https://doi.org/10.1016/j.foreco.2017.06.036

Cortini, F., Filipescu, C.N., Groot, A., MacIsaac, D.A., Nunifu, T., 2011. Regional models of diameter as a function of individual tree attributes, climate and site characteristics for six major tree species in Alberta, Canada. Forests 2, 814–831. https://doi.org/10.3390/f2040814

Curtis, R.O., 1967. Height-Diameter and Height-Diameter-Age Equations For Second-Growth Douglas-Fir. Science (80-.). 13, 365–375.

Curtis, R.O., Clendenen, G.W., DeMars, D.J., 1981. A new stand simulator for coast Douglas-fir:

DFSIM user's guide, US Department of Agriculture, Forest Service, General Technical Report.

Enquist, B.J., Brown, J.H., West, G.B., 1998. Allometric scaling of plant energetics and population density. Nature 395, 163–165.

Enquist, B.J., Niklas, K.J., 2001. Invariant scaling relations across tree-dominated communities. Nature 410, 655–660. https://doi.org/10.1038/nature02023

Farr, W.A., DeMars, D.J., Dealy, J.E., 1989. Height and crown width related to diameter for open-grown western hemlock and Sitka spruce. Can. J. For. Res. 19, 1203–1207. https://doi.org/10.1139/x89-181

Firbank, L.G., Watkinson, A.R., 1990. On the effects of competition: from monocultures to mixtures, in: Grace, J.B., Tilman, D. (Eds.), Perspectives on Plant Competition. Academic Press, San Diego, California, USA, pp. 165–192.

Ford, E.D., 1975. Competition and Stand Structure in Some Even-Aged Plant Monocultures. J. Ecol. 63, 311–333. https://doi.org/10.2307/2258857

Forest Management Branch, 2005. Permanent sample plot (PSP) field procedures manual. Public Lands and Forests Division, Alberta Sustainable Resource Development.

Garcia-Gonzalo, J., Peltola, H., Zubizarreta Gerendiain, A., Kellomäki, S., 2007. Impacts of forest landscape structure and management on timber production and carbon stocks in the boreal forest ecosystem under changing climate. For. Ecol. Manage. 241, 243–257. https://doi.org/10.1016/j.foreco.2007.01.008

Gentry, A.H., 1993. In Biodiversity and Conservation of Neotropical and Montane Forests, in: Churchill, S.P. et al. (Ed.), . New York Botanical Garden, New York, pp. 103–126.

Gentry, A.H., 1988. Changes in plant community diversity and floristic composition on

environmental and geographical gradients. Ann. Missouri Bot. Gard. 75, 1–34.

Glazier, D.S., 2005. Beyond the'3/4-power law':variation in the intra-and interspecific scaling of metabolic rate in animals. Biol. Rev. 80, 611–662.

Gove, J.H., 2003. Estimation and applications of size-biased distributions in forestry., in: Amaro, D.R., Soares, P. (Eds.), Modelling Forest Systems. CAB International, Oxford, UK, pp. 201–212. https://doi.org/10.1079/9780851996936.0201

Granda, E., Alla, A.Q., Laskurain, N.A., Loidi, J., Sánchez-Lorenzo, A., Camarero, J.J., 2018. Coexisting oak species, including rear-edge populations, buffer climate stress through xylem adjustments. Tree Physiol. 38, 159–172. https://doi.org/10.1093/treephys/tpx157

Hadden, D., Grelle, A., 2016. Changing temperature response of respiration turns boreal forest from carbon sink into carbon source. Agric. For. Meteorol. 223, 30–38. https://doi.org/10.1016/j.agrformet.2016.03.020

Hafley, W.L., Schreuder, H.T., 1977. Statistical distributions for fitting diameter and height data in even-aged stands. Can. J. For. Res. 7, 481–487.

Harper, J.L., 1977. Population biology of plants. Academic Press, London, UK.

Henry, H.A.L., Aarssen, L.W., 1997. On the Relationship between Shade Tolerance and Shade Avoidance Strategies in Woodland Plants. Oikos 80, 575–582.

Hogg, E.H. (Ted., 1994. Climate and the southern limit of the western Canadian boreal forest. Can. J. For. Res. 24, 1835–1845.

Hogg, E.H., Brandt, J.P., Kochtubajda, B., 2005. Factors affecting interannual variation in growth of western Canadian aspen forests during 1951-2000. Can. J. For. Res. 35, 610–622. https://doi.org/10.1139/x04-211

Hogg, E.H., Brandt, J.P., Kochtubajda, B., 2002. Growth and dieback of aspen forests in

northwestern Alberta, Canada, in relation to climate and insects. Can. J. For. Res. 32, 823–832. https://doi.org/10.1139/x01-152

Hogg, E.H., Brandt, J.P., Michaelian, M., 2008. Impacts of a regional drought on the productivity, dieback, and biomass of western Canadian aspen forests. Can. J. For. Res. 38, 1373–1384. https://doi.org/10.1139/X08-001

Homeier, J., Siegmar, W.B., Sven, G., Rütger, T.R., Christoph, L., 2010. Tree diversity, forest structure and productivity along altitudinal and topographical gradients in a species-rich ecuadorian montane rain forest. Biotropica 42, 140–148.

Huang, J.A., Tardif, J.C., Bergeron, Y., Denneler, B., Berninger, F., Girardin, M.P., 2010. Radial growth response of four dominant boreal tree species to climate along a latitudinal gradient in the eastern Canadian boreal forest. Glob. Chang. Biol. 16, 711–731. https://doi.org/10.1111/j.1365-2486.2009.01990.x

Huang, J.G., Bergeron, Y., Berninger, F., Zhai, L., Tardif, J.C., Denneler, B., 2013. Impact of Future Climate on Radial Growth of Four Major Boreal Tree Species in the Eastern Canadian Boreal Forest. PLoS One 8. https://doi.org/10.1371/journal.pone.0056758

Huang, S., Price, D., Titus, S.J., 2000. Development of ecoregion-based height-diameter models for white spruce in boreal forests. For. Ecol. Manage. 129, 125–141. https://doi.org/10.1016/S0378-1127(99)00151-6

Huang, S., Titus, S.J., 1999. An individual tree height increment model for mixed white spruce–aspen stands in Alberta, Canada. For. Ecol. Manage. 123, 41–53. https://doi.org/10.1016/S0378-1127(99)00015-8

Huang, S., Titus, S.J., 1994. An age-independent individual tree height prediction model for boreal spruce–aspen stands in Alberta. Can. J. For. Res. 24, 1295–1301.

https://doi.org/10.1139/x94-169

Huang, S., Titus, S.J., Wiens, D.P., 1992. Comparison of nonlinear height-diameter functions for major Alberta tree species. Can. J. For. Res. 22, 1297–1304.

Huang, S., Wiens, D.P., Yang, Y., Meng, S.X., Vanderschaaf, C.L., 2009. Assessing the impacts of species composition, top height and density on individual tree height prediction of quaking aspen in boreal mixedwoods. For. Ecol. Manage. 258, 1235–1247. https://doi.org/10.1016/j.foreco.2009.06.017

Huang, S., Yang, Y., Aitkin, D., 2013. Population and plot-specific individual tree height-diameter models for major Alberta tree species.

Hubbell, S.P., Foster, R.B., 1983. Diversity of canopy trees in a neotropical forest and implications for conservation., in: Whitmore, T.C., Chadwick, A.C., Sutton, S.L. (Eds.), Tropical Rain Forest: Ecology and Management. Blackwell Scientific Publications, Oxford., pp. 24–41.

Hulshof, C.M., Swenson, N.G., Weiser, M.D., 2015. Tree height-diameter allometry across the United States. Ecol. Evol. 5, 1193–1204. https://doi.org/10.1002/ece3.1328

Hynynen, J., Ojansuu, R., 2003. Impact of plot size on individual-tree competition measures for growth and yield simulators. Can. J. For. Res. 33, 455–465. https://doi.org/10.1139/x02-173

IPCC, 2001. Climate Change 2001: The Scientific Basis, in: Contribution of Working Group I to the Third Assessment Report of the Intergovernmental Panel on Climate Change. Cambridge University Press, New York, USA, p. 881.

Jiang, X., Huang, J.G., Stadt, K.J., Comeau, P.G., Chen, H.Y.H., 2016. Spatial climate-dependent growth response of boreal mixedwood forest in western Canada. Glob. Planet. Change 139, 141–150. https://doi.org/10.1016/j.gloplacha.2016.02.002

Kalbi, S., Fallah, A., Bettinger, P., Shataee, S., Yousefpour, R., 2018. Mixed-effects modeling for tree height prediction models of Oriental beech in the Hyrcanian forests. J. For. Res. 29, 1195–1204. https://doi.org/10.1007/s11676-017-0551-z

Kramer, K., Leinonen, I., Loustau, D., 2000. The importance of phenology for the evaluation of impact of climate change on growth of boreal, temperate and Mediterranean forests ecosystems: An overview. Int. J. Biometeorol. 44, 67–75. https://doi.org/10.1007/s004840000066

Kreuzwieser, J., Gessler, A., 2010. Global climate change and tree nutrition: Influence of water availability. Tree Physiol. 30, 1221–1234. https://doi.org/10.1093/treephys/tpq055

Kueppers, L.M., Conlisk, E., Castanha, C., Moyes, A.B., Germino, M.J., de Valpine, P., Torn, M.S., Mitton, J.B., 2017. Warming and provenance limit tree recruitment across and beyond the elevation range of subalpine forest. Glob. Chang. Biol. 23, 2383–2395. https://doi.org/10.1111/gcb.13561

Kunneke, A., Aardt, J. van, Roberts, W., Seifert, T., 2014. Bioenergy from Wood, Managing Forest Ecosystems. Springer Netherlands, Dordrecht. https://doi.org/10.1007/978-94-007-7448-3

Lai, J., Coomes, D.A., Du, X., Hsieh, C. fu, Sun, I.F., Chao, W.C., Mi, X., Ren, H., Wang, X., Hao, Z., Ma, K., 2013. A general combined model to describe tree-diameter distributions within subtropical and temperate forest communities. Oikos 122, 1636–1642. https://doi.org/10.1111/j.1600-0706.2013.00436.x

Leak, B., 1965. The J-shaped Probability Distribution. For. Sci. 11, 405–409.

Li, F., Zhang, L., Davis, C.J., 2002. Modeling the Joint Distribution of Tree Diameters and Heights by Bivariate Generalized Beta Distribution. For. Sci. 48, 47–58.

Lindroth, A., Grelle, A., Morén, A.S., 1998. Long-term measurements of boreal forest carbon balance reveal large temperature sensitivity. Glob. Chang. Biol. 4, 443–450. https://doi.org/10.1046/j.1365-2486.1998.00165.x

Lines, E.R., Zavala, M.A., Purves, D.W., Coomes, D.A., 2012. Predictable changes in aboveground allometry of trees along gradients of temperature, aridity and competition. Glob. Ecol. Biogeogr. 21, 1017–1028. https://doi.org/10.1111/j

Liu, M., Feng, Z., Zhang, Z., Ma, C., Wang, M., Lian, B. ling, Sun, R., Zhang, L., 2017. Development and evaluation of height diameter at breast models for native Chinese Metasequoia. PLoS One 12, 1–17. https://doi.org/10.1371/journal.pone.0182170

Liu, Y., El-Kassaby, Y.A., 2018. Evapotranspiration and favorable growing degree-days are key to tree height growth and ecosystem functioning: Meta-Analyses of Pacific Northwest historical data. Sci. Rep. 8, 1–12. https://doi.org/10.1038/s41598-018-26681-1

Loehle, C., 2000. Strategy space and the disturbance spectrum: A life-history model for tree species coexistence. Am. Nat. 156, 14–33. https://doi.org/10.1086/303369

Loetsch, F., Zöhrer, F., Haller, K.E., 1973. Forest inventory. BLV, Verlagsgesellschaft mbH, München, Germany.

Lorimer, C.G., Krug, A.G., 1983. Diameter distributions in even-aged stands of shade-tolerant and midtolerant tree species. Am. Midl. Nat. 109, 331–345. https://doi.org/10.2307/2425414

Ma, Z., Peng, C., Zhu, Q., Chen, H., Yu, G., Li, W., Zhou, X., Wang, W., Zhang, W., 2012. Regional Drought-Induced Reduction in the Biomass Carbon Sink of Canada's Boreal Forests. Proc. Natl. Acad. Sci. 109, 2423–2427. https://doi.org/10.1073/pnas.1111576109

Mandelbrot, B.B., 1990. The fractal geometry of nature. W.H. Freeman, New York.

Merganič, J., Sterba, H., 2006. Characterisation of diameter distribution using the Weibull function: Method of moments. Eur. J. For. Res. 125, 427–439. https://doi.org/10.1007/s10342-006-0138-2

Messaoud, Y., Chen, H.Y.H., 2011. The influence of recent climate change on tree height growth differs with species and spatial environment. PLoS One 6. https://doi.org/10.1371/journal.pone.0014691

Michaelian, M., Hogg, E.H., Hall, R.J., Arsenault, E., 2011. Massive mortality of aspen following severe drought along the southern edge of the Canadian boreal forest. Glob. Chang. Biol. 17, 2084–2094. https://doi.org/10.1111/j.1365-2486.2010.02357.x

Moles, A.T., Warton, D.I., Warman, L., Swenson, N.G., Laffan, S.W., Zanne, A.E., Pitman, A., Hemmings, F.A., Leishman, M.R., 2009. Global patterns in plant height. J. Ecol. 97, 923–932. https://doi.org/10.1111/j.1365-2745.2009.01526.x

Natural Regions Committee, 2006. Natural regions and subregions of Alberta, Natural regions and subregions of Alberta : Natural Regions Committee /. https://doi.org/10.5962/bhl.title.115367

Nelson, T.C., 1964. Diameter distribution and growth of Loblolly pine. For. Sci. 10, 105–114.

Oboite, F.O., Comeau, P.G., 2019. Competition and climate influence growth of black spruce in western boreal forests. For. Ecol. Manage. 443, 84–94. https://doi.org/10.1016/j.foreco.2019.04.017

Olson, M.E., Soriano, D., Rosell, J.A., Anfodillo, T., Donoghue, M.J., Edwards, E.J., León-Gómez, C., Dawson, T., Julio Camarero Martínez, J., Castorena, M., Echeverría, A., Espinosa, C.I., Fajardo, A., Gazol, A., Isnard, S., Lima, R.S., Marcati, C.R., Méndez-Alonzo, R., 2018. Plant height and hydraulic vulnerability to drought and cold. Proc. Natl.

Acad. Sci. U. S. A. 115, 7551–7556. https://doi.org/10.1073/pnas.1721728115

Pacala, S.W., Canham, C.D., Silander, J.A., JR., Kobe, R.K., 1994. Sapling growth as a function of resources in a north temperate forest. Can. J. For. Res. 24, 2172–2183.

Parker, G.R., Leopold, D.J., Eichenberger, J.K., 1985. Tree dynamics in an old-growth, deciduous forest. For. Ecol. Manage. 11, 31–57. https://doi.org/10.1016/0378-1127(85)90057-X

Pearl, R., Reed, L.J., 1920. On the rate of growth of the population of the United States since 1790 and its mathematical representation. Proc. Natl. Acad. Sci. 6, 275–288.

Peng, C., Zhang, L., Liu, J., 2001. Developing and validating nonlinear height-diameter models for major tree species of Ontario's boreal forests. North. J. Appl. For. 18, 87–94. https://doi.org/10.1093/njaf/18.3.87

Pepin, N., Bradley, R.S., Diaz, H.F., Baraer, M., Caceres, E.B., Forsythe, N., Fowler, H., Greenwood, G., Hashmi, M.Z., Liu, X.D., Miller, J.R., Ning, L., Ohmura, A., Palazzi, E., Rangwala, I., Schöner, W., Severskiy, I., Shahgedanova, M., Wang, M.B., Williamson, S.N., Yang, D.Q., 2015. Elevation-dependent warming in mountain regions of the world. Nat. Clim. Chang. 5, 424–430. https://doi.org/10.1038/nclimate2563

Pinheiro, J., Bates, D., DebRoy, S., Sarkar, D., R Core Team, 2020. nlme: Linear and Nonlinear Mixed Effects Models.

Pretzsch, H., 2009a. Forest dynamics, growth and yield: From measurement to model, Forest Dynamics, Growth and Yield: From Measurement to Model. Springer Berlin Heidelberg. https://doi.org/10.1007/978-3-540-88307-4

Pretzsch, H., 2009b. Forest dynamics, growth and yield: Chapter 6 standard analysis of long-term experimental plots, Forest Dynamics, Growth and Yield. Springer Berlin Heidelberg.

https://doi.org/10.1007/978-3-540-88307-4

Pretzsch, H., Biber, P., Schütze, G., Uhl, E., Rötzer, T., 2014. Forest stand growth dynamics in Central Europe have accelerated since 1870. Nat. Commun. 5, 1–10. https://doi.org/10.1038/ncomms5967

Price, D.T., Alfaro, R.I., Brown, K.J., Flannigan, M.D., Fleming, R.A., Hogg, E.H., Girardin, M.P., Lakusta, T., Johnston, M., McKenney, D.W., Pedlar, J.H., Stratton, T., Sturrock, R.N., Thompson, I.D., Trofymow, J.A., Venier, L.A., 2013. Anticipating the consequences of climate change for Canada's boreal forest ecosystems. Environ. Rev. 21, 322–365. https://doi.org/10.1139/er-2013-0042

R Core Team, 2019. R: A language and environment for statistical computing.

Ratkowsky, D.A., 1990. Handbook of Nonlinear Regression Models. Marcel Dekker, Inc., New York. https://doi.org/10.2307/2347928

Ratkowsky, D.A., Reedy, T.J., 1986. Choosing Near-Linear Parameters in the Four-Parameter Logistic Model for Radioligand and Related Assays. Int. Biometric Soc. 42, 575–582.

Reed, W.J., Hughes, B.D., 2002. From gene families and genera to incomes and internet file sizes: Why power laws are so common in nature. Phys. Rev. E 66, 4. https://doi.org/10.1103/PhysRevE.66.067103

Reynolds, J.H., David Ford, E., 2005. Improving competition representation in theoretical models of self-thinning: A critical review. J. Ecol. 93, 362–372. https://doi.org/10.1111/j.1365-2745.2005.00976.x

Reynolds, J.H., Ford, E.D., 2005. Improving competition representation in theoretical models of self-thinning : a critical review. J. Ecol. 93, 362–372. https://doi.org/10.1111/j.1365-2745.2005.00976.x

Rijal, B., Weiskittel, A.R., Kershaw, J.A., 2012. Development of regional height to diameter equations for 15 tree species in the North American Acadian Region. Forestry 85, 379–390. https://doi.org/10.1093/forestry/cps036

Seely, B., Nelson, J., Wells, R., Peter, B., Meitner, M., Anderson, A., Harshaw, H., Sheppard, S., Bunnell, F.L., Kimmins, H., Harrison, D., 2004. The application of a hierarchical, decision-support system to evaluate multi-objective forest management strategies: A case study in northeastern British Columbia, Canada. For. Ecol. Manage. 199, 283–305. https://doi.org/10.1016/j.foreco.2004.05.048

Segura, M., Kanninen, M., 2005. Allometric Models for Tree Volume and Total Aboveground Biomass in a Tropical Humid Forest in Costa Rica. Biotropica 37, 2–8. https://doi.org/10.1111/j.1744-7429.2005.02027.x

Sette Jr, C.R., Tomazello Fo, M., Lousada, J.L., Lopes, D., Laclau, J.P., 2016. Relationship between climate variables, trunk growth rate and wood density of Eucalyptus grandis W. Mill ex Maiden trees. Rev. Arvore 40, 337–346. https://doi.org/10.1590/0100-67622016000200016

Sharma, M., Parton, J., 2007. Height-diameter equations for boreal tree species in Ontario using a mixed-effects modeling approach. For. Ecol. Manage. 249, 187–198. https://doi.org/10.1016/j.foreco.2007.05.006

Silvertown, J., Charlesworth, D., 2001. Introduction to plant population biology, 4th editio. ed. Blackwell Science, Oxford, UK.

Solow, A.R., 2005. Power law without complexity. Ecol. l 8, 361–363.

Spies, T.A., Franklin, J.F., 2014. Gap Characteristics and Vegetation Response in Coniferous Forests of the Pacific Northwest Author (s): Thomas A . Spies and Jerry F . Franklin

Published by : Ecological Society of America GAP CHARACTERISTICS AND VEGETATION RESPONSE IN. Ecol. Soc. Am. 70, 543–545.

Tomppo, E., Olsson, H., Ståhl, G., Nilsson, M., Hagner, O., Katila, M., 2008. Combining national forest inventory field plots and remote sensing data for forest databases. Remote Sens. Environ. 112, 1982–1999. https://doi.org/10.1016/j.rse.2007.03.032

Tsega, M., Guadie, A., Teffera, Z.L., Belayneh, Y., Niu, D., 2018. Development and Validation of Height-Diameter Models for Cupressus lusitanica in Gergeda Forest, Ethiopia. Forest Sci. Technol. 14, 138–144. https://doi.org/10.1080/21580103.2018.1482794

Turner, M.D., Deborah, R., 1983. Factors Affecting Frequency Distributions of Plant Mass : The Absence of Dominance and Suppression in Competing Monocultures of Festuca Paradoxa. Ecology 64, 469–475.

Tyree, M.T., Dixon, M.A., 1986. Water stress induced cavitation and embolism in some woody plants. Physiol. Plant. 66, 397–405. https://doi.org/10.1111/j.1399-3054.1986.tb05941.x

Wang, X., Hao, Z., Zhang, J., Lian, J., Li, B., Ye, J., Yao, X., 2009. Tree size distributions in an old-growth temperate forest. Oikos 118, 25–36. https://doi.org/10.1111/j.0030-1299.2008.16598.x

Wang, X., Piao, S., Ciais, P., Li, J., Friedlingstein, P., Koven, C., Chen, A., 2011. Spring temperature change and its implication in the change of vegetation growth in North America from 1982 to 2006. Proc. Natl. Acad. Sci. U. S. A. 108, 1240–1245. https://doi.org/10.1073/pnas.1014425108

Weiner, J., 1986. How Competition for Light and Nutrients Affects Size Variability in Ipomoea Tricolor Populations. Ecology 67, 1425–1427.

Weiner, J., Solbrig, O.T., 1984. The meaning and measurement of size hierarchies in plant

populations. Oecologia 61, 334–336. https://doi.org/10.1007/BF00379630

Winsor, C.P., 1932. The Gompertz Curve as a Growth Curve. Proc. Natl. Acad. Sci. 18, 1–8. https://doi.org/10.1073/pnas.18.1.1

Wykoff, W.R., Crookston, N.L., Stage, A.R., 1982. User's guide to the stand prognosis model, US Department of Agriculture, Forest Service, General Technical Report. Ogden, Utah.

Yamamoto, S.-I., 2000. Forest Gap Dynamics and Tree Regeneration. J. For. Res. 5, 223–229. https://doi.org/10.1007/bf02767114

Yeh, H.-Y., Wensel, L.C., 2000. The relationship between tree diameter growth and climate for coniferous species in northern California. Can. J. For. Res. 30, 1463–1471. https://doi.org/10.1139/cjfr-30-9-1463

Yoda, K., Kira, T., Ogawa, H., Hozumi, K., 1963. Self-thinning in overcrowded pure stands under cultivated and natural conditions. J. Biol. Osaka City Univ. 14, 107–129.

Zhai, L., Bergeron, Y., Huang, J.G., Berninger, F., 2012. Variation in intra-annual wood formation, foliage and shoot development of three major Canadian boreal tree species. Am. J. Bot. 99, 827–837. https://doi.org/10.3732/ajb.1100235

Zhang, B., Cadotte, M.W., Chen, S., Tan, X., You, C., Ren, T., Chen, M., Wang, S., Li, W., Chu, C., Jiang, L., Bai, Y., Huang, J., Han, X., 2019. Plants alter their vertical root distribution rather than biomass allocation in response to changing precipitation. Ecology 100, 1–10. https://doi.org/10.1002/ecy.2828

Zhang, J., Huang, S., He, F., 2015. Half-century evidence from western Canada shows forest dynamics are primarily driven by competition followed by climate. Proc. Natl. Acad. Sci. U. S. A. 112, 4009–4014. https://doi.org/10.1073/pnas.1420844112

Zhang, L., Gove, J.H., Liu, C., Leak, W.B., 2001. A finite mixture of two Weibull distributions

for modeling the diameter distributions of rotated-sigmoid, uneven-aged stands. Can. J. For. Res. 31, 1654–1659. https://doi.org/10.1139/cjfr-31-9-1654

Zhou, Y., Lei, Z., Zhou, F., Han, Y., Yu, D., Zhang, Y., 2019. Impact of climate factors on height growth of pinus sylvestris var. Mongolica. PLoS One 14, 1–15. https://doi.org/10.1371/journal.pone.0213509

Appendix A: Location of permanent sampling plots (PSP)

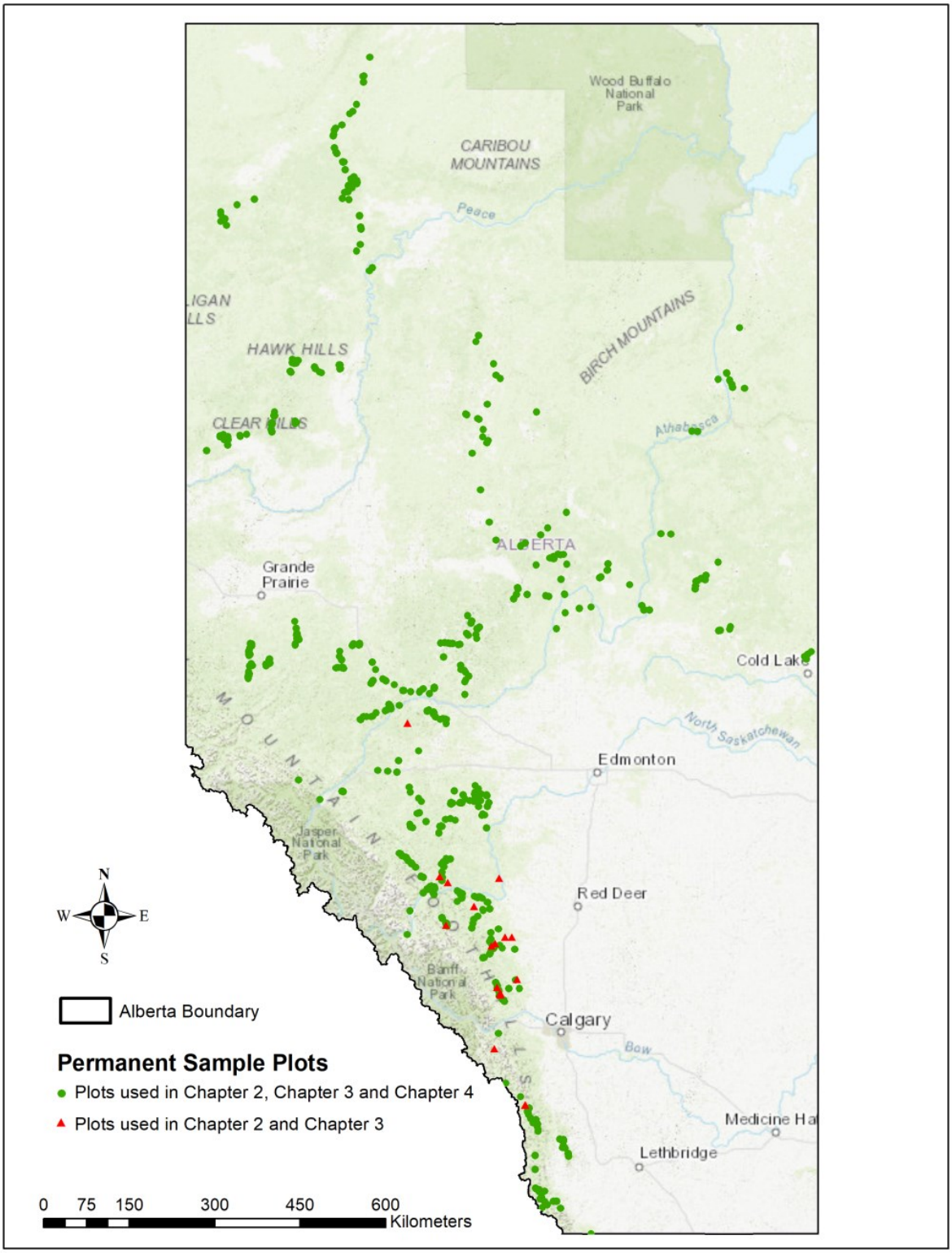

Appendix B: Detailed model selection results for Chapter 3

Table B.1 Model selection criteria for species Aspen

Model name	AIC	RMSE	R^2	a	b	c	d
aw1nlme	38018.65	1.84	0.86	4.453	0.481		
aw1a	39623.47	1.88	0.86	5.123	0.421		
aw1b	38316.76	0.97	0.96	4.101	0.489		
aw1nls	44468.97	2.57	0.74	4.133	0.494		
aw2nlme	37334.04	1.75	0.88	3.416	-10.439		
aw2a	37621.1	0.97	0.96	3.429	-10.598		
aw2b	38477.61	1.03	0.96	3.465	-11.210		
aw2nls	43546.83	2.45	0.76	3.495	-11.646		
aw3nlme	37480.43	1.77	0.88	33.819	16.512		
aw3a	38240.81	1.07	0.95	30.426	12.665		
aw3b	37730.47	1.83	0.87	36.479	19.852		
aw3nls	43703	2.47	0.76	39.092	22.133		
aw4nlme	NA	NA	NA	NA	NA		
aw4a	NA	NA	NA	NA	NA		
aw4b	37724.7	1.85	0.86	28.430	0.053		
aw4nls	43535.51	2.45	0.76	28.030	0.055		
aw5nlme	37363.04	0.90	0.97	1.117	0.178		
aw5a	38157.51	0.99	0.96	1.187	0.173		
aw5b	37688.29	1.02	0.96	1.118	0.177		
aw5nls	43553.94	2.45	0.76	1.227	0.169		
aw6nlme	37298.88	1.74	0.88	29.465	-9.030		
aw6a	37862.66	1.02	0.96	28.491	-8.235		
aw6b	38603.27	1.04	0.96	31.294	-10.138		
aw6nls	43576.76	2.45	0.76	32.109	-10.467		
aw7nlme	38338.15	0.82	0.97	10.918	0.387		
aw7a	39400.93	0.99	0.96	10.176	0.341		
aw7b	39293.4	0.99	0.96	9.696	0.412		
aw7nls	45481.72	2.71	0.71	10.578	0.388		
aw8nlme	37299.16	1.75	0.88	29.829	9.528		
aw8a	37849.42	1.02	0.96	28.793	8.698		
aw8b	38537	1.03	0.96	31.634	10.662		
aw8nls	43558.85	2.45	0.76	32.529	11.043		
aw9nlme	NA	NA	NA	NA	NA	NA	
aw9a	37582.17	0.95	0.96	3.603	-5.778	-0.710	
aw9b	NA	NA	NA	NA	NA	NA	
aw9c	NA	NA	NA	NA	NA	NA	
aw9ab	NA	NA	NA	NA	NA	NA	
aw9ac	NA	NA	NA	NA	NA	NA	
aw9bc	NA	NA	NA	NA	NA	NA	
aw9nls	43551.88	2.45	0.76	3.556	-7.906	-0.851	

Model name	AIC	RMSE	R^2	a	b	c	d
aw10nlme	37366.42	1.73	0.88	23.956	3.345	0.122	
aw10a	37916.92	1.02	0.96	23.567	3.415	0.132	
aw10b	39655.66	1.88	0.86	27.844	2.251	0.071	
aw10c	39099.87	1.83	0.87	26.821	2.518	0.084	
aw10ab	37441.99	1.75	0.88	24.229	3.162	0.116	
aw10ac	37488.59	1.74	0.88	23.360	4.012	0.147	
aw10bc	37193.07	1.79	0.87	27.480	2.863	0.083	
aw10nls	43546.53	2.45	0.76	25.662	3.547	0.113	
aw11nlme	NA	NA	NA	NA	NA	NA	
aw11a	37906.52	1.02	0.96	23.878	0.094	1.361	
aw11b	NA	NA	NA	NA	NA	NA	
aw11c	NA	NA	NA	NA	NA	NA	
aw11ab	NA	NA	NA	NA	NA	NA	
aw11ac	NA	NA	NA	NA	NA	NA	
aw11bc	NA	NA	NA	NA	NA	NA	
aw11nls	43511.84	2.44	0.76	27.108	0.065	1.145	
aw12nlme	NA	NA	NA	NA	NA	NA	
aw12a	37914.15	1.02	0.96	23.717	0.047	1.183	
aw12b	37694.35	1.85	0.86	29.062	0.058	0.954	
aw12c	37577.99	1.82	0.87	29.642	0.072	0.870	
aw12ab	NA	NA	NA	NA	NA	NA	
aw12ac	NA	NA	NA	NA	NA	NA	
aw12bc	NA	NA	NA	NA	NA	NA	
aw12nls	43511.18	2.44	0.76	26.923	0.047	1.083	
aw13nlme	NA	NA	NA	NA	NA	NA	
aw13a	37576.02	1.80	0.87	25.163	1.778	0.089	
aw13b	39629.73	1.88	0.86	29.196	1.317	0.051	
aw13c	37737.83	1.84	0.86	28.037	1.573	0.065	
aw13ab	37361.56	1.75	0.88	24.721	1.788	0.092	
aw13ac	37401.84	1.74	0.88	24.172	2.181	0.115	
aw13bc	37503.23	1.79	0.87	28.785	1.489	0.058	
aw13nls	43514.14	2.44	0.76	26.266	1.912	0.087	
aw14nlme	NA	NA	NA	NA	NA	NA	
aw14a	39356.1	1.86	0.86	0.052	1.234	27.849	
aw14b	40491.36	1.45	0.92	0.081	0.462	28.272	
aw14c	37756.84	1.01	0.96	0.084	0.800	25.416	
aw14ab	NA	NA	NA	NA	NA	NA	
aw14ac	37347.36	1.74	0.88	0.095	0.614	25.392	
aw14bc	37314.78	1.74	0.88	0.090	0.650	25.540	
aw14nls	43513.27	2.44	0.51	0.074	0.735	27.400	
aw15nlme	NA	NA		NA	NA	NA	
aw15a	39480.59	1.47	0.91	1.874	0.366	0.031	
aw15b	37903.18	0.98	0.96	1.375	0.416	0.030	
aw15c	37875.74	1.10	0.95	1.234	0.381	0.033	

Model name	AIC	RMSE	R^2	a	b	c	d
aw15ab	37319.53	1.75	0.88	1.751	0.358	0.032	
aw15ac	37385.58	1.75	0.88	2.451	0.268	0.035	
aw15bc	37437.14	0.92	0.97	1.878	0.326	0.034	
aw15nls	43537.86	2.45	0.76	2.251	0.339	0.030	
aw16nlme	NA	NA	NA	NA	NA	NA	
aw16a	38233.12	1.04	0.96	24.718	-24.934	1.902	
aw16b	NA	NA	NA	NA	NA	NA	
aw16c	37646.92	1.83	0.87	39.555	-5.066	0.997	
aw16ab	NA	NA	NA	NA	NA	NA	
aw16ac	NA	NA	NA	NA	NA	NA	
aw16bc	NA	NA	NA	NA	NA	NA	
aw16nls	43538.41	2.45	0.76	32.720	-9.077	1.302	
aw17nlme	NA	NA	NA	NA	NA	NA	
aw17a	37507.5	1.80	0.87	31.058	-10.725	1.192	
aw17b	39103.33	1.83	0.87	33.059	-13.634	3.724	
aw17c	39879.49	1.60	0.90	35.683	-15.746	4.387	
aw17ab	37338.19	1.74	0.88	28.022	-7.160	-1.948	
aw17ac	38431.44	1.04	0.96	24.069	-2.848	-6.962	
aw17bc	NA	NA	NA	NA	NA	NA	
aw17nls	43542.18	2.45	0.76	33.669	-12.643	1.823	
aw18nlme	NA	NA	NA	NA	NA	NA	
aw18a	37510.79	1.80	0.87	28.718	0.028	1.407	
aw18b	37740.83	1.86	0.86	32.368	0.028	1.298	
aw18c	38815.02	1.80	0.87	34.537	0.056	1.007	
aw18ab	NA	NA	NA	NA	NA	NA	
aw18ac	NA	NA	NA	NA	NA	NA	
aw18bc	NA	NA	NA	NA	NA	NA	
aw18nls	43526.17	2.44	0.76	30.759	0.024	1.401	
aw19nlme	NA	NA	NA	NA	NA	NA	NA
aw19a	37517.47	1.80	0.87	26.274	1.157	0.058	0.748
aw19b	NA	NA	NA	NA	NA	NA	NA
aw19c	NA	NA	NA	NA	NA	NA	NA
aw19d	NA	NA	NA	NA	NA	NA	NA
aw19ab	NA	NA	NA	NA	NA	NA	NA
aw19ac	NA	NA	NA	NA	NA	NA	NA
aw19ad	NA	NA	NA	NA	NA	NA	NA
aw19bc	NA	NA	NA	NA	NA	NA	NA
aw19bd	NA	NA	NA	NA	NA	NA	NA
aw19cd	NA	NA	NA	NA	NA	NA	NA
aw19abc	37527.51	1.80		26.272	1.156	0.058	0.749
aw19abd	NA	NA	NA	NA	NA	NA	NA
aw19acd	NA	NA	NA	NA	NA	NA	NA
aw19bcd	NA	NA	NA	NA	NA	NA	NA
aw19nls	43511.15	2.44	0.76	26.724	0.727	0.074	1.933

Table B.2 Model selection criteria for species White birch

Model name	AIC	RMSE	R^2	a	b	c	d
bw1nlme	NA	NA	NA	NA	NA		
bw1a	2655.24	1.63	0.74	2.870	0.580		
bw1b	2600.97	0.99	0.90	3.113	0.548		
bw1nls	2853.69	2.15	0.54	3.283	0.538		
bw2nlme	2580.86	1.09	0.88	3.284	-10.102		
bw2a	2597.26	0.96	0.91	3.226	-9.262		
bw2b	2663.02	1.26	0.84	3.242	-9.355		
bw2nls	2835.12	2.12	0.55	3.274	-9.656		
bw3nlme	NA	NA	NA	NA	NA		
bw3a	2690.33	1.12	0.88	20.334	7.043		
bw3b	2703.73	1.17	0.86	21.647	8.340		
bw3nls	2839.52	2.13	0.55	32.379	19.028		
bw4nlme	NA	NA	NA	NA	NA		
bw4a	2640.38	1.06	0.89	17.580	0.107		
bw4b	2688.23	1.68	0.72	27.338	0.048		
bw4nls	2836.43	2.12	0.55	22.333	0.069		
bw5nlme	2607.93	1.18	0.86	1.164	0.188		
bw5a	2646.75	1.13	0.87	1.105	0.192		
bw5b	2595.12	0.99	0.90	1.081	0.195		
bw5nls	2835.82	2.12	0.55	1.119	0.189		
bw6nlme	2594.93	1.55	0.76	23.827	-7.745		
bw6a	2641.98	1.06	0.89	20.631	-5.808		
bw6b	2668.82	1.30	0.83	24.687	-8.175		
bw6nls	2835.26	2.12	0.55	25.455	-8.445		
bw7nlme	2616.18	1.57	0.76	6.691	0.504		
bw7a	2656.89	1.08	0.89	7.669	0.432		
bw7b	2608.89	1.00	0.90	6.893	0.478		
bw7nls	2871.61	2.18	0.53	7.645	0.451		
bw8nlme	2620.12	1.34	0.82	24.014	8.116		
bw8a	2643.76	1.07	0.89	20.825	6.168		
bw8b	2665.82	1.28	0.84	25.121	8.747		
bw8nls	2835.12	2.12	0.55	25.923	9.032		
bw9nlme	NA	NA	NA	NA	NA	NA	
bw9a	2599.09	0.96	0.91	3.364	-5.587	-0.757	
bw9b	NA	NA	NA	NA	NA	NA	
bw9c	NA	NA	NA	NA	NA	NA	
bw9ab	NA	NA	NA	NA	NA	NA	
bw9ac	NA	NA	NA	NA	NA	NA	
bw9bc	NA	NA	NA	NA	NA	NA	

Model name	AIC	RMSE	R^2	a	b	c	d
bw9nls	2837.11	2.12	0.55	3.289	-7.321	-0.914	
bw10nlme	NA	NA	NA	NA	NA	NA	
bw10a	2634.01	1.00	0.90	16.577	5.260	0.237	
bw10b	2691.18	1.66	0.73	27.556	2.479	0.059	
bw10c	NA	NA	NA	NA	NA	NA	
bw10ab	NA	NA	NA	NA	NA	NA	
bw10ac	2609.91	1.53	0.77	16.432	9.085	0.290	
bw10bc	NA	NA	NA	NA	NA	NA	
bw10nls	2838.76	2.12	0.55	19.666	3.637	0.154	
bw11nlme	NA	NA	NA	NA	NA	NA	
bw11a	2640.38	1.00	0.90	16.535	0.203	2.814	
bw11b	NA	NA	NA	NA	NA	NA	
bw11c	NA	NA	NA	NA	NA	NA	
bw11ab	NA	NA	NA	NA	NA	NA	
bw11ac	NA	NA	NA	NA	NA	NA	
bw11bc	NA	NA	NA	NA	NA	NA	
bw11nls	2837.26	2.12	0.55	20.915	0.090	1.233	
bw12nlme	NA	NA	NA	NA	NA	NA	
bw12a	2638.70	1.60	0.75	18.448	0.060	1.186	
bw12b	NA	NA	NA	NA	NA	NA	
bw12c	NA	NA	NA	NA	NA	NA	
bw12ab	2590.85	1.65	0.73	17.945	0.048	1.286	
bw12ac	NA	NA	NA	NA	NA	NA	
bw12bc	NA	NA	NA	NA	NA	NA	
bw12nls	2837.32	2.12	0.55	20.731	0.057	1.124	
bw13nlme	NA	NA	NA	NA	NA	NA	
bw13a	2637.12	1.00	0.90	16.587	3.206	0.208	
bw13b	NA	NA	NA	NA	NA	NA	
bw13c	NA	NA	NA	NA	NA	NA	
bw13ab	NA	NA	NA	NA	NA	NA	
bw13ac	NA	NA	NA	NA	NA	NA	
bw13bc	NA	NA	NA	NA	NA	NA	
bw13nls	2837.77	2.12	0.55	20.209	1.988	0.119	
bw14nlme	NA	NA	NA	NA	NA	NA	
bw14a	NA	NA	NA	NA	NA	NA	
bw14b	2698.70	1.69	0.72	0.032	1.408	28.474	
bw14c	2633.05	1.03	0.90	0.163	0.340	18.137	
bw14ab	2655.00	1.75	0.70	0.042	1.210	27.409	
bw14ac	NA	NA	NA	NA	NA	NA	
bw14bc	2596.24	1.53	0.77	0.194	-0.159	19.116	

Model name	AIC	RMSE	R^2	a	b	c	d
bw14nls	2837.28	2.12	0.55	0.093	0.719	22.098	
bw15nlme	2596.71	1.55	0.76	3.903	0.103	0.046	
bw15a	2695.13	1.70	0.71	0.681	0.507	0.034	
bw15b	2631.74	1.04	0.89	1.559	0.382	0.038	
bw15c	2602.31	1.05	0.89	0.844	0.455	0.038	
bw15ab	2613.90	1.51	0.77	4.265	0.045	0.048	
bw15ac	2587.22	1.55	0.76	3.769	0.112	0.046	
bw15bc	2587.12	1.09	0.88	2.315	0.312	0.039	
bw15nls	2837.09	2.12	0.55	2.115	0.307	0.039	
bw16nlme	NA	NA	NA	NA	NA	NA	
bw16a	2660.86	1.01	0.90	16.483	-195.472	3.067	
bw16b	2677.36	1.64	0.73	251.788	-4.642	0.539	
bw16c	2970.30	1.06	0.89	0.000	23.234	0.351	
bw16ab	NA	NA	NA	NA	NA	NA	
bw16ac	2611.02	1.54	0.76	18.330	-112.911	2.687	
bw16bc	NA	NA	NA	NA	NA	NA	
bw16nls	2837.09	2.12	0.55	24.975	-9.164	1.409	
bw17nlme	NA	NA	NA	NA	NA	NA	
bw17a	2643.97	1.60	0.75	21.562	-5.458	-1.800	
bw17b	2648.16	1.72	0.70	22.362	-5.193	-2.955	
bw17c	2692.49	1.68	0.72	41.443	-31.089	13.559	
bw17ab	NA	NA	NA	NA	NA	NA	
bw17ac	2610.82	1.56	0.76	19.908	-3.080	-5.091	
bw17bc	NA	NA	NA	NA	NA	NA	
bw17nls	2837.10	2.12	0.55	26.141	-9.304	0.715	
bw18nlme	NA	NA	NA	NA	NA	NA	
bw18a	2655.52	1.00	0.90	16.505	0.002	3.028	
bw18b	NA	NA	NA	NA	NA	NA	
bw18c	NA	NA	NA	NA	NA	NA	
bw18ab	NA	NA	NA	NA	NA	NA	
bw18ac	2613.73	1.54	0.76	17.331	0.001	3.171	
bw18bc	NA	NA	NA	NA	NA	NA	
bw18nls	2837.10	2.12	0.55	23.716	0.029	1.468	
bw19nlme	NA	NA	NA	NA	NA	NA	NA
bw19a	NA	NA	NA	NA	NA	NA	NA
bw19b	NA	NA	NA	NA	NA	NA	NA
bw19c	NA	NA	NA	NA	NA	NA	NA
bw19d	NA	NA	NA	NA	NA	NA	NA
bw19ab	NA	NA	NA	NA	NA	NA	NA
bw19ac	NA	NA	NA	NA	NA	NA	NA

Model name	AIC	RMSE	R^2	a	b	c	d
bw19ad	NA	NA	NA	NA	NA	NA	NA
bw19bc	NA	NA	NA	NA	NA	NA	NA
bw19bd	NA	NA	NA	NA	NA	NA	NA
bw19cd	NA	NA	NA	NA	NA	NA	NA
bw19abc	NA	NA	NA	NA	NA	NA	NA
bw19abd	NA	NA	NA	NA	NA	NA	NA
bw19acd	NA	NA	NA	NA	NA	NA	NA
bw19bcd	NA	NA	NA	NA	NA	NA	NA
bw19nls	2839.08	2.12	0.55	21.964	1.266	0.063	0.624

Table B.3 Model selection criteria for species White spruce

Model name	AIC	RMSE	R^2	a	b	c	d
sw1nlme	129478.90	2.16	0.89	2.020	0.705		
sw1a	130364.60	2.23	0.88	2.187	0.660		
sw1b	131167.40	2.27	0.88	2.358	0.632		
sw1nls	163110.80	3.26	0.74	2.464	0.649		
sw2nlme	128515.70	0.91	0.98	3.612	-17.243		
sw2a	130836.10	1.00	0.98	3.591	-16.550		
sw2b	132843.00	0.92	0.98	3.697	-18.620		
sw2nls	158456.70	3.03	0.78	3.717	-17.699		
sw3nlme	NA	NA	NA	NA	NA		
sw3a	128598.90	2.13	0.89	54.321	47.558		
sw3b	128366.30	2.13	0.89	58.979	54.776		
sw3nls	160407.50	3.12	0.77	59.249	48.155		
sw4nlme	NA	NA	NA	NA	NA		
sw4a	131878.60	0.99	0.98	28.835	0.041		
sw4b	NA	NA	NA	NA	NA		
sw4nls	159803.40	3.09	0.77	37.980	0.031		
sw5nlme	127171.40	2.03	0.90	1.949	0.152		
sw5a	128425.20	2.13	0.89	2.031	0.147		
sw5b	131410.30	1.07	0.97	1.809	0.160		
sw5nls	158869.20	3.05	-0.68	1.843	0.147		
sw6nlme	127778.20	2.03	0.90	36.235	-15.525		
sw6a	131697.10	1.00	0.98	32.966	-13.496		
sw6b	133696.40	0.92	0.98	39.155	-16.986		
sw6nls	158501.40	3.03	0.78	39.896	-16.142		
sw7nlme	130828.30	0.78	0.99	5.06	0.54		
sw7a	132893.50	2.36	0.87	6.126	0.488		
sw7b	NA	NA	NA	NA	NA		
sw7nls	166262.20	3.43	0.72	7.358	0.497		

Model name	AIC	RMSE	R^2	a	b	c	d
sw8nlme	127632.20	2.03	0.90	36.899	16.335		
sw8a	131435.10	1.00	0.98	33.474	14.216		
sw8b	133256.60	0.92	0.98	39.725	17.785		
sw8nls	158468.50	3.03	0.78	40.509	16.906		
sw9nlme	127250.10	2.04	0.90	4.142	-7.280	-0.560	
sw9a	129385.80	0.92	0.98	4.450	-6.309	-0.441	
sw9b	NA	NA	NA	NA	NA	NA	
sw9c	128020.50	2.11	0.89	4.304	-6.645	-0.493	
sw9ab	127250.10	2.04	0.90	4.142	-7.280	-0.560	
sw9ac	NA	NA	NA	NA	NA	NA	
sw9bc	127451.30	2.05	0.90	4.584	-6.230	-0.411	
sw9nls	158480.60	3.03	0.78	3.733	-14.071	-0.934	
sw10nlme	NA	NA	NA	NA	NA	NA	
sw10a	131566.40	0.99	0.98	25.458	5.433	0.113	
sw10b	141040.80	2.23	0.88	32.640	5.055	0.074	
sw10c	129074.30	2.16	0.89	31.156	5.013	0.081	
sw10ab	127692.50	2.04	0.90	28.294	5.415	0.096	
sw10ac	127830.80	2.04	0.90	28.835	5.593	0.097	
sw10bc	NA	NA	NA	NA	NA	NA	
sw10nls	158629.50	3.04	0.78	28.680	6.503	0.114	
sw11nlme	NA	NA	NA	NA	NA	NA	
sw11a	131482.60	1.00	0.98	26.327	0.071	1.667	
sw11b	128122.10	2.12	0.89	39.306	0.027	1.002	
sw11c	129384.20	2.19	0.89	60.236	0.011	0.809	
sw11ab	127156.60	2.03	0.90	34.664	0.041	1.248	
sw11ac	127149.30	2.03	0.90	32.189	0.043	1.258	
sw11bc	NA	NA	NA	NA	NA	NA	
sw11nls	158312.80	3.02	0.78	30.870	0.063	1.693	
sw12nlme	NA	NA	NA	NA	NA	NA	
sw12a	131431.00	1.00	0.98	25.887	0.019	1.340	
sw12b	128084.10	2.12	0.89	36.558	0.024	1.070	
sw12c	127983.70	2.11	0.89	35.288	0.025	1.059	
sw12ab	NA	NA	NA	NA	NA	NA	
sw12ac	127347.30	2.04	0.90	36.237	0.021	1.125	
sw12bc	127230.80	2.03	0.90	34.285	0.021	1.163	
sw12nls	158323.30	3.02	0.78	30.010	0.015	1.361	
sw13nlme	127117.50	2.01	0.90	32.459	2.355	0.061	
sw13a	131214.80	0.99	0.98	26.057	2.521	0.085	
sw13b	129753.80	2.27	0.88	35.74	2.241	0.050	
sw13c	128356.10	2.13	0.89	33.170	2.193	0.055	

Model name	AIC	RMSE	R^2	a	b	c	d
sw13ab	127335.70	2.03	0.90	29.790	2.356	0.067	
sw13ac	127330.40	2.03	0.90	31.191	2.423	0.067	
sw13bc	127503.40	2.05	0.90	33.141	2.260	0.056	
sw13nls	158355.90	3.02	0.78	29.770	2.750	0.082	
sw14nlme	127194.90	2.02	0.90	0.060	0.565	29.214	
sw14a	129899.10	2.32	0.87	0.053	0.612	30.853	
sw14b	144308.40	1.42	0.95	0.082	0.054	31.327	
sw14c	129913.00	0.96	0.98	0.059	0.667	27.601	
sw14ab	130169.00	2.19	0.89	0.053	0.706	30.374	
sw14ac	127426.80	2.04	0.90	0.063	0.511	28.962	
sw14bc	127368.20	2.03	0.90	0.066	0.456	28.755	
sw14nls	158412.70	3.03	0.78	0.082	0.220	29.878	
sw15nlme	127002.70	2.01	0.90	3.215	0.663	0.021	
sw15a	130274.30	2.24	0.88	5.499	0.550	0.021	
sw15b	130088.40	0.96	0.98	1.639	0.812	0.019	
sw15c	129529.60	2.16	0.89	3.722	0.491	0.028	
sw15ab	127126.80	2.03	0.90	3.730	0.612	0.022	
sw15ac	127342.50	2.03	0.90	4.847	0.498	0.025	
sw15bc	127167.30	2.03	0.90	3.483	0.628	0.022	
sw15nls	158366.80	3.02	0.78	6.911	0.246	0.027	
sw16nlme	NA	NA	NA	NA	NA	NA	
sw16a	128183.10	2.11	0.89	44.117	-8.743	1.093	
sw16b	128465.90	2.14	0.89	67.591	-6.418	0.864	
sw16c	128001.20	2.11	0.89	55.868	-7.168	0.952	
sw16ab	127164.80	2.03	0.90	45.502	-8.846	1.085	
sw16ac	127173.10	2.02	0.90	46.926	-9.539	1.113	
sw16bc	NA	NA	NA	NA	NA	NA	
sw16nls	158429.10	3.03	0.78	39.012	-15.481	1.360	
sw17nlme	NA	NA	NA	NA	NA	NA	
sw17a	132794.00	1.02	0.97	31.412	-11.399	-1.455	
sw17b	137858.80	0.96	0.98	35.656	-12.242	-3.100	
sw17c	130100.80	2.30	0.87	61.171	-45.406	13.988	
sw17ab	127183.70	2.02	0.90	40.983	-21.540	3.514	
sw17ac	127275.70	2.03	0.90	41.658	-22.361	3.988	
sw17bc	127211.80	2.03	0.90	44.512	-25.870	5.248	
sw17nls	158458.60	3.03	0.78	41.167	-17.730	1.020	
sw18nlme	NA	NA	NA	NA	NA	NA	
sw18a	128197.60	2.11	0.89	38.580	0.014	1.316	
sw18b	128104.90	2.12	0.89	46.633	0.014	1.209	
sw18c	127935.40	2.11	0.89	44.311	0.015	1.210	

Model name	AIC	RMSE	R^2	a	b	c	d
sw18ab	127277.70	2.02	0.90	35.414	0.009	1.554	
sw18ac	127228.10	2.03	0.90	43.192	0.011	1.366	
sw18bc	126445.40	2.03	0.90	41.176	0.013	1.334	
sw18nls	158337.70	3.02	0.78	34.700	0.006	1.698	
sw19nlme	NA	NA	NA	NA	NA	NA	NA
sw19a	128182.10	2.11	0.89	33.749	1.101	0.033	0.855
sw19b	NA	NA	NA	NA	NA	NA	NA
sw19c	NA	NA	NA	NA	NA	NA	NA
sw19d	NA	NA	NA	NA	NA	NA	NA
sw19ab	NA	NA	NA	NA	NA	NA	NA
sw19ac	NA	NA	NA	NA	NA	NA	NA
sw19ad	NA	NA	NA	NA	NA	NA	NA
sw19bc	NA	NA	NA	NA	NA	NA	NA
sw19bd	NA	NA	NA	NA	NA	NA	NA
sw19cd	NA	NA	NA	NA	NA	NA	NA
sw19abc	NA	NA	NA	NA	NA	NA	NA
sw19abd	NA	NA	NA	NA	NA	NA	NA
sw19acd	NA	NA	NA	NA	NA	NA	NA
sw19bcd	NA	NA	NA	NA	NA	NA	NA
sw19nls	158313.20	3.02	0.78	30.682	0.912	0.066	1.993

Table B.4 Model selection criteria for species Lodgepole pine

Model name	AIC	RMSE	R^2	a	b	c	d
pl1nlme	114432.00	1.55	0.89	3.359	0.553		
pl1a	115360.60	1.58	0.88	3.375	0.536		
pl1b	117212.60	0.86	0.97	3.188	0.550		
pl1nls	152264.80	2.61	0.69	2.490	0.642		
pl2nlme	115251.40	0.79	0.97	3.379	-11.532		
pl2a	117014.50	0.91	0.96	3.373	-11.045		
pl2b	117332.20	1.64	0.88	3.455	-12.439		
pl2nls	151864.30	2.59	0.69	3.553	-14.410		
pl3nlme	NA	NA	NA	NA	NA		
pl3a	118407.00	0.97	0.96	29.315	13.978		
pl3b	114935.00	1.56	0.89	39.202	26.353		
pl3nls	151534.80	2.58	0.69	50.573	38.697		
pl4nlme	114077.70	1.53	0.89	26.657	0.056		
pl4a	117472.60	0.93	0.96	23.126	0.070		
pl4b	115491.70	1.60	0.88	29.194	0.045		
pl4nls	151436.10	2.58	0.69	32.600	0.038		
pl5nlme	114019.10	1.52	0.89	1.289	0.179		

Model name	AIC	RMSE	R^2	a	b	c	d
pl5a	118279.20	0.86	0.97	1.367	0.172		
pl5b	117168.40	0.95	0.96	1.226	0.182		
pl5nls	151508.70	2.58	0.69	1.593	0.160		
pl6nlme	113375.80	1.52	0.89	28.598	-10.041		
pl6a	117893.50	0.95	0.96	26.772	-8.548		
pl6b	117955.50	1.66	0.87	30.726	-11.157		
pl6nls	152107.70	2.60	0.69	33.683	-12.932		
pl7nlme	115365.70	0.70	0.98	8.157	0.453		
pl7a	117858.30	0.80	0.97	8.499	0.430		
pl7b	118631.90	0.81	0.97	7.512	0.464		
pl7nls	153426.70	2.66	0.67	6.806	0.517		
pl8nlme	114197.30	1.52	0.89	29.184	10.710		
pl8a	117767.00	0.94	0.96	27.111	9.049		
pl8b	120213.50	0.85	0.97	31.010	11.633		
pl8nls	151979.40	2.60	0.69	34.287	13.654		
pl9nlme	NA	NA	NA	NA	NA	NA	
pl9a	116103.80	0.85	0.97	4.548	-4.433	-0.316	
pl9b	114911.60	1.56	0.89	6.290	-5.520	-0.155	
pl9c	114904.20	1.56	0.89	4.855	-4.487	-0.265	
pl9ab	NA	NA	NA	NA	NA	NA	
pl9ac	NA	NA	NA	NA	NA	NA	
pl9bc	NA	NA	NA	NA	NA	NA	
pl9nls	151477.90	2.58	0.69	4.121	-5.993	-0.518	
pl10nlme	NA	NA	NA	NA	NA	NA	
pl10a	117472.70	0.92	0.96	21.982	3.298	0.127	
pl10b	116158.70	1.60	0.88	30.915	3.138	0.064	
pl10c	115536.00	1.59	0.88	27.623	3.138	0.080	
pl10ab	114179.20	1.53	0.89	24.183	3.099	0.100	
pl10ac	NA	NA	NA	NA	NA	NA	
pl10bc	114474.60	1.55	0.89	29.143	3.071	0.071	
pl10nls	151451.10	2.58	0.69	26.353	4.335	0.105	
pl11nlme	NA	NA	NA	NA	NA	NA	
pl11a	114746.10	1.55	0.89	27.512	0.043	0.858	
pl11b	NA	NA	NA	NA	NA	NA	
pl11c	NA	NA	NA	NA	NA	NA	
pl11ab	NA	NA	NA	NA	NA	NA	
pl11ac	113006.50	1.53	0.89	27.589	0.043	0.865	
pl11bc	NA	NA	NA	NA	NA	NA	
pl11nls	151417.20	2.57	-0.92	30.918	0.044	1.085	
pl12nlme	NA	NA	NA	NA	NA	NA	
pl12a	114747.20	1.55	0.89	27.784	0.063	0.909	

Model name	AIC	RMSE	R^2	a	b	c	d
pl12b	NA	NA	NA	NA	NA	NA	
pl12c	114754.60	1.56	0.89	32.708	0.063	0.817	
pl12ab	114178.50	1.53	0.89	24.842	0.048	1.096	
pl12ac	114569.40	1.53	0.89	36.342	0.053	0.881	
pl12bc	NA	NA	NA	NA	NA	NA	
pl12nls	151415.10	2.57	0.69	30.510	0.035	1.060	
pl13nlme	NA	NA	NA	NA	NA	NA	
pl13a	114842.50	1.56	0.89	25.338	1.654	0.072	
pl13b	116114.70	1.60	0.88	35.608	1.622	0.038	
pl13c	NA	NA	NA	NA	NA	NA	
pl13ab	113986.40	1.53	0.89	25.382	1.669	0.072	
pl13ac	114369.50	1.53	0.89	23.796	1.925	0.094	
pl13bc	114254.80	1.55	0.89	31.386	1.598	0.047	
pl13nls	151398.10	2.57	0.69	27.937	2.073	0.073	
pl14nlme	113842.30	1.52	0.89	0.060	1.010	25.979	
pl14a	121482.60	0.80	0.97	0.014	1.600	33.637	
pl14b	116827.70	1.64	0.88	0.023	1.640	30.738	
pl14c	114723.60	1.55	0.89	0.049	1.169	26.747	
pl14ab	NA	NA	NA	NA	NA	NA	
pl14ac	113958.30	1.53	0.89	0.053	1.113	26.635	
pl14bc	113891.40	1.53	0.89	0.057	1.037	26.196	
pl14nls	151438.90	2.58	0.69	0.055	0.787	29.098	
pl15nlme	NA	NA	NA	NA	NA	NA	
pl15a	122531.10	1.01	0.95	-1.171	0.801	0.022	
pl15b	117044.40	0.88	0.96	-1.097	0.785	0.023	
pl15c	117936.80	0.99	0.95	0.053	0.598	0.030	
pl15ab	114015.10	1.53	0.89	-0.135	0.676	0.026	
pl15ac	114011.70	1.53	0.89	0.653	0.566	0.030	
pl15bc	115471.10	0.79	0.97	-0.141	0.663	0.027	
pl15nls	151453.80	2.58	0.69	1.374	0.628	0.023	
pl16nlme	NA	NA	NA	NA	NA	NA	
pl16a	114753.50	1.55	0.89	35.827	-5.818	1.057	
pl16b	115014.00	1.57	0.89	68.151	-4.199	0.733	
pl16c	114752.30	1.56	0.89	51.195	-4.532	0.838	
pl16ab	NA	NA	NA	NA	NA	NA	
pl16ac	114080.90	1.52	0.89	30.670	-8.402	1.283	
pl16bc	NA	NA	NA	NA	NA	NA	
pl16nls	151447.90	2.58	0.69	45.713	-6.874	1.020	
pl17nlme	NA	NA	NA	NA	NA	NA	
pl17a	114739.50	1.55	0.89	34.550	-18.333	6.157	
pl17b	128006.00	0.89	0.96	26.301	-5.473	-5.048	

Model name	AIC	RMSE	R^2	a	b	c	d
pl17c	124568.50	0.64	0.98	64.136	-43.823	12.484	
pl17ab	113985.50	1.52	0.89	31.291	-13.583	2.796	
pl17ac	113920.80	1.52	0.89	32.912	-15.938	4.534	
pl17bc	114057.80	1.53	0.89	35.910	-20.480	6.725	
pl17nls	151437.20	2.58	0.69	41.878	-23.281	6.386	
pl18nlme	NA	NA	NA	NA	NA	NA	
pl18a	114753.50	1.55	0.89	33.503	0.040	1.095	
pl18b	NA	NA	NA	NA	NA	NA	
pl18c	114730.50	1.56	0.89	42.608	0.043	0.913	
pl18ab	113349.50	1.52	0.89	26.661	0.021	1.529	
pl18ac	NA	NA	NA	NA	NA	NA	
pl18bc	NA	NA	NA	NA	NA	NA	
pl18nls	151438.40	2.58	0.69	39.340	0.022	1.195	
pl19nlme	NA	NA	NA	NA	NA	NA	NA
pl19a	NA	NA	NA	NA	NA	NA	NA
pl19b	NA	NA	NA	NA	NA	NA	NA
pl19c	NA	NA	NA	NA	NA	NA	NA
pl19d	NA	NA	NA	NA	NA	NA	NA
pl19ab	NA	NA	NA	NA	NA	NA	NA
pl19ac	NA	NA	NA	NA	NA	NA	NA
pl19ad	NA	NA	NA	NA	NA	NA	NA
pl19bc	NA	NA	NA	NA	NA	NA	NA
pl19bd	NA	NA	NA	NA	NA	NA	NA
pl19cd	NA	NA	NA	NA	NA	NA	NA
pl19abc	NA	NA	NA	NA	NA	NA	NA
pl19abd	NA	NA	NA	NA	NA	NA	NA
pl19acd	NA	NA	NA	NA	NA	NA	NA
pl19bcd	NA	NA	NA	NA	NA	NA	NA
pl19nls	151397.60	2.57	0.69	28.523	0.423	0.065	4.115

Table B.5 Model selection criteria for species Balsam poplar

Model name	AIC	RMSE	R^2	a	b	c	d
pb1nlme	NA	NA	NA	NA	NA		
pb1a	11312.11	1.84	0.86	4.021	0.484		
pb1b	10931.79	0.96	0.96	3.521	0.524		
pb1nls	12263.50	2.40	0.76	3.410	0.535		
pb2nlme	10805.84	1.77	0.87	3.448	-12.055		
pb2a	10907.14	0.95	0.96	3.435	-11.720		
pb2b	11161.63	0.90	0.97	3.495	-12.938		
pb2nls	12269.32	2.41	0.76	3.495	-13.129		

Model name	AIC	RMSE	R^2	a	b	c	d
pb3nlme	10765.20	1.74	0.88	35.038	19.790		
pb3a	11029.19	1.01	0.96	31.374	15.253		
pb3b	11103.97	0.99	0.96	32.044	16.087		
pb3nls	12171.27	2.36	0.77	41.612	28.333		
pb4nlme	NA	NA	NA	NA	NA		
pb4a	10959.50	0.98	0.96	25.078	0.062		
pb4b	10909.14	1.93	0.85	30.535	0.042		
pb4nls	12201.80	2.38	0.77	29.170	0.045		
pb5nlme	10774.68	1.76	0.87	1.313	0.173		
pb5a	11000.93	0.89	0.97	1.388	0.169		
pb5b	10900.73	1.01	0.96	1.275	0.175		
pb5nls	12208.68	2.38	0.77	1.436	0.168		
pb6nlme	10915.61	0.96	0.96	28.478	-9.153		
pb6a	11005.25	0.99	0.96	28.615	-9.220		
pb6b	11224.38	0.91	0.97	32.191	-11.772		
pb6nls	12307.25	2.42	0.76	32.026	-11.833		
pb7nlme	10965.72	1.83	0.86	10.410	0.369		
pb7a	11123.42	0.90	0.97	10.462	0.353		
pb7b	11142.97	0.98	0.96	8.756	0.416		
pb7nls	12508.33	2.52	0.74	9.392	0.388		
pb8nlme	10905.30	0.96	0.96	28.805	9.640		
pb8a	10990.31	0.99	0.96	28.954	9.735		
pb8b	11192.10	0.90	0.97	32.555	12.342		
pb8nls	12287.52	2.42	0.76	32.480	12.467		
pb9nlme	NA	NA	NA	NA	NA	NA	
pb9a	10813.99	0.91	0.97	4.217	-4.440	-0.393	
pb9b	NA	NA	NA	NA	NA	NA	
pb9c	NA	NA	NA	NA	NA	NA	
pb9ab	NA	NA	NA	NA	NA	NA	
pb9ac	NA	NA	NA	NA	NA	NA	
pb9bc	NA	NA	NA	NA	NA	NA	
pb9nls	12170.25	2.36	0.77	4.186	-4.860	-0.430	
pb10nlme	NA	NA	NA	NA	NA	NA	
pb10a	10991.15	0.98	0.96	24.103	3.175	0.109	
pb10b	11435.92	1.88	0.86	31.316	2.328	0.051	
pb10c	11370.52	1.86	0.86	29.774	2.545	0.061	
pb10ab	11174.92	1.73	0.88	25.989	2.460	0.080	
pb10ac	NA	NA	NA	NA	NA	NA	
pb10bc	NA	NA	NA	NA	NA	NA	
pb10nls	12234.73	2.39	0.77	27.740	3.140	0.080	

Model name	AIC	RMSE	R^2	a	b	c	d
pb11nlme	NA	NA	NA	NA	NA	NA	
pb11a	10999.83	0.98	0.96	24.409	0.075	1.215	
pb11b	NA	NA	NA	NA	NA	NA	
pb11c	NA	NA	NA	NA	NA	NA	
pb11ab	NA	NA	NA	NA	NA	NA	
pb11ac	NA	NA	NA	NA	NA	NA	
pb11bc	NA	NA	NA	NA	NA	NA	
pb11nls	12176.61	2.36	0.77	32.909	0.029	0.796	
pb12nlme	NA	NA	NA	NA	NA	NA	
pb12a	11228.71	1.81	0.87	28.242	0.069	0.882	
pb12b	NA	NA	NA	NA	NA	NA	
pb12c	11260.94	1.82	0.87	48.885	0.069	0.613	
pb12ab	NA	NA	NA	NA	NA	NA	
pb12ac	NA	NA	NA	NA	NA	NA	
pb12bc	NA	NA	NA	NA	NA	NA	
pb12nls	12175.44	2.36	0.77	34.019	0.055	0.848	
pb13nlme	NA	NA	NA	NA	NA	NA	
pb13a	10981.21	0.98	0.96	24.332	1.827	0.088	
pb13b	10952.77	1.90	0.85	35.375	1.443	0.034	
pb13c	11332.69	1.85	0.86	32.010	1.433	0.041	
pb13ab	10788.98	1.77	0.87	27.976	1.539	0.058	
pb13ac	NA	NA	NA	NA	NA	NA	
pb13bc	NA	NA	NA	NA	NA	NA	
pb13nls	12205.21	2.38	0.77	29.024	1.678	0.057	
pb14nlme	NA	NA	NA	NA	NA	NA	
pb14a	10940.75	1.92	0.85	0.039	1.366	28.410	
pb14b	12040.59	1.05	0.95	0.080	0.269	29.021	
pb14c	10892.23	0.96	0.96	0.062	1.022	25.948	
pb14ab	NA	NA	NA	NA	NA	NA	
pb14ac	NA	NA	NA	NA	NA	NA	
pb14bc	10788.70	1.77	0.87	0.059	0.945	26.971	
pb14nls	12219.12	2.38	0.77	0.053	0.985	27.532	
pb15nlme	NA	NA	NA	NA	NA	NA	
pb15a	11393.69	1.30	0.93	-1.622	0.758	0.023	
pb15b	10884.56	0.90	0.97	-0.595	0.701	0.024	
pb15c	10944.63	1.07	0.95	-0.052	0.619	0.027	
pb15ab	10786.60	1.79	0.87	-0.130	0.646	0.026	
pb15ac	10778.82	1.77	0.87	0.192	0.600	0.027	
pb15bc	10780.48	0.91	0.97	0.115	0.622	0.026	
pb15nls	12173.20	2.36	0.77	-0.097	0.690	0.024	

Model name	AIC	RMSE	R^2	a	b	c	d
pb16nlme	NA	NA	NA	NA	NA	NA	
pb16a	11231.64	1.81	0.87	33.288	-6.486	1.143	
pb16b	NA	NA	NA	NA	NA	NA	
pb16c	11256.99	1.81	0.87	0.22	2.774	0.212	
pb16ab	NA	NA	NA	NA	NA	NA	
pb16ac	NA	NA	NA	NA	NA	NA	
pb16bc	NA	NA	NA	NA	NA	NA	
pb16nls	12173.57	2.36	0.77	45.895	-5.328	0.931	
pb17nlme	NA	NA	NA	NA	NA	NA	
pb17a	11094.29	1.00	0.96	27.252	-7.288	-1.884	
pb17b	11839.44	1.00	0.96	28.426	-6.434	-4.990	
pb17c	11604.26	0.83	0.97	48.733	-31.445	9.537	
pb17ab	10792.43	1.76	0.87	31.553	-12.444	1.689	
pb17ac	10788.66	1.78	0.87	33.548	-15.124	3.562	
pb17bc	NA	NA	NA	NA	NA	NA	
pb17nls	12175.99	2.36	0.77	40.281	-24.528	8.810	
pb18nlme	NA	NA	NA	NA	NA	NA	
pb18a	10822.30	1.83	0.86	32.924	0.033	1.180	
pb18b	NA	NA	NA	NA	NA	NA	
pb18c	10894.55	1.86	0.86	245.324	0.015	0.544	
pb18ab	10826.27	1.83	0.86	32.928	0.033	1.180	
pb18ac	NA	NA	NA	NA	NA	NA	
pb18bc	NA	NA	NA	NA	NA	NA	
pb18nls	12172.85	2.36	0.77	43.193	0.036	0.969	
pb19nlme	NA	NA	NA	NA	NA	NA	NA
pb19a	NA	NA	NA	NA	NA	NA	NA
pb19b	NA	NA	NA	NA	NA	NA	NA
pb19c	NA	NA	NA	NA	NA	NA	NA
pb19d	NA	NA	NA	NA	NA	NA	NA
pb19ab	NA	NA	NA	NA	NA	NA	NA
pb19ac	NA	NA	NA	NA	NA	NA	NA
pb19ad	NA	NA	NA	NA	NA	NA	NA
pb19bc	NA	NA	NA	NA	NA	NA	NA
pb19bd	NA	NA	NA	NA	NA	NA	NA
pb19cd	NA	NA	NA	NA	NA	NA	NA
pb19abc	NA	NA	NA	NA	NA	NA	NA
pb19abd	NA	NA	NA	NA	NA	NA	NA
pb19acd	NA	NA	NA	NA	NA	NA	NA
pb19bcd	NA	NA	NA	NA	NA	NA	NA
pb19nls	12169.90	2.36	0.77	43.590	1.048	0.009	0.451

Table B.6 Model selection criteria for species Black spruce

Model name	AIC	RMSE	R^2	a	b	c	d
sb1nlme	32358.31	1.41	0.84	1.218	0.858		
sb1a	34627.41	1.42	0.84	1.711	0.715		
sb1b	32682.15	0.63	0.97	1.467	0.767		
sb1nls	40804.67	2.05	0.66	1.555	0.770		
sb2nlme	32480.63	0.60	0.97	3.360	-14.038		
sb2a	32920.23	0.63	0.97	3.312	-13.082		
sb2b	33384.32	0.60	0.97	3.429	-14.892		
sb2nls	40730.94	2.04	0.66	3.428	-13.940		
sb3nlme	NA	NA	NA	NA	NA		
sb3a	34661.72	1.42	0.84	40.815	35.967		
sb3b	34611.42	1.42	0.84	44.564	41.545		
sb3nls	40699.56	2.04	0.66	59.803	56.138		
sb4nlme	NA	NA	NA	NA	NA		
sb4a	32474.61	1.43	0.83	29.977	0.034		
sb4b	32445.14	1.45	0.83	40.285	0.024		
sb4nls	40689.88	2.04	0.66	35.200	0.030		
sb5nlme	32258.28	1.40	0.84	1.834	0.167		
sb5a	32955.72	0.61	0.97	1.855	0.166		
sb5b	33016.10	0.67	0.96	1.617	0.182		
sb5nls	40664.86	2.03	0.66	1.713	0.166		
sb6nlme	32419.41	1.40	0.84	27.614	-12.186		
sb6a	33839.60	0.73	0.96	21.604	-8.512		
sb6b	33594.30	0.60	0.97	29.289	-13.108		
sb6nls	40781.15	2.05	0.66	29.200	-12.207		
sb7nlme	32195.91	0.57	0.97	2.17	0.65		
sb7a	32801.22	0.61	0.97	2.653	0.617		
sb7b	32583.75	0.61	0.97	2.801	0.609		
sb7nls	40947.48	2.06	0.65	3.37	0.618		
sb8nlme	32386.93	1.40	0.84	28.382	13.038		
sb8a	33832.93	0.73	0.96	21.949	9.065		
sb8b	33485.91	0.60	0.97	30.035	13.972		
sb8nls	40754.39	2.04	0.66	29.976	13.047		
sb9nlme	NA	NA	NA	NA	NA	NA	
sb9a	32494.92	0.61	0.97	31.475	-31.240	-0.027	
sb9b	NA	NA	NA	NA	NA	NA	
sb9c	NA	NA	NA	NA	NA	NA	
sb9ab	NA	NA	NA	NA	NA	NA	
sb9ac	NA	NA	NA	NA	NA	NA	
sb9bc	NA	NA	NA	NA	NA	NA	

Model name	AIC	RMSE	R^2	a	b	c	d
sb9nls	40654.99	2.03	0.67	4.151	-6.239	-0.501	
sb10nlme	NA	NA	NA	NA	NA	NA	
sb10a	33575.94	0.69	0.96	16.386	5.928	0.194	
sb10b	34638.25	1.42	0.84	28.190	5.181	0.085	
sb10c	32525.54	1.45	0.83	24.723	5.210	0.104	
sb10ab	32232.86	1.39	0.84	21.747	5.552	0.126	
sb10ac	32409.43	1.41	0.84	22.704	5.565	0.127	
sb10bc	32275.98	1.40	0.84	26.754	5.703	0.098	
sb10nls	40755.76	2.04	0.66	22.173	5.472	0.132	
sb11nlme	NA	NA	NA	NA	NA	NA	
sb11a	32497.66	1.44	0.83	26.543	0.046	1.125	
sb11b	NA	NA	NA	NA	NA	NA	
sb11c	NA	NA	NA	NA	NA	NA	
sb11ab	NA	NA	NA	NA	NA	NA	
sb11ac	NA	NA	NA	NA	NA	NA	
sb11bc	NA	NA	NA	NA	NA	NA	
sb11nls	40669.61	2.03	0.66	28.105	0.048	1.195	
sb12nlme	NA	NA	NA	NA	NA	NA	
sb12a	33816.27	0.69	0.96	16.080	0.022	1.562	
sb12b	NA	NA	NA	NA	NA	NA	
sb12c	32494.04	1.44	0.83	34.484	0.031	0.970	
sb12ab	NA	NA	NA	NA	NA	NA	
sb12ac	NA	NA	NA	NA	NA	NA	
sb12bc	NA	NA	NA	NA	NA	NA	
sb12nls	40671.73	2.03	0.66	27.560	0.029	1.127	
sb13nlme	NA	NA	NA	NA	NA	NA	
sb13a	32482.75	1.44	0.83	23.898	2.192	0.077	
sb13b	34619.80	1.42	0.84	38.352	2.228	0.042	
sb13c	32456.97	1.44	0.83	28.492	2.204	0.062	
sb13ab	32207.03	1.39	0.84	24.534	2.342	0.079	
sb13ac	32454.85	1.41	0.84	24.855	2.250	0.079	
sb13bc	NA	NA	NA	NA	NA	NA	
sb13nls	40703.23	2.04	0.66	24.083	2.359	0.087	
sb14nlme	NA	NA	NA	NA	NA	NA	
sb14a	32414.82	1.43	0.83	0.019	1.213	33.126	
sb14b	32456.83	1.44	0.83	0.029	0.996	32.275	
sb14c	32468.71	1.44	0.83	0.040	0.965	27.611	
sb14ab	32252.71	1.40	0.84	0.023	1.197	31.966	
sb14ac	NA	NA	NA	NA	NA	NA	
sb14bc	32229.10	1.40	0.84	0.057	0.640	26.868	

Model name	AIC	RMSE	R^2	a	b	c	d
sb14nls	40667.47	2.03	0.66	0.055	0.724	27.400	
sb15nlme	NA	NA	NA	NA	NA	NA	
sb15a	33807.55	0.72	0.96	1.243	0.945	0.017	
sb15b	32770.98	0.65	0.97	-1.033	1.174	0.012	
sb15c	33219.82	0.71	0.96	-2.556	1.282	0.012	
sb15ab	32501.59	0.63	0.97	-0.701	1.162	0.012	
sb15ac	32223.74	1.40	0.84	1.339	0.884	0.020	
sb15bc	32494.86	0.62	0.97	-1.268	1.243	0.009	
sb15nls	40659.11	2.03	0.67	2.046	0.681	0.024	
sb16nlme	NA	NA	NA	NA	NA	NA	
sb16a	NA	NA	NA	NA	NA	NA	
sb16b	32446.74	1.43	0.83	131.674	-5.885	0.697	
sb16c	32494.19	1.44	0.83	111.82	-5.791	0.717	
sb16ab	NA	NA	NA	NA	NA	NA	
sb16ac	NA	NA	NA	NA	NA	NA	
sb16bc	NA	NA	NA	NA	NA	NA	
sb16nls	40661.32	2.03	0.67	41.721	-7.611	1.054	
sb17nlme	NA	NA	NA	NA	NA	NA	
sb17a	32492.69	1.44	0.83	37.223	-24.441	6.707	
sb17b	32416.16	1.43	0.83	43.272	-29.845	8.138	
sb17c	32505.63	1.43	0.83	63.028	-49.978	14.887	
sb17ab	NA	NA	NA	NA	NA	NA	
sb17ac	32269.66	1.40	0.84	33.783	-18.926	3.477	
sb17bc	32291.41	1.40	0.84	35.727	-20.825	3.994	
sb17nls	40663.15	2.03	0.67	38.182	-22.232	5.232	
sb18nlme	NA	NA	NA	NA	NA	NA	
sb18a	34329.58	0.72	0.96	16.318	0.003	2.594	
sb18b	NA	NA	NA	NA	NA	NA	
sb18c	34713.69	1.43	0.84	67.952	0.021	0.847	
sb18ab	NA	NA	NA	NA	NA	NA	
sb18ac	NA	NA	NA	NA	NA	NA	
sb18bc	NA	NA	NA	NA	NA	NA	
sb18nls	40663.84	2.03	0.67	35.900	0.018	1.259	
sb19nlme	NA	NA	NA	NA	NA	NA	NA
sb19a	NA	NA	NA	NA	NA	NA	NA
sb19b	NA	NA	NA	NA	NA	NA	NA
sb19c	NA	NA	NA	NA	NA	NA	NA
sb19d	NA	NA	NA	NA	NA	NA	NA
sb19ab	NA	NA	NA	NA	NA	NA	NA
sb19ac	NA	NA	NA	NA	NA	NA	NA

Model name	AIC	RMSE	R^2	a	b	c	d
sb19ad	NA	NA	NA	NA	NA	NA	NA
sb19bc	NA	NA	NA	NA	NA	NA	NA
sb19bd	NA	NA	NA	NA	NA	NA	NA
sb19cd	NA	NA	NA	NA	NA	NA	NA
sb19abc	NA	NA	NA	NA	NA	NA	NA
sb19abd	NA	NA	NA	NA	NA	NA	NA
sb19acd	NA	NA	NA	NA	NA	NA	NA
sb19bcd	NA	NA	NA	NA	NA	NA	NA
sb19nls	NA	NA	NA	NA	NA	NA	NA

Table B.7 Model selection criteria for species Balsam fir

Model name	AIC	RMSE	R^2	a	b	c	d
fb1nlme	NA	NA	NA	NA	NA		
fb1a	21218.24	1.94	0.85	1.217	0.847		
fb1b	21010.60	0.64	0.98	0.968	0.925		
fb1nls	25010.08	2.40	0.77	1.401	0.798		
fb2nlme	20534.64	1.80	0.87	3.586	-17.033		
fb2a	20870.00	0.66	0.98	3.608	-17.299		
fb2b	21065.76	0.64	0.98	3.632	-17.763		
fb2nls	24551.46	2.30	0.79	3.575	-16.803		
fb3nlme	NA	NA	NA	NA	NA		
fb3a	21055.02	1.89	0.86	80.561	83.738		
fb3b	21051.29	1.89	0.86	81.372	85.479		
fb3nls	24805.46	2.36	0.78	73.960	75.547		
fb4nlme	NA	NA	NA	NA	NA		
fb4a	21033.18	1.88	0.86	46.310	0.020		
fb4b	22727.72	1.88	0.86	48.968	0.019		
fb4nls	24777.33	2.35	0.78	42.554	0.023		
fb5nlme	20527.21	0.62	0.98	2.116	0.146		
fb5a	20725.25	0.63	0.98	2.132	0.145		
fb5b	20952.16	0.69	0.98	2.119	0.145		
fb5nls	24578.18	2.31	0.79	1.987	0.152		
fb6nlme	21021.54	0.63	0.98	32.447	-13.891		
fb6a	21606.28	0.74	0.98	29.176	-12.436		
fb6b	21186.67	0.65	0.98	35.971	-15.814		
fb6nls	24572.53	2.31	0.79	34.048	-14.958		
fb7nlme	21274.27	1.90	0.85	2.03	0.681		
fb7a	21534.04	0.62	0.98	2.420	0.647		
fb7b	21155.20	0.63	0.98	1.009	0.730		
fb7nls	25223.61	2.45	0.76	3.045	0.612		

Model name	AIC	RMSE	R^2	a	b	c	d
fb8nlme	20817.98	1.79	0.87	35.248	15.925		
fb8a	21591.51	0.73	0.98	29.733	13.188		
fb8b	21123.21	0.64	0.98	36.845	16.762		
fb8nls	24560.09	2.30	0.79	34.857	15.857		
fb9nlme	NA	NA	NA	NA	NA	NA	
fb9a	20678.41	0.62	0.98	4.840	-7.220	-0.416	
fb9b	NA	NA	NA	NA	NA	NA	
fb9c	22544.59	1.85	0.86	4.388	-7.167	-0.495	
fb9ab	NA	NA	NA	NA	NA	NA	
fb9ac	NA	NA	NA	NA	NA	NA	
fb9bc	NA	NA	NA	NA	NA	NA	
fb9nls	24548.27	2.30	0.79	3.729	-10.557	-0.801	
fb10nlme	NA	NA	NA	NA	NA	NA	
fb10a	21503.42	0.75	0.98	20.871	8.648	0.171	
fb10b	22876.00	1.91	0.85	25.776	6.553	0.115	
fb10c	20969.22	1.87	0.86	25.905	7.227	0.122	
fb10ab	20872.35	1.81	0.87	24.511	7.297	0.131	
fb10ac	20849.87	1.81	0.87	24.704	8.158	0.139	
fb10bc	20881.07	1.81	0.87	26.199	7.281	0.120	
fb10nls	24643.51	2.32	0.78	23.350	7.484	0.140	
fb11nlme	NA	NA	NA	NA	NA	NA	
fb11a	20869.70	1.85	0.86	29.557	0.056	1.554	
fb11b	20936.12	1.87	0.86	39.886	0.030	1.174	
fb11c	NA	NA	NA	NA	NA	NA	
fb11ab	NA	NA	NA	NA	NA	NA	
fb11ac	20774.42	1.79	0.87	28.799	0.058	1.567	
fb11bc	NA	NA	NA	NA	NA	NA	
fb11nls	24557.27	2.30	0.79	26.565	0.068	1.698	
fb12nlme	NA	NA	NA	NA	NA	NA	
fb12a	20874.37	1.86	0.86	28.178	0.015	1.334	
fb12b	20893.86	1.86	0.86	29.561	0.015	1.325	
fb12c	20852.67	1.85	0.86	30.229	0.016	1.279	
fb12ab	NA	NA	NA	NA	NA	NA	
fb12ac	NA	NA	NA	NA	NA	NA	
fb12bc	NA	NA	NA	NA	NA	NA	
fb12nls	24565.97	2.30	0.79	25.480	0.016	1.385	
fb13nlme	NA	NA	NA	NA	NA	NA	
fb13a	21554.31	0.76	0.98	21.169	3.519	0.129	
fb13b	22863.47	1.91	0.85	28.703	2.532	0.072	
fb13c	22560.22	1.85	0.86	27.587	2.663	0.079	

Model name	AIC	RMSE	R^2	a	b	c	d
fb13ab	20799.32	1.80	0.87	26.455	2.810	0.086	
fb13ac	20797.73	1.80	0.87	26.11	2.958	0.092	
fb13bc	20810.00	1.81	0.87	28.805	2.709	0.076	
fb13nls	24580.13	2.31	0.79	24.835	2.903	0.094	
fb14nlme	NA	NA	NA	NA	NA	NA	
fb14a	22595.19	1.86	0.86	0.064	0.450	28.848	
fb14b	21052.24	1.90	0.86	0.063	0.435	29.537	
fb14c	21682.12	0.77	0.98	0.100	0.233	22.790	
fb14ab	NA	NA	NA	NA	NA	NA	
fb14ac	20777.28	1.80	0.87	0.075	0.312	27.759	
fb14bc	20774.56	1.79	0.87	0.076	0.300	27.619	
fb14nls	24559.42	2.30	0.79	0.080	0.288	26.669	
fb15nlme	NA	NA	NA	NA	NA	NA	
fb15a	21339.82	0.72	0.98	5.811	0.471	0.025	
fb15b	20685.83	0.66	0.98	3.667	0.722	0.018	
fb15c	21330.77	0.76	0.98	1.986	0.913	0.013	
fb15ab	20580.11	0.66	0.98	4.291	0.639	0.021	
fb15ac	20782.64	1.80	0.87	5.607	0.459	0.026	
fb15bc	20576.74	0.63	0.98	4.585	0.601	0.022	
fb15nls	24548.28	2.30	0.79	6.121	0.366	0.029	
fb16nlme	NA	NA	NA	NA	NA	NA	
fb16a	22178.65	0.80	0.97	21.488	-67.643	2.193	
fb16b	22130.52	0.69	0.98	12729.091	-9.306	0.472	
fb16c	20877.77	1.86	0.86	55.99	-8.499	1.004	
fb16ab	NA	NA	NA	NA	NA	NA	
fb16ac	NA	NA	NA	NA	NA	NA	
fb16bc	NA	NA	NA	NA	NA	NA	
fb16nls	24547.49	2.30	0.79	36.266	-12.619	1.279	
fb17nlme	NA	NA	NA	NA	NA	NA	
fb17a	20865.55	1.85	0.86	42.249	-22.838	3.637	
fb17b	20935.90	1.87	0.86	43.505	-24.075	4.077	
fb17c	22296.71	0.62	0.98	52.154	-28.608	4.537	
fb17ab	20789.18	1.79	0.87	37.381	-18.118	1.596	
fb17ac	20781.45	1.79	0.87	39.317	-19.983	2.432	
fb17bc	20775.90	1.80	0.87	40.101	-20.825	2.622	
fb17nls	24547.62	2.30	0.79	37.362	-18.672	1.975	
fb18nlme	NA	NA	NA	NA	NA	NA	
fb18a	21894.54	0.78	0.98	21.477	0.002	2.440	
fb18b	20900.96	1.86	0.86	37.159	0.008	1.513	
fb18c	20853.39	1.85	0.86	40.218	0.010	1.402	

Model name	AIC	RMSE	R^2	a	b	c	d
fb18ab	NA	NA	NA	NA	NA	NA	
fb18ac	20819.89	1.80	0.87	29.240	0.006	1.801	
fb18bc	NA	NA	NA	NA	NA	NA	
fb18nls	24550.72	2.30	0.79	30.760	0.008	1.644	
fb19nlme	NA	NA	NA	NA	NA	NA	NA
fb19a	NA	NA	NA	NA	NA	NA	NA
fb19b	NA	NA	NA	NA	NA	NA	NA
fb19c	NA	NA	NA	NA	NA	NA	NA
fb19d	NA	NA	NA	NA	NA	NA	NA
fb19ab	NA	NA	NA	NA	NA	NA	NA
fb19ac	NA	NA	NA	NA	NA	NA	NA
fb19ad	NA	NA	NA	NA	NA	NA	NA
fb19bc	NA	NA	NA	NA	NA	NA	NA
fb19bd	NA	NA	NA	NA	NA	NA	NA
fb19cd	NA	NA	NA	NA	NA	NA	NA
fb19abc	NA	NA	NA	NA	NA	NA	NA
fb19abd	NA	NA	NA	NA	NA	NA	NA
fb19acd	NA	NA	NA	NA	NA	NA	NA
fb19bcd	NA	NA	NA	NA	NA	NA	NA
fb19nls	24552.72	2.30	0.79	28.86	1.20	0.05	0.938

Appendix C: Detailed model selection results for Chapter 4

Table C.1a CMI added models selection criteria for species Aspen

Model name	MSE	R^2	AIC
AW_1nls	8.54	0.635801	29392.56
AW_1nlme	8.30	0.645924	25422.22
AW_1nlmea	9.33	0.602191	25576.94
AW_1nlmeb	9.52	0.593922	25583.51
AW_1nlscmi	8.00	0.65882	29318.82
AW_1nlmecmirandomab	NA	NA	NA
AW_1nlmecmirandoma	8.82	0.623808	25497.68
AW_1nlmecmirandomb	8.82	0.623749	25580.08
AW_1nlscmia	8.09	0.655124	29344.57
AW_1nlmecmiarandomab	NA	NA	NA
AW_1nlmecmiarandoma	8.79	0.625395	25502.18
AW_1nlmecmiarandomb	8.99	0.616732	25518.77
AW_1nlscmib	8.14	0.653091	29354.05
AW_1nlmecmibrandomab	NA	NA	NA
AW_1nlmecmibrandoma	8.76	0.626541	25495.25
AW_1nlmecmibrandomb	8.98	0.617099	25516.78
AW_2nls	7.86	0.664748	28717.68
AW_2nlme	8.99	0.616532	24884.82
AW_2nlmea	8.80	0.624888	25011.94
AW_2nlmeb	8.28	0.646952	25675.01
AW_2nlscmi	7.27	0.690178	28646.02
AW_2nlmecmirandomab	8.34	0.644522	24803.9
AW_2nlmecmirandoma	7.91	0.662767	24997.35
AW_2nlmecmirandomb	7.19	0.693431	25695.94
AW_2nlscmia	7.45	0.682456	28684.78
AW_2nlmecmiarandomab	8.38	0.642756	24803.97
AW_2nlmecmiarandoma	8.05	0.656964	24903.46
AW_2nlmecmiarandomb	7.60	0.676159	25229.56
AW_2nlscmib	7.21	0.692629	28617.73
AW_2nlmecmibrandomab	8.39	0.642299	24798.09
AW_2nlmecmibrandoma	8.10	0.654726	24894.78
AW_2nlmecmibrandomb	7.47	0.681643	25187.2
AW_3nls	7.88	0.664211	28729.63
AW_3nlme	8.98	0.616969	24929.64
AW_3nlmea	8.42	0.640899	25461.36
AW_3nlmeb	9.07	0.613274	25073.38

Model name	MSE	R^2	AIC
AW_3nlscmi	7.27	0.690119	28651.54
AW_3nlmecmirandomab	8.31	0.64561	24845.28
AW_3nlmecmirandoma	7.57	0.677402	25104.6
AW_3nlmecmirandomb	8.21	0.649777	25102.92
AW_3nlscmia	7.29	0.689378	28646.78
AW_3nlmecmiarandomab	8.35	0.643813	24836.79
AW_3nlmecmiarandoma	7.57	0.677388	25072.61
AW_3nlmecmiarandomb	8.39	0.642097	25102.92
AW_3nlscmib	7.52	0.679412	28704.17
AW_3nlmecmibrandomab	8.40	0.641849	24850.68
AW_3nlmecmibrandoma	7.71	0.671475	25118.99
AW_3nlmecmibrandomb	8.35	0.644085	24925.25
AW_4nls	7.87	0.664505	28723.46
AW_4nlme	8.93	0.619084	24844.91
AW_4nlmea	8.64	0.631622	24969.93
AW_4nlmeb	8.20	0.650489	25303.76
AW_4nlscmi	7.28	0.689716	28654.11
AW_4nlmecmirandomab	8.33	0.644989	24770.48
AW_4nlmecmirandoma	8.00	0.658871	24894.02
AW_4nlmecmirandomb	7.53	0.67898	25255.06
AW_4nlscmia	7.45	0.682289	28691.79
AW_4nlmecmiarandomab	8.35	0.644166	24780.73
AW_4nlmecmiarandoma	8.01	0.658543	24899.12
AW_4nlmecmiarandomb	7.59	0.67631	25260.43
AW_4nlscmib	7.21	0.69273	28622.15
AW_4nlmecmibrandomab	8.36	0.643384	24763.64
AW_4nlmecmibrandoma	8.04	0.657119	24881.11
AW_4nlmecmibrandomb	7.46	0.68199	25216.49
AW_5nls	7.76	0.669041	28684.67
AW_5nlme	NA	NA	NA
AW_5nlmea	8.99	0.616716	25176.5
AW_5nlmeb	NA	NA	NA
AW_5nlmec	NA	NA	NA
AW_5nlmeab	NA	NA	NA
AW_5nlmeac	NA	NA	NA
AW_5nlmebc	NA	NA	NA
AW_5nlscmi	7.16	0.694749	28610.13
AW_5nlmecmirandomabc	NA	NA	NA

Model name	MSE	R^2	AIC
AW_5nlmecmirandoma	8.24	0.648717	25076.36
AW_5nlmecmirandomb	NA	NA	NA
AW_5nlmecmirandomc	NA	NA	NA
AW_5nlmecmirandomab	NA	NA	NA
AW_5nlmecmirandomac	NA	NA	NA
AW_5nlmecmirandombc	NA	NA	NA
AW_5nlscmia	7.33	0.687536	28649.23
AW_5nlmecmiarandomabc	NA	NA	NA
AW_5nlmecmiarandoma	8.33	0.644779	25092.73
AW_5nlmecmiarandomb	NA	NA	NA
AW_5nlmecmiarandomc	NA	NA	NA
AW_5nlmecmiarandomab	NA	NA	NA
AW_5nlmecmiarandomac	NA	NA	NA
AW_5nlmecmiarandombc	NA	NA	NA
AW_5nlscmib	7.01	0.701248	28577.33
AW_5nlmecmibrandomabc	NA	NA	NA
AW_5nlmecmibrandoma	8.22	0.649684	25065.1
AW_5nlmecmibrandomb	NA	NA	NA
AW_5nlmecmibrandomc	NA	NA	NA
AW_5nlmecmibrandomab	7.84	0.665623	24721.27
AW_5nlmecmibrandomac	NA	NA	NA
AW_5nlmecmibrandombc	NA	NA	NA
AW_5nlscmic	7.06	0.699087	28543.67
AW_5nlmecmicrandomabc	NA	NA	NA
AW_5nlmecmicrandoma	8.45	0.63986	25070.64
AW_5nlmecmicrandomb	NA	NA	NA
AW_5nlmecmicrandomc	NA	NA	NA
AW_5nlmecmicrandomab	NA	NA	NA
AW_5nlmecmicrandomac	NA	NA	NA
AW_5nlmecmicrandombc	NA	NA	NA
AW_6nls	7.75	0.669381	28683.46
AW_6nlme	NA	NA	NA
AW_6nlmea	8.43	0.640417	24960.93
AW_6nlmeb	7.98	0.659961	25130.46
AW_6nlmec	8.43	0.640728	25026.78
AW_6nlmeab	NA	NA	NA
AW_6nlmeac	7.77	0.668884	24911.29
AW_6nlmebc	NA	NA	NA

Model name	MSE	R^2	AIC
AW_6nlscmi	7.15	0.695054	28608.94
AW_6nlmecmirandomabc	NA	NA	NA
AW_6nlmecmirandoma	7.77	0.668823	24879.23
AW_6nlmecmirandomb	7.39	0.684832	25058.95
AW_6nlmecmirandomc	7.75	0.669765	24949.56
AW_6nlmecmirandomab	NA	NA	NA
AW_6nlmecmirandomac	NA	NA	NA
AW_6nlmecmirandombc	NA	NA	NA
AW_6nlscmia	7.32	0.687875	28647.98
AW_6nlmecmiarandomabc	NA	NA	NA
AW_6nlmecmiarandoma	7.77	0.668843	24885.02
AW_6nlmecmiarandomb	7.35	0.686746	25064.87
AW_6nlmecmiarandomc	7.76	0.669362	24955.07
AW_6nlmecmiarandomab	NA	NA	NA
AW_6nlmecmiarandomac	8.18	0.651396	24820.95
AW_6nlmecmiarandombc	NA	NA	NA
AW_6nlscmib	6.99	0.702156	28574.85
AW_6nlmecmibrandomabc	NA	NA	NA
AW_6nlmecmibrandoma	7.71	0.67109	24870.21
AW_6nlmecmibrandomb	7.33	0.687354	25068.33
AW_6nlmecmibrandomc	7.72	0.670742	24947.21
AW_6nlmecmibrandomab	NA	NA	NA
AW_6nlmecmibrandomac	NA	NA	NA
AW_6nlmecmibrandombc	NA	NA	NA
AW_6nlscmic	7.12	0.69647	28608.15
AW_6nlmecmicrandomabc	NA	NA	NA
AW_6nlmecmicrandoma	7.72	0.670869	24870.85
AW_6nlmecmicrandomb	7.28	0.689688	25061.35
AW_6nlmecmicrandomc	7.75	0.669669	24953.16
AW_6nlmecmicrandomab	NA	NA	NA
AW_6nlmecmicrandomac	NA	NA	NA
AW_6nlmecmicrandombc	NA	NA	NA
AW_7nls	7.70	0.671627	28677.83
AW_7nlme	NA	NA	NA
AW_7nlmea	8.34	0.644296	24971.87
AW_7nlmeb	NA	NA	NA
AW_7nlmec	8.14	0.652769	25134.09
AW_7nlmeab	8.64	0.631538	24828.84

Model name	MSE	R^2	AIC
AW_7nlmeac	8.44	0.640361	24844.32
AW_7nlmebc	NA	NA	NA
AW_7nlscmi	7.10	0.697476	28602.48
AW_7nlmecmirandomabc	NA	NA	NA
AW_7nlmecmirandoma	7.65	0.673643	24886.71
AW_7nlmecmirandomb	NA	NA	NA
AW_7nlmecmirandomc	7.50	0.680442	25073.81
AW_7nlmecmirandomab	7.95	0.660892	24745.59
AW_7nlmecmirandomac	7.96	0.660571	24762.08
AW_7nlmecmirandombc	NA	NA	NA
AW_7nlscmia	7.27	0.690242	28642
AW_7nlmecmiarandomabc	NA	NA	NA
AW_7nlmecmiarandoma	7.66	0.673499	24892.87
AW_7nlmecmiarandomb	8.06	0.656423	25485.88
AW_7nlmecmiarandomc	7.52	0.67949	25086.29
AW_7nlmecmiarandomab	7.98	0.65962	24754.44
AW_7nlmecmiarandomac	7.71	0.671426	24768.75
AW_7nlmecmiarandombc	NA	NA	NA
AW_7nlscmib	7.01	0.701247	28530.31
AW_7nlmecmibrandomabc	NA	NA	NA
AW_7nlmecmibrandoma	7.83	0.666003	24889.67
AW_7nlmecmibrandomb	NA	NA	NA
AW_7nlmecmibrandomc	7.64	0.674446	25074.49
AW_7nlmecmibrandomab	8.11	0.654414	24747.16
AW_7nlmecmibrandomac	NA	NA	NA
AW_7nlmecmibrandombc	NA	NA	NA
AW_7nlscmic	6.95	0.703478	28574.19
AW_7nlmecmicrandomabc	NA	NA	NA
AW_7nlmecmicrandoma	7.61	0.675628	24878.58
AW_7nlmecmicrandomb	NA	NA	NA
AW_7nlmecmicrandomc	7.48	0.681048	25077.13
AW_7nlmecmicrandomab	7.86	0.665001	24726.01
AW_7nlmecmicrandomac	7.99	0.659156	24739.37
AW_7nlmecmicrandombc	NA	NA	NA

Table C.1b Tmax added models selection criteria for species Aspen

Model name	MSE	R^2	AIC
AW_1nls	8.54	0.635801	29392.56
AW_1nlme	8.30	0.645924	25422.22
AW_1nlmea	9.33	0.602191	25576.94
AW_1nlmeb	9.52	0.593922	25583.51
AW_1nlstmax	8.57	0.634822	29368.97
AW_1nlmetmaxrandomab	NA	NA	NA
AW_1nlmetmaxrandoma	9.23	0.606611	25591.4
AW_1nlmetmaxrandomb	10.36	0.558473	26350.35
AW_1nlstmaxa	8.56	0.634983	29390.75
AW_1nlmetmaxarandomab	NA	NA	NA
AW_1nlmetmaxarandoma	9.29	0.603752	26185.68
AW_1nlmetmaxarandomb	9.14	0.610373	25538.76
AW_1nlstmaxb	8.56	0.635103	29392.04
AW_1nlmetmaxbrandomab	NA	NA	NA
AW_1nlmetmaxbrandoma	9.01	0.61586	25531.1
AW_1nlmetmaxbrandomb	9.11	0.611516	25543.35
AW_2nls	7.86	0.664748	28717.68
AW_2nlme	9.19	0.608032	24818.5
AW_2nlmea	8.80	0.624888	25011.94
AW_2nlmeb	8.28	0.646952	25675.01
AW_2nlstmax	7.86	0.664797	28719.6
AW_2nlmetmaxrandomab	NA	NA	NA
AW_2nlmetmaxrandoma	8.65	0.631387	24945.93
AW_2nlmetmaxrandomb	8.50	0.637459	25866.04
AW_2nlstmaxa	7.86	0.664723	28719
AW_2nlmetmaxarandomab	8.79	0.625367	24807.1
AW_2nlmetmaxarandoma	8.64	0.631557	24949.45
AW_2nlmetmaxarandomb	8.28	0.646853	25620.95
AW_2nlstmaxb	7.85	0.665237	28716.83
AW_2nlmetmaxbrandomab	9.14	0.610414	24768.01
AW_2nlmetmaxbrandoma	8.76	0.626529	24990.7
AW_2nlmetmaxbrandomb	8.57	0.634516	25615
AW_3nls	7.88	0.664211	28729.63
AW_3nlme	9.30	0.603675	24895.22
AW_3nlmea	8.42	0.640899	25461.36
AW_3nlmeb	9.07	0.613274	25073.38
AW_3nlstmax	7.87	0.664412	28729.4
AW_3nlmetmaxrandomab	9.00	0.616216	24935.55
AW_3nlmetmaxrandoma	8.48	0.63862	25798.64

Model name	MSE	R^2	AIC
AW_3nlmetmaxrandomb	8.93	0.619244	25005.58
AW_3nlstmaxa	7.87	0.664418	28729.22
AW_3nlmetmaxarandomab	9.15	0.609804	24837.75
AW_3nlmetmaxarandoma	8.57	0.634441	25394.08
AW_3nlmetmaxarandomb	8.96	0.618016	25005.58
AW_3nlstmaxb	7.87	0.664275	28731.05
AW_3nlmetmaxbrandomab	8.74	0.627526	24849.57
AW_3nlmetmaxbrandoma	8.33	0.645034	25411.9
AW_3nlmetmaxbrandomb	8.76	0.62666	25019.08
AW_4nls	7.87	0.664505	28723.46
AW_4nlme	NA	NA	NA
AW_4nlmea	9.47	0.596293	25175.93
AW_4nlmeb	8.27	0.647592	25716.53
AW_4nlstmax	7.87	0.664496	28725.46
AW_4nlmetmaxrandomab	8.84	0.622899	24803.89
AW_4nlmetmaxrandoma	9.83	0.581065	25296.15
AW_4nlmetmaxrandomb	8.42	0.640889	25150.25
AW_4nlstmaxa	7.87	0.664455	28724.45
AW_4nlmetmaxarandomab	NA	NA	NA
AW_4nlmetmaxarandoma	9.39	0.599753	25124.96
AW_4nlmetmaxarandomb	8.27	0.647419	25664.46
AW_4nlstmaxb	7.86	0.665025	28722.84
AW_4nlmetmaxbrandomab	NA	NA	NA
AW_4nlmetmaxbrandoma	9.46	0.596472	25160.95
AW_4nlmetmaxbrandomb	8.57	0.634571	25658.35
AW_5nls	7.76	0.669041	28684.67
AW_5nlme	NA	NA	NA
AW_5nlmea	8.99	0.616716	25176.5
AW_5nlmeb	NA	NA	NA
AW_5nlmec	NA	NA	NA
AW_5nlmeab	NA	NA	NA
AW_5nlmeac	NA	NA	NA
AW_5nlmebc	NA	NA	NA
AW_5nlstmax	7.76	0.669111	28686.46
AW_5nlmetmaxrandomabc	NA	NA	NA
AW_5nlmetmaxrandoma	8.99	0.616824	25176.51
AW_5nlmetmaxrandomb	NA	NA	NA
AW_5nlmetmaxrandomc	NA	NA	NA
AW_5nlmetmaxrandomab	NA	NA	NA
AW_5nlmetmaxrandomac	NA	NA	NA

Model name	MSE	R^2	AIC
AW_5nlmetmaxrandombc	NA	NA	NA
AW_5nlstmaxa	7.76	0.669015	28685.96
AW_5nlmetmaxarandomabc	NA	NA	NA
AW_5nlmetmaxarandoma	9.04	0.614524	25121.29
AW_5nlmetmaxarandomb	NA	NA	NA
AW_5nlmetmaxarandomc	NA	NA	NA
AW_5nlmetmaxarandomab	NA	NA	NA
AW_5nlmetmaxarandomac	NA	NA	NA
AW_5nlmetmaxarandombc	NA	NA	NA
AW_5nlstmaxb	7.75	0.669381	28684.09
AW_5nlmetmaxbrandomabc	NA	NA	NA
AW_5nlmetmaxbrandoma	9.00	0.616468	25165.78
AW_5nlmetmaxbrandomb	NA	NA	NA
AW_5nlmetmaxbrandomc	NA	NA	NA
AW_5nlmetmaxbrandomab	NA	NA	NA
AW_5nlmetmaxbrandomac	NA	NA	NA
AW_5nlmetmaxbrandombc	NA	NA	NA
AW_5nlstmaxc	7.73	0.670569	28674.94
AW_5nlmetmaxcrandomabc	NA	NA	NA
AW_5nlmetmaxcrandoma	9.01	0.616068	25175.2
AW_5nlmetmaxcrandomb	NA	NA	NA
AW_5nlmetmaxcrandomc	NA	NA	NA
AW_5nlmetmaxcrandomab	NA	NA	NA
AW_5nlmetmaxcrandomac	NA	NA	NA
AW_5nlmetmaxcrandombc	NA	NA	NA
AW_6nls	7.75	0.669381	28683.46
AW_6nlme	NA	NA	NA
AW_6nlmea	8.91	0.61993	25175.07
AW_6nlmeb	8.14	0.653016	25769.03
AW_6nlmec	8.43	0.640728	25026.78
AW_6nlmeab	NA	NA	NA
AW_6nlmeac	7.77	0.668884	24911.29
AW_6nlmebc	NA	NA	NA
AW_6nlstmax	7.75	0.669436	28685.27
AW_6nlmetmaxrandomabc	NA	NA	NA
AW_6nlmetmaxrandoma	8.91	0.620215	25173.58
AW_6nlmetmaxrandomb	NA	NA	NA
AW_6nlmetmaxrandomc	8.35	0.644131	24988.96
AW_6nlmetmaxrandomab	NA	NA	NA
AW_6nlmetmaxrandomac	NA	NA	NA

Model name	MSE	R^2	AIC
AW_6nlmetmaxrandombc	NA	NA	NA
AW_6nlstmaxa	7.76	0.669359	28684.73
AW_6nlmetmaxarandomabc	NA	NA	NA
AW_6nlmetmaxarandoma	8.98	0.617249	25119.2
AW_6nlmetmaxarandomb	8.07	0.655945	25743.95
AW_6nlmetmaxarandomc	8.29	0.64654	24978.1
AW_6nlmetmaxarandomab	NA	NA	NA
AW_6nlmetmaxarandomac	NA	NA	NA
AW_6nlmetmaxarandombc	NA	NA	NA
AW_6nlstmaxb	7.75	0.669724	28682.84
AW_6nlmetmaxbrandomabc	NA	NA	NA
AW_6nlmetmaxbrandoma	8.92	0.619646	25165.99
AW_6nlmetmaxbrandomb	8.14	0.653158	25071.26
AW_6nlmetmaxbrandomc	8.40	0.641724	24981.37
AW_6nlmetmaxbrandomab	NA	NA	NA
AW_6nlmetmaxbrandomac	NA	NA	NA
AW_6nlmetmaxbrandombc	NA	NA	NA
AW_6nlstmaxc	7.75	0.669457	28684.93
AW_6nlmetmaxcrandomabc	NA	NA	NA
AW_6nlmetmaxcrandoma	8.90	0.620434	25157.98
AW_6nlmetmaxcrandomb	8.01	0.658458	25064.91
AW_6nlmetmaxcrandomc	8.52	0.636747	25631.59
AW_6nlmetmaxcrandomab	NA	NA	NA
AW_6nlmetmaxcrandomac	NA	NA	NA
AW_6nlmetmaxcrandombc	NA	NA	NA
AW_7nls	7.70	0.671627	28677.83
AW_7nlme	NA	NA	NA
AW_7nlmea	8.83	0.623371	25132.61
AW_7nlmeb	NA	NA	NA
AW_7nlmec	8.14	0.652769	25134.09
AW_7nlmeab	8.64	0.631538	24828.84
AW_7nlmeac	8.44	0.640361	24844.32
AW_7nlmebc	NA	NA	NA
AW_7nlstmax	7.70	0.671739	28679.43
AW_7nlmetmaxrandomabc	NA	NA	NA
AW_7nlmetmaxrandoma	8.85	0.622784	25143.63
AW_7nlmetmaxrandomb	NA	NA	NA
AW_7nlmetmaxrandomc	NA	NA	NA
AW_7nlmetmaxrandomab	NA	NA	NA
AW_7nlmetmaxrandomac	8.47	0.639023	24779.02

Model name	MSE	R^2	AIC
AW_7nlmetmaxrandombc	NA	NA	NA
AW_7nlstmaxa	7.70	0.671584	28679.11
AW_7nlmetmaxarandomabc	NA	NA	NA
AW_7nlmetmaxarandoma	8.89	0.621036	25075.19
AW_7nlmetmaxarandomb	NA	NA	NA
AW_7nlmetmaxarandomc	NA	NA	NA
AW_7nlmetmaxarandomab	8.52	0.636862	24760.54
AW_7nlmetmaxarandomac	NA	NA	NA
AW_7nlmetmaxarandombc	NA	NA	NA
AW_7nlstmaxb	7.66	0.673468	28664.38
AW_7nlmetmaxbrandomabc	NA	NA	NA
AW_7nlmetmaxbrandoma	8.85	0.62276	25131.53
AW_7nlmetmaxbrandomb	NA	NA	NA
AW_7nlmetmaxbrandomc	8.21	0.650119	25108.94
AW_7nlmetmaxbrandomab	NA	NA	NA
AW_7nlmetmaxbrandomac	8.71	0.628832	24801.82
AW_7nlmetmaxbrandombc	8.62	0.632601	25046.93
AW_7nlstmaxc	7.70	0.671905	28677.09
AW_7nlmetmaxcrandomabc	NA	NA	NA
AW_7nlmetmaxcrandoma	8.83	0.623434	25121.22
AW_7nlmetmaxcrandomb	NA	NA	NA
AW_7nlmetmaxcrandomc	8.24	0.648494	25752.16
AW_7nlmetmaxcrandomab	NA	NA	NA
AW_7nlmetmaxcrandomac	NA	NA	NA
AW_7nlmetmaxcrandombc	NA	NA	NA

Table C.2a CMI added models selection criteria for species Balsam poplar

Model name	MSE	R^2	AIC
PB_1nls	9.319654	0.72916	9014.353
PB_1nlme	NA	NA	NA
PB_1nlmea	9.556318	0.722282	8280.584
PB_1nlmeb	9.441157	0.725629	8044.154
PB_1nlscmi	9.550572	0.722449	9013.02
PB_1nlmecmirandomab	NA	NA	NA
PB_1nlmecmirandoma	9.052727	0.736917	8270.19
PB_1nlmecmirandomb	8.458545	0.754185	8050.069
PB_1nlscmia	9.572547	0.72181	9012.04
PB_1nlmecmiarandomab	NA	NA	NA
PB_1nlmecmiarandoma	8.993172	0.738648	8273.801
PB_1nlmecmiarandomb	8.999812	0.738455	8038.266

Model name	MSE	R^2	AIC
PB_1nlscmib	9.551337	0.722427	9012.49
PB_1nlmecmibrandomab	NA	NA	NA
PB_1nlmecmibrandoma	9.074897	0.736273	8275.138
PB_1nlmecmibrandomb	9.028251	0.737628	8039.665
PB_2nls	7.667463	0.777174	8999.787
PB_2nlme	8.428776	0.75505	7928.059
PB_2nlmea	8.615087	0.749635	7987.029
PB_2nlmeb	7.656429	0.777495	8210.97
PB_2nlscmi	7.62111	0.778521	9001.677
PB_2nlmecmirandomab	7.856744	0.771674	7920.97
PB_2nlmecmirandoma	7.420263	0.784358	7991.132
PB_2nlmecmirandomb	6.722793	0.804628	8229.895
PB_2nlscmia	7.711948	0.775882	9001.692
PB_2nlmecmiarandomab	7.983044	0.768003	7923.896
PB_2nlmecmiarandoma	8.017267	0.767009	7978.46
PB_2nlmecmiarandomb	7.303216	0.78776	8207.384
PB_2nlscmib	7.502998	0.781954	9000.145
PB_2nlmecmibrandomab	7.926271	0.769653	7916.018
PB_2nlmecmibrandoma	7.956038	0.768788	7964.435
PB_2nlmecmibrandomb	7.195595	0.790887	8200.366
PB_3nls	7.810187	0.773027	8954.133
PB_3nlme	8.680241	0.747742	7915.177
PB_3nlmea	7.930644	0.769526	8087.555
PB_3nlmeb	8.766382	0.745238	7991.847
PB_3nlscmi	7.785587	0.773742	8956.1
PB_3nlmecmirandomab	7.34219	0.786627	7946.395
PB_3nlmecmirandoma	6.711088	0.804968	8131.652
PB_3nlmecmirandomb	7.322816	0.78719	8008.162
PB_3nlscmia	7.727751	0.775422	8955.71
PB_3nlmecmiarandomab	8.108382	0.764361	7902.116
PB_3nlmecmiarandoma	7.424253	0.784242	8076.325
PB_3nlmecmiarandomb	8.047564	0.766128	8008.162
PB_3nlscmib	7.886758	0.770801	8955.822
PB_3nlmecmibrandomab	8.199245	0.76172	7911.071
PB_3nlmecmibrandoma	7.568618	0.780047	8084.052
PB_3nlmecmibrandomb	8.13258	0.763658	7984.211
PB_4nls	7.642104	0.777911	9013.996
PB_4nlme	8.772719	0.745054	7934.981
PB_4nlmea	10.11745	0.705975	8052.643
PB_4nlmeb	7.595838	0.779256	8235.524

Model name	MSE	R^2	AIC
PB_4nlscmi	7.592894	0.779341	9015.875
PB_4nlmecmirandomab	8.240178	0.760531	7927.66
PB_4nlmecmirandoma	9.199056	0.732664	8037.54
PB_4nlmecmirandomb	6.66736	0.806239	8255.229
PB_4nlscmia	7.687951	0.776579	9015.896
PB_4nlmecmiarandomab	8.340355	0.757619	7930.682
PB_4nlmecmiarandoma	9.603028	0.720925	8044.993
PB_4nlmecmiarandomb	7.251134	0.789273	8232.26
PB_4nlscmib	7.461015	0.783174	9014.023
PB_4nlmecmibrandomab	8.266767	0.759758	7922.894
PB_4nlmecmibrandoma	9.507967	0.723687	8031.934
PB_4nlmecmibrandomb	7.137708	0.79257	8225.01
PB_5nls	8.283372	0.759275	8931.629
PB_5nlme	NA	NA	NA
PB_5nlmea	9.414782	0.726395	8064.471
PB_5nlmeb	NA	NA	NA
PB_5nlmec	NA	NA	NA
PB_5nlmeab	NA	NA	NA
PB_5nlmeac	NA	NA	NA
PB_5nlmebc	NA	NA	NA
PB_5nlscmi	8.326245	0.758029	8933.54
PB_5nlmecmirandomabc	NA	NA	NA
PB_5nlmecmirandoma	8.600651	0.750055	8045.52
PB_5nlmecmirandomb	NA	NA	NA
PB_5nlmecmirandomc	NA	NA	NA
PB_5nlmecmirandomab	NA	NA	NA
PB_5nlmecmirandomac	NA	NA	NA
PB_5nlmecmirandombc	NA	NA	NA
PB_5nlscmia	8.370995	0.756729	8933.249
PB_5nlmecmiarandomabc	NA	NA	NA
PB_5nlmecmiarandoma	8.863786	0.742408	8056.18
PB_5nlmecmiarandomb	NA	NA	NA
PB_5nlmecmiarandomc	NA	NA	NA
PB_5nlmecmiarandomab	NA	NA	NA
PB_5nlmecmiarandomac	NA	NA	NA
PB_5nlmecmiarandombc	NA	NA	NA
PB_5nlscmib	8.351077	0.757308	8933.415
PB_5nlmecmibrandomabc	NA	NA	NA
PB_5nlmecmibrandoma	8.793878	0.744439	8051.98
PB_5nlmecmibrandomb	NA	NA	NA

Model name	MSE	R^2	AIC
PB_5nlmecmibrandomc	NA	NA	NA
PB_5nlmecmibrandomab	NA	NA	NA
PB_5nlmecmibrandomac	NA	NA	NA
PB_5nlmecmibrandombc	NA	NA	NA
PB_5nlscmic	8.295194	0.758932	8933.622
PB_5nlmecmicrandomabc	NA	NA	NA
PB_5nlmecmicrandoma	8.911487	0.741022	8047.708
PB_5nlmecmicrandomb	NA	NA	NA
PB_5nlmecmicrandomc	NA	NA	NA
PB_5nlmecmicrandomab	NA	NA	NA
PB_5nlmecmicrandomac	NA	NA	NA
PB_5nlmecmicrandombc	NA	NA	NA
PB_6nls	8.277724	0.759439	8930.778
PB_6nlme	NA	NA	NA
PB_6nlmea	9.333236	0.728765	8070.559
PB_6nlmeb	NA	NA	NA
PB_6nlmec	9.024972	0.737724	7974.236
PB_6nlmeab	NA	NA	NA
PB_6nlmeac	NA	NA	NA
PB_6nlmebc	NA	NA	NA
PB_6nlscmi	8.322253	0.758145	8932.682
PB_6nlmecmirandomabc	NA	NA	NA
PB_6nlmecmirandoma	8.543787	0.751707	8053.986
PB_6nlmecmirandomb	NA	NA	NA
PB_6nlmecmirandomc	8.453856	0.754321	8211.38
PB_6nlmecmirandomab	NA	NA	NA
PB_6nlmecmirandomac	NA	NA	NA
PB_6nlmecmirandombc	NA	NA	NA
PB_6nlscmia	8.369338	0.756777	8932.36
PB_6nlmecmiarandomabc	NA	NA	NA
PB_6nlmecmiarandoma	8.776709	0.744938	8062.238
PB_6nlmecmiarandomb	NA	NA	NA
PB_6nlmecmiarandomc	8.612022	0.749724	8215.853
PB_6nlmecmiarandomab	NA	NA	NA
PB_6nlmecmiarandomac	NA	NA	NA
PB_6nlmecmiarandombc	NA	NA	NA
PB_6nlscmib	8.346061	0.757454	8932.558
PB_6nlmecmibrandomabc	NA	NA	NA
PB_6nlmecmibrandoma	8.711369	0.746837	8057.528
PB_6nlmecmibrandomb	NA	NA	NA

Model name	MSE	R^2	AIC
PB_6nlmecmibrandomc	8.544867	0.751676	8211.976
PB_6nlmecmibrandomab	NA	NA	NA
PB_6nlmecmibrandomac	NA	NA	NA
PB_6nlmecmibrandombc	NA	NA	NA
PB_6nlscmic	8.373991	0.756642	8932.338
PB_6nlmecmicrandomabc	NA	NA	NA
PB_6nlmecmicrandoma	8.750732	0.745693	8062.877
PB_6nlmecmicrandomb	NA	NA	NA
PB_6nlmecmicrandomc	8.59489	0.750222	8215.282
PB_6nlmecmicrandomab	NA	NA	NA
PB_6nlmecmicrandomac	NA	NA	NA
PB_6nlmecmicrandombc	NA	NA	NA
PB_7nls	8.346194	0.75745	8952.296
PB_7nlme	NA	NA	NA
PB_7nlmea	9.246823	0.731276	8043.238
PB_7nlmeb	NA	NA	NA
PB_7nlmec	9.068015	0.736473	8024.402
PB_7nlmeab	8.828302	0.743439	7920.087
PB_7nlmeac	NA	NA	NA
PB_7nlmebc	NA	NA	NA
PB_7nlscmi	8.378059	0.756524	8954.25
PB_7nlmecmirandomabc	NA	NA	NA
PB_7nlmecmirandoma	8.442085	0.754663	8025.561
PB_7nlmecmirandomb	NA	NA	NA
PB_7nlmecmirandomc	8.581927	0.750599	8266.048
PB_7nlmecmirandomab	8.335504	0.75776	7912.226
PB_7nlmecmirandomac	NA	NA	NA
PB_7nlmecmirandombc	NA	NA	NA
PB_7nlscmia	8.407252	0.755675	8954.121
PB_7nlmecmiarandomabc	NA	NA	NA
PB_7nlmecmiarandoma	8.686032	0.747574	8034.7
PB_7nlmecmiarandomb	NA	NA	NA
PB_7nlmecmiarandomc	8.691608	0.747412	8269.705
PB_7nlmecmiarandomab	8.448864	0.754466	7916.127
PB_7nlmecmiarandomac	NA	NA	NA
PB_7nlmecmiarandombc	NA	NA	NA
PB_7nlscmib	8.351746	0.757288	8954.295
PB_7nlmecmibrandomabc	NA	NA	NA
PB_7nlmecmibrandoma	8.780741	0.744821	8028.324
PB_7nlmecmibrandomb	9.570186	0.721879	8319.226

Model name	MSE	R^2	AIC
PB_7nlmecmibrandomc	8.739338	0.746024	8268.725
PB_7nlmecmibrandomab	8.433692	0.754907	7909.497
PB_7nlmecmibrandomac	NA	NA	NA
PB_7nlmecmibrandombc	NA	NA	NA
PB_7nlscmic	8.410885	0.75557	8954.111
PB_7nlmecmicrandomabc	NA	NA	NA
PB_7nlmecmicrandoma	8.663512	0.748228	8035.059
PB_7nlmecmicrandomb	NA	NA	NA
PB_7nlmecmicrandomc	8.673114	0.747949	8019.754
PB_7nlmecmicrandomab	8.377976	0.756526	7913.276
PB_7nlmecmicrandomac	NA	NA	NA
PB_7nlmecmicrandombc	NA	NA	NA

Table C.2b Tmax added models selection criteria for species Balsam poplar

Model name	MSE	R^2	AIC
PB_1nls	9.319654	0.72916	9014.353
PB_1nlme	NA	NA	NA
PB_1nlmea	9.556318	0.722282	8280.584
PB_1nlmeb	9.441157	0.725629	8044.154
PB_1nlstmax	8.72559	0.746424	9013.034
PB_1nlmetmaxrandomab	NA	NA	NA
PB_1nlmetmaxrandoma	11.78839	0.657415	8045.023
PB_1nlmetmaxrandomb	7.26922	0.788748	8305.427
PB_1nlstmaxa	9.400273	0.726817	9016.276
PB_1nlmetmaxarandomab	NA	NA	NA
PB_1nlmetmaxarandoma	11.1348	0.676409	8280.212
PB_1nlmetmaxarandomb	10.32542	0.699931	8044.969
PB_1nlstmaxb	9.50297	0.723832	9015.865
PB_1nlmetmaxbrandomab	NA	NA	NA
PB_1nlmetmaxbrandoma	11.65079	0.661414	8278.361
PB_1nlmetmaxbrandomb	10.84035	0.684967	8043.57
PB_2nls	7.667463	0.777174	8999.787
PB_2nlme	8.428776	0.75505	7928.059
PB_2nlmea	8.615087	0.749635	7987.029
PB_2nlmeb	7.656429	0.777495	8210.97
PB_2nlstmax	7.093041	0.793868	8997.086
PB_2nlmetmaxrandomab	7.758361	0.774533	7937.355
PB_2nlmetmaxrandoma	NA	NA	NA
PB_2nlmetmaxrandomb	8.724934	0.746443	8073.532
PB_2nlstmaxa	6.922526	0.798823	8991.303

Model name	MSE	R^2	AIC
PB_2nlmetmaxarandomab	10.33782	0.699571	7924.525
PB_2nlmetmaxarandoma	10.061	0.707615	7985.837
PB_2nlmetmaxarandomb	7.527047	0.781255	8212.896
PB_2nlstmaxb	6.830752	0.80149	8991.872
PB_2nlmetmaxbrandomab	8.99972	0.738457	7929.276
PB_2nlmetmaxbrandoma	9.009413	0.738176	7988.495
PB_2nlmetmaxbrandomb	8.876645	0.742034	8209.821
PB_3nls	7.810187	0.773027	8954.133
PB_3nlme	8.680241	0.747742	7915.177
PB_3nlmea	7.930644	0.769526	8087.555
PB_3nlmeb	8.766382	0.745238	7991.847
PB_3nlstmax	7.290678	0.788124	8952.625
PB_3nlmetmaxrandomab	NA	NA	NA
PB_3nlmetmaxrandoma	8.041009	0.766319	8302.393
PB_3nlmetmaxrandomb	7.549927	0.78059	8219.895
PB_3nlstmaxa	7.042296	0.795343	8948.193
PB_3nlmetmaxarandomab	9.317984	0.729208	7916.391
PB_3nlmetmaxarandoma	9.179848	0.733223	8086.449
PB_3nlmetmaxarandomb	8.923021	0.740686	8219.895
PB_3nlstmaxb	7.217553	0.790249	8948.913
PB_3nlmetmaxbrandomab	10.75716	0.687384	7910.796
PB_3nlmetmaxbrandoma	8.013165	0.767128	8089.51
PB_3nlmetmaxbrandomb	10.10505	0.706335	7991.268
PB_4nls	7.642104	0.777911	9013.996
PB_4nlme	8.772719	0.745054	7934.981
PB_4nlmea	10.11745	0.705975	8052.643
PB_4nlmeb	7.595838	0.779256	8235.524
PB_4nlstmax	7.079243	0.794269	9011.467
PB_4nlmetmaxrandomab	9.108053	0.735309	7934.495
PB_4nlmetmaxrandoma	7.183034	0.791252	8120.607
PB_4nlmetmaxrandomb	8.776347	0.744949	8405.626
PB_4nlstmaxa	6.883614	0.799954	9004.902
PB_4nlmetmaxarandomab	10.36667	0.698732	7933.581
PB_4nlmetmaxarandoma	12.06802	0.649289	8051.822
PB_4nlmetmaxarandomb	7.428839	0.784109	8237.388
PB_4nlstmaxb	6.79342	0.802575	9005.72
PB_4nlmetmaxbrandomab	9.41879	0.726279	7936.224
PB_4nlmetmaxbrandoma	11.6518	0.661385	8055.104
PB_4nlmetmaxbrandomb	8.795847	0.744382	8234.429
PB_5nls	8.283372	0.759275	8931.629

Model name	MSE	R^2	AIC
PB_5nlme	NA	NA	NA
PB_5nlmea	9.414782	0.726395	8064.471
PB_5nlmeb	NA	NA	NA
PB_5nlmec	NA	NA	NA
PB_5nlmeab	NA	NA	NA
PB_5nlmeac	NA	NA	NA
PB_5nlmebc	NA	NA	NA
PB_5nlstmax	7.600536	0.779119	8928.018
PB_5nlmetmaxrandomabc	NA	NA	NA
PB_5nlmetmaxrandoma	7.681244	0.776774	8076.391
PB_5nlmetmaxrandomb	NA	NA	NA
PB_5nlmetmaxrandomc	NA	NA	NA
PB_5nlmetmaxrandomab	NA	NA	NA
PB_5nlmetmaxrandomac	NA	NA	NA
PB_5nlmetmaxrandombc	NA	NA	NA
PB_5nlstmaxa	7.728582	0.775398	8929.47
PB_5nlmetmaxarandomabc	NA	NA	NA
PB_5nlmetmaxarandoma	11.07888	0.678035	8062.214
PB_5nlmetmaxarandomb	NA	NA	NA
PB_5nlmetmaxarandomc	NA	NA	NA
PB_5nlmetmaxarandomab	NA	NA	NA
PB_5nlmetmaxarandomac	NA	NA	NA
PB_5nlmetmaxarandombc	NA	NA	NA
PB_5nlstmaxb	7.633939	0.778149	8928.956
PB_5nlmetmaxbrandomabc	NA	NA	NA
PB_5nlmetmaxbrandoma	10.84968	0.684696	8061.911
PB_5nlmetmaxbrandomb	NA	NA	NA
PB_5nlmetmaxbrandomc	NA	NA	NA
PB_5nlmetmaxbrandomab	NA	NA	NA
PB_5nlmetmaxbrandomac	NA	NA	NA
PB_5nlmetmaxbrandombc	NA	NA	NA
PB_5nlstmaxc	7.570282	0.779999	8928.235
PB_5nlmetmaxcrandomabc	NA	NA	NA
PB_5nlmetmaxcrandoma	9.866205	0.713276	8065.251
PB_5nlmetmaxcrandomb	NA	NA	NA
PB_5nlmetmaxcrandomc	NA	NA	NA
PB_5nlmetmaxcrandomab	NA	NA	NA
PB_5nlmetmaxcrandomac	NA	NA	NA
PB_5nlmetmaxcrandombc	NA	NA	NA
PB_6nls	8.277724	0.759439	8930.778

Model name	MSE	R^2	AIC
PB_6nlme	NA	NA	NA
PB_6nlmea	9.333236	0.728765	8070.559
PB_6nlmeb	NA	NA	NA
PB_6nlmec	9.024972	0.737724	7974.236
PB_6nlmeab	NA	NA	NA
PB_6nlmeac	NA	NA	NA
PB_6nlmebc	NA	NA	NA
PB_6nlstmax	7.599985	0.779135	8927.273
PB_6nlmetmaxrandomabc	NA	NA	NA
PB_6nlmetmaxrandoma	7.955831	0.768794	8081.766
PB_6nlmetmaxrandomb	NA	NA	NA
PB_6nlmetmaxrandomc	NA	NA	NA
PB_6nlmetmaxrandomab	NA	NA	NA
PB_6nlmetmaxrandomac	NA	NA	NA
PB_6nlmetmaxrandombc	NA	NA	NA
PB_6nlstmaxa	7.734465	0.775227	8928.805
PB_6nlmetmaxarandomabc	NA	NA	NA
PB_6nlmetmaxarandoma	10.96498	0.681345	8070.127
PB_6nlmetmaxarandomb	NA	NA	NA
PB_6nlmetmaxarandomc	11.1087	0.677168	8222.927
PB_6nlmetmaxarandomab	NA	NA	NA
PB_6nlmetmaxarandomac	NA	NA	NA
PB_6nlmetmaxarandombc	NA	NA	NA
PB_6nlstmaxb	7.633509	0.778161	8928.172
PB_6nlmetmaxbrandomabc	NA	NA	NA
PB_6nlmetmaxbrandoma	10.72241	0.688394	8067.01
PB_6nlmetmaxbrandomb	NA	NA	NA
PB_6nlmetmaxbrandomc	10.44174	0.696551	8225.199
PB_6nlmetmaxbrandomab	NA	NA	NA
PB_6nlmetmaxbrandomac	NA	NA	NA
PB_6nlmetmaxbrandombc	NA	NA	NA
PB_6nlstmaxc	7.681711	0.77676	8928.687
PB_6nlmetmaxcrandomabc	NA	NA	NA
PB_6nlmetmaxcrandoma	11.09242	0.677641	8064.868
PB_6nlmetmaxcrandomb	NA	NA	NA
PB_6nlmetmaxcrandomc	10.88272	0.683735	8226.002
PB_6nlmetmaxcrandomab	NA	NA	NA
PB_6nlmetmaxcrandomac	NA	NA	NA
PB_6nlmetmaxcrandombc	NA	NA	NA
PB_7nls	8.346194	0.75745	8952.296

Model name	MSE	R^2	AIC
PB_7nlme	NA	NA	NA
PB_7nlmea	9.246823	0.731276	8043.238
PB_7nlmeb	NA	NA	NA
PB_7nlmec	9.068015	0.736473	8024.402
PB_7nlmeab	8.828302	0.743439	7920.087
PB_7nlmeac	NA	NA	NA
PB_7nlmebc	NA	NA	NA
PB_7nlstmax	7.547256	0.780668	8946.238
PB_7nlmetmaxrandomabc	NA	NA	NA
PB_7nlmetmaxrandoma	7.44149	0.783741	8055.88
PB_7nlmetmaxrandomb	8.699958	0.747169	8066.173
PB_7nlmetmaxrandomc	9.166436	0.733612	8280.107
PB_7nlmetmaxrandomab	NA	NA	NA
PB_7nlmetmaxrandomac	NA	NA	NA
PB_7nlmetmaxrandombc	NA	NA	NA
PB_7nlstmaxa	7.671868	0.777046	8947.78
PB_7nlmetmaxarandomabc	NA	NA	NA
PB_7nlmetmaxarandoma	10.82828	0.685317	8042.964
PB_7nlmetmaxarandomb	NA	NA	NA
PB_7nlmetmaxarandomc	10.88066	0.683795	8282.472
PB_7nlmetmaxarandomab	10.94165	0.682023	7917.329
PB_7nlmetmaxarandomac	NA	NA	NA
PB_7nlmetmaxarandombc	NA	NA	NA
PB_7nlstmaxb	7.623753	0.778445	8948.602
PB_7nlmetmaxbrandomabc	NA	NA	NA
PB_7nlmetmaxbrandoma	9.665393	0.719112	8044.023
PB_7nlmetmaxbrandomb	NA	NA	NA
PB_7nlmetmaxbrandomc	10.12144	0.705859	8277.523
PB_7nlmetmaxbrandomab	9.713172	0.717724	7922.184
PB_7nlmetmaxbrandomac	NA	NA	NA
PB_7nlmetmaxbrandombc	NA	NA	NA
PB_7nlstmaxc	7.668479	0.777145	8949.549
PB_7nlmetmaxcrandomabc	NA	NA	NA
PB_7nlmetmaxcrandoma	10.82079	0.685535	8039.576
PB_7nlmetmaxcrandomb	9.43003	0.725952	8328.03
PB_7nlmetmaxcrandomc	10.85748	0.684469	8023.757
PB_7nlmetmaxcrandomab	11.11699	0.676927	7915.093
PB_7nlmetmaxcrandomac	NA	NA	NA
PB_7nlmetmaxcrandombc	NA	NA	NA

Table C.3a CMI added models selection criteria for species Lodgepole pine

Model name	MSE	R^2	AIC
PL_1nls	7.537567	0.527677	109501.7
PL_1nlme	NA	NA	NA
PL_1nlmea	7.592931	0.524207	81587.08
PL_1nlmeb	7.112863	0.55429	82660.39
PL_1nlscmi	7.04191	0.558736	106431.7
PL_1nlmecmirandomab	8.268105	0.481899	80562.84
PL_1nlmecmirandoma	NA	NA	NA
PL_1nlmecmirandomb	6.672411	0.58189	82410.63
PL_1nlscmia	6.789437	0.574556	106511.2
PL_1nlmecmiarandomab	NA	NA	NA
PL_1nlmecmiarandoma	7.182672	0.549915	84360.31
PL_1nlmecmiarandomb	6.551506	0.589466	82057.85
PL_1nlscmib	6.663428	0.582453	106711.6
PL_1nlmecmibrandomab	NA	NA	NA
PL_1nlmecmibrandoma	6.910933	0.566943	80841.81
PL_1nlmecmibrandomb	6.506181	0.592306	82025.84
PL_2nls	7.8411	0.508657	108997.3
PL_2nlme	7.400234	0.536282	80786.26
PL_2nlmea	7.696537	0.517715	81451.76
PL_2nlmeb	8.076878	0.493882	83091.63
PL_2nlscmi	7.28274	0.543645	106523.2
PL_2nlmecmirandomab	NA	NA	NA
PL_2nlmecmirandoma	7.279605	0.543841	81030.6
PL_2nlmecmirandomb	NA	NA	NA
PL_2nlscmia	6.99956	0.56139	106095.1
PL_2nlmecmiarandomab	NA	NA	NA
PL_2nlmecmiarandoma	7.022768	0.559935	80627.66
PL_2nlmecmiarandomb	7.283884	0.543573	81997.44
PL_2nlscmib	7.368451	0.538274	106582.7
PL_2nlmecmibrandomab	NA	NA	NA
PL_2nlmecmibrandoma	7.276468	0.544038	81055.89
PL_2nlmecmibrandomb	7.565858	0.525904	82620.75
PL_3nls	7.68865	0.518209	108801.5
PL_3nlme	7.310821	0.541885	80751.55
PL_3nlmea	7.589368	0.524431	82079.1
PL_3nlmeb	7.444349	0.533518	82174.71
PL_3nlscmi	7.166371	0.550937	106233.1
PL_3nlmecmirandomab	6.863238	0.569932	80287.95
PL_3nlmecmirandoma	7.474775	0.531611	83878.36

Model name	MSE	R^2	AIC
PL_3nlmecmirandomb	7.004388	0.561087	80977.79
PL_3nlscmia	7.152218	0.551824	106152
PL_3nlmecmiarandomab	6.833762	0.571779	80168.5
PL_3nlmecmiarandoma	7.054676	0.557936	81468.81
PL_3nlmecmiarandomb	6.999578	0.561389	80977.79
PL_3nlscmib	6.777566	0.5753	105941.7
PL_3nlmecmibrandomab	6.673755	0.581805	79806.82
PL_3nlmecmibrandoma	6.840938	0.571329	80934.77
PL_3nlmecmibrandomb	6.779053	0.575207	81335.61
PL_4nls	7.879844	0.506229	109067
PL_4nlme	NA	NA	NA
PL_4nlmea	8.952951	0.438985	82526.69
PL_4nlmeb	8.13492	0.490245	83328
PL_4nlscmi	7.318369	0.541412	106625.9
PL_4nlmecmirandomab	7.292759	0.543017	80342.87
PL_4nlmecmirandoma	8.290404	0.480502	82140.5
PL_4nlmecmirandomb	7.7045	0.517216	82934.49
PL_4nlscmia	7.01903	0.56017	106113.9
PL_4nlmecmiarandomab	7.138626	0.552675	80205.93
PL_4nlmecmiarandoma	8.180475	0.48739	81843.98
PL_4nlmecmiarandomb	7.410489	0.53564	83265.3
PL_4nlscmib	7.410615	0.535632	106691
PL_4nlmecmibrandomab	7.334775	0.540384	80366.55
PL_4nlmecmibrandoma	8.449981	0.470503	82132.69
PL_4nlmecmibrandomb	7.626926	0.522077	82867.27
PL_5nls	7.628434	0.521983	108764.5
PL_5nlme	NA	NA	NA
PL_5nlmea	7.733813	0.515379	81164.59
PL_5nlmeb	NA	NA	NA
PL_5nlmec	NA	NA	NA
PL_5nlmeab	NA	NA	NA
PL_5nlmeac	NA	NA	NA
PL_5nlmebc	NA	NA	NA
PL_5nlscmi	7.047532	0.558384	106026.4
PL_5nlmecmirandomabc	NA	NA	NA
PL_5nlmecmirandoma	8.156439	0.488897	82175.54
PL_5nlmecmirandomb	NA	NA	NA
PL_5nlmecmirandomc	NA	NA	NA
PL_5nlmecmirandomab	NA	NA	NA
PL_5nlmecmirandomac	NA	NA	NA

Model name	MSE	R^2	AIC
PL_5nlmecmirandombc	NA	NA	NA
PL_5nlscmia	6.811951	0.573146	105795.5
PL_5nlmecmiarandomabc	NA	NA	NA
PL_5nlmecmiarandoma	8.033537	0.496598	82015.95
PL_5nlmecmiarandomb	NA	NA	NA
PL_5nlmecmiarandomc	NA	NA	NA
PL_5nlmecmiarandomab	NA	NA	NA
PL_5nlmecmiarandomac	NA	NA	NA
PL_5nlmecmiarandombc	NA	NA	NA
PL_5nlscmib	6.94583	0.564756	105850.6
PL_5nlmecmibrandomabc	NA	NA	NA
PL_5nlmecmibrandoma	NA	NA	NA
PL_5nlmecmibrandomb	NA	NA	NA
PL_5nlmecmibrandomc	NA	NA	NA
PL_5nlmecmibrandomab	NA	NA	NA
PL_5nlmecmibrandomac	NA	NA	NA
PL_5nlmecmibrandombc	NA	NA	NA
PL_5nlscmic	7.112638	0.554304	106204.6
PL_5nlmecmicrandomabc	NA	NA	NA
PL_5nlmecmicrandoma	NA	NA	NA
PL_5nlmecmicrandomb	NA	NA	NA
PL_5nlmecmicrandomc	NA	NA	NA
PL_5nlmecmicrandomab	NA	NA	NA
PL_5nlmecmicrandomac	NA	NA	NA
PL_5nlmecmicrandombc	NA	NA	NA
PL_6nls	7.627598	0.522035	108763
PL_6nlme	NA	NA	NA
PL_6nlmea	7.74116	0.514919	81163.23
PL_6nlmeb	NA	NA	NA
PL_6nlmec	7.520093	0.528772	81171.94
PL_6nlmeab	8.47296	0.469063	80893.93
PL_6nlmeac	9.906173	0.379254	81035.29
PL_6nlmebc	NA	NA	NA
PL_6nlscmi	7.050157	0.558219	106030.4
PL_6nlmecmirandomabc	NA	NA	NA
PL_6nlmecmirandoma	7.241629	0.546221	80679.14
PL_6nlmecmirandomb	NA	NA	NA
PL_6nlmecmirandomc	7.04503	0.55854	80689.25
PL_6nlmecmirandomab	8.089673	0.49308	80421.11
PL_6nlmecmirandomac	NA	NA	NA

Model name	MSE	R^2	AIC
PL_6nlmecmirandombc	NA	NA	NA
PL_6nlscmia	6.812235	0.573128	105794.9
PL_6nlmecmiarandomabc	NA	NA	NA
PL_6nlmecmiarandoma	7.095839	0.555357	80538.95
PL_6nlmecmiarandomb	NA	NA	NA
PL_6nlmecmiarandomc	6.86779	0.569647	80428.92
PL_6nlmecmiarandomab	7.99473	0.49903	80143.24
PL_6nlmecmiarandomac	NA	NA	NA
PL_6nlmecmiarandombc	NA	NA	NA
PL_6nlscmib	6.951026	0.564431	105853.4
PL_6nlmecmibrandomabc	NA	NA	NA
PL_6nlmecmibrandoma	7.114958	0.554158	80599.54
PL_6nlmecmibrandomb	NA	NA	NA
PL_6nlmecmibrandomc	6.914724	0.566706	80688.7
PL_6nlmecmibrandomab	8.420266	0.472365	79882.47
PL_6nlmecmibrandomac	NA	NA	NA
PL_6nlmecmibrandombc	8.358479	0.476236	79884.48
PL_6nlscmic	6.87691	0.569075	105794.7
PL_6nlmecmicrandomabc	NA	NA	NA
PL_6nlmecmicrandoma	7.032047	0.559354	80449.32
PL_6nlmecmicrandomb	NA	NA	NA
PL_6nlmecmicrandomc	NA	NA	NA
PL_6nlmecmicrandomab	8.353153	0.47657	80079.22
PL_6nlmecmicrandomac	9.724146	0.39066	80065.23
PL_6nlmecmicrandombc	NA	NA	NA
PL_7nls	7.602723	0.523594	108764.3
PL_7nlme	NA	NA	NA
PL_7nlmea	7.699632	0.517521	81245.22
PL_7nlmeb	7.644128	0.520999	81780.97
PL_7nlmec	7.729359	0.515659	81521.17
PL_7nlmeab	NA	NA	NA
PL_7nlmeac	8.483465	0.468404	80996.75
PL_7nlmebc	7.747669	0.514511	81012
PL_7nlscmi	7.023221	0.559907	106001.8
PL_7nlmecmirandomabc	NA	NA	NA
PL_7nlmecmirandoma	7.192484	0.549301	80752.76
PL_7nlmecmirandomb	7.171304	0.550628	81281.59
PL_7nlmecmirandomc	7.199592	0.548855	81027.29
PL_7nlmecmirandomab	7.114225	0.554204	80264.21
PL_7nlmecmirandomac	NA	NA	NA

Model name	MSE	R^2	AIC
PL_7nlmecmirandombc	7.240157	0.546313	80547.14
PL_7nlscmia	6.789852	0.57453	105793.9
PL_7nlmecmiarandomabc	NA	NA	NA
PL_7nlmecmiarandoma	7.059985	0.557603	80622.87
PL_7nlmecmiarandomb	6.990095	0.561983	80992.61
PL_7nlmecmiarandomc	7.01973	0.560126	80800.56
PL_7nlmecmiarandomab	6.960852	0.563815	80089.07
PL_7nlmecmiarandomac	9.611965	0.39769	80147.79
PL_7nlmecmiarandombc	7.06957	0.557003	80292.64
PL_7nlscmib	7.201424	0.54874	106382.3
PL_7nlmecmibrandomabc	NA	NA	NA
PL_7nlmecmibrandoma	7.281555	0.543719	80924.36
PL_7nlmecmibrandomb	NA	NA	NA
PL_7nlmecmibrandomc	7.327295	0.540853	81290
PL_7nlmecmibrandomab	7.231928	0.546829	80419.83
PL_7nlmecmibrandomac	NA	NA	NA
PL_7nlmecmibrandombc	7.230851	0.546896	80803.69
PL_7nlscmic	6.908551	0.567093	105804.6
PL_7nlmecmicrandomabc	NA	NA	NA
PL_7nlmecmicrandoma	7.039229	0.558904	80682.98
PL_7nlmecmicrandomb	NA	NA	NA
PL_7nlmecmicrandomc	7.104359	0.554823	81147.27
PL_7nlmecmicrandomab	6.908595	0.56709	80072.06
PL_7nlmecmicrandomac	8.421631	0.472279	79996
PL_7nlmecmicrandombc	7.111948	0.554347	80648.07

Table C.3b Tmax added models selection criteria for species Lodgepole pine

Model name	MSE	R^2	AIC
PL_1nls	7.537567	0.527677	109501.7
PL_1nlme	9.166756	0.425588	81052.31
PL_1nlmea	7.592931	0.524207	81587.08
PL_1nlmeb	7.112863	0.55429	82660.39
PL_1nlstmax	6.612228	0.585661	107756.4
PL_1nlmetmaxrandomab	11.36272	0.287983	80366.13
PL_1nlmetmaxrandoma	7.068235	0.557086	81164.45
PL_1nlmetmaxrandomb	NA	NA	NA
PL_1nlstmaxa	6.4159	0.597963	107477.2
PL_1nlmetmaxarandomab	8.741095	0.452261	79977.13
PL_1nlmetmaxarandoma	7.186995	0.549644	80522.35
PL_1nlmetmaxarandomb	6.517141	0.591619	81639

Model name	MSE	R^2	AIC
PL_1nlstmaxb	6.40931	0.598376	107579.5
PL_1nlmetmaxbrandomab	8.615497	0.460131	80195.27
PL_1nlmetmaxbrandoma	7.140744	0.552543	80539.36
PL_1nlmetmaxbrandomb	6.456883	0.595395	81690.53
PL_2nls	7.8411	0.508657	108997.3
PL_2nlme	7.400234	0.536282	80786.26
PL_2nlmea	7.696537	0.517715	81451.76
PL_2nlmeb	8.076878	0.493882	83091.63
PL_2nlstmax	6.601656	0.586323	106806.7
PL_2nlmetmaxrandomab	6.825474	0.572298	79573.87
PL_2nlmetmaxrandoma	NA	NA	NA
PL_2nlmetmaxrandomb	7.658387	0.520106	83760.78
PL_2nlstmaxa	6.711174	0.579461	107234.3
PL_2nlmetmaxarandomab	7.012488	0.56058	79505.8
PL_2nlmetmaxarandoma	7.390481	0.536894	80188.79
PL_2nlmetmaxarandomb	7.839189	0.508776	82040.66
PL_2nlstmaxb	6.839893	0.571395	106993.2
PL_2nlmetmaxbrandomab	7.418604	0.535131	79638.04
PL_2nlmetmaxbrandoma	7.427147	0.534596	80488.77
PL_2nlmetmaxbrandomb	NA	NA	NA
PL_3nls	7.68865	0.518209	108801.5
PL_3nlme	7.310821	0.541885	80751.55
PL_3nlmea	7.589368	0.524431	82079.1
PL_3nlmeb	7.444349	0.533518	82174.71
PL_3nlstmax	6.523755	0.591205	106753.2
PL_3nlmetmaxrandomab	6.63401	0.584296	79672.64
PL_3nlmetmaxrandoma	6.714965	0.579223	80101.74
PL_3nlmetmaxrandomb	NA	NA	NA
PL_3nlstmaxa	6.652472	0.583139	106686.4
PL_3nlmetmaxarandomab	7.282818	0.54364	79513.48
PL_3nlmetmaxarandoma	8.288235	0.480638	81682.59
PL_3nlmetmaxarandomb	7.084335	0.556077	81148.02
PL_3nlstmaxb	6.561997	0.588808	107067.6
PL_3nlmetmaxbrandomab	6.814411	0.572992	79470.88
PL_3nlmetmaxbrandoma	7.41886	0.535115	81868.9
PL_3nlmetmaxbrandomb	7.00474	0.561065	80976.85
PL_4nls	7.879844	0.506229	109067
PL_4nlme	NA	NA	NA
PL_4nlmea	8.952951	0.438985	82526.69
PL_4nlmeb	8.13492	0.490245	83328

Model name	MSE	R^2	AIC
PL_4nlstmax	6.62124	0.585096	106850.1
PL_4nlmetmaxrandomab	NA	NA	NA
PL_4nlmetmaxrandoma	NA	NA	NA
PL_4nlmetmaxrandomb	7.691586	0.518025	83837.23
PL_4nlstmaxa	6.734598	0.577993	107370.7
PL_4nlmetmaxarandomab	7.462091	0.532406	79563.64
PL_4nlmetmaxarandoma	7.734735	0.515322	80338.66
PL_4nlmetmaxarandomb	8.136573	0.490142	83315.67
PL_4nlstmaxb	6.881855	0.568765	107087
PL_4nlmetmaxbrandomab	8.004999	0.498386	79667.23
PL_4nlmetmaxbrandoma	9.260333	0.419724	81580.57
PL_4nlmetmaxbrandomb	9.189143	0.424185	83206.1
PL_5nls	7.628434	0.521983	108764.5
PL_5nlme	NA	NA	NA
PL_5nlmea	7.733813	0.515379	81164.59
PL_5nlmeb	NA	NA	NA
PL_5nlmec	NA	NA	NA
PL_5nlmeab	NA	NA	NA
PL_5nlmeac	NA	NA	NA
PL_5nlmebc	NA	NA	NA
PL_5nlstmax	6.517811	0.591577	106712.3
PL_5nlmetmaxrandomabc	NA	NA	NA
PL_5nlmetmaxrandoma	8.396492	0.473854	82051.28
PL_5nlmetmaxrandomb	NA	NA	NA
PL_5nlmetmaxrandomc	NA	NA	NA
PL_5nlmetmaxrandomab	NA	NA	NA
PL_5nlmetmaxrandomac	NA	NA	NA
PL_5nlmetmaxrandombc	NA	NA	NA
PL_5nlstmaxa	6.449464	0.59586	106915.3
PL_5nlmetmaxarandomabc	NA	NA	NA
PL_5nlmetmaxarandoma	9.056072	0.432523	81390.91
PL_5nlmetmaxarandomb	NA	NA	NA
PL_5nlmetmaxarandomc	NA	NA	NA
PL_5nlmetmaxarandomab	NA	NA	NA
PL_5nlmetmaxarandomac	7.3483	0.539537	79476.2
PL_5nlmetmaxarandombc	NA	NA	NA
PL_5nlstmaxb	6.487983	0.593446	106806
PL_5nlmetmaxbrandomabc	NA	NA	NA
PL_5nlmetmaxbrandoma	7.322057	0.541181	80173.54
PL_5nlmetmaxbrandomb	NA	NA	NA

Model name	MSE	R^2	AIC
PL_5nlmetmaxbrandomc	NA	NA	NA
PL_5nlmetmaxbrandomab	NA	NA	NA
PL_5nlmetmaxbrandomac	NA	NA	NA
PL_5nlmetmaxbrandombc	NA	NA	NA
PL_5nlstmaxc	6.662026	0.58254	106579.2
PL_5nlmetmaxcrandomabc	NA	NA	NA
PL_5nlmetmaxcrandoma	NA	NA	NA
PL_5nlmetmaxcrandomb	NA	NA	NA
PL_5nlmetmaxcrandomc	NA	NA	NA
PL_5nlmetmaxcrandomab	NA	NA	NA
PL_5nlmetmaxcrandomac	NA	NA	NA
PL_5nlmetmaxcrandombc	NA	NA	NA
PL_6nls	7.627598	0.522035	108763
PL_6nlme	NA	NA	NA
PL_6nlmea	7.74116	0.514919	81163.23
PL_6nlmeb	NA	NA	NA
PL_6nlmec	7.520093	0.528772	81171.94
PL_6nlmeab	8.47296	0.469063	80893.93
PL_6nlmeac	9.906173	0.379254	81035.29
PL_6nlmebc	NA	NA	NA
PL_6nlstmax	6.508572	0.592156	106715.5
PL_6nlmetmaxrandomabc	NA	NA	NA
PL_6nlmetmaxrandoma	8.296321	0.480131	81971.52
PL_6nlmetmaxrandomb	NA	NA	NA
PL_6nlmetmaxrandomc	6.871645	0.569405	80367.12
PL_6nlmetmaxrandomab	NA	NA	NA
PL_6nlmetmaxrandomac	7.630238	0.52187	80063.71
PL_6nlmetmaxrandombc	NA	NA	NA
PL_6nlstmaxa	6.449422	0.595863	106915.1
PL_6nlmetmaxarandomabc	NA	NA	NA
PL_6nlmetmaxarandoma	7.383212	0.537349	80033.8
PL_6nlmetmaxarandomb	NA	NA	NA
PL_6nlmetmaxarandomc	NA	NA	NA
PL_6nlmetmaxarandomab	8.376497	0.475107	79634.57
PL_6nlmetmaxarandomac	NA	NA	NA
PL_6nlmetmaxarandombc	NA	NA	NA
PL_6nlstmaxb	6.480935	0.593888	106810.5
PL_6nlmetmaxbrandomabc	NA	NA	NA
PL_6nlmetmaxbrandoma	7.74666	0.514574	83462.85
PL_6nlmetmaxbrandomb	NA	NA	NA

Model name	MSE	R^2	AIC
PL_6nlmetmaxbrandomc	NA	NA	NA
PL_6nlmetmaxbrandomab	8.258655	0.482492	79653.01
PL_6nlmetmaxbrandomac	10.90741	0.316514	79871.62
PL_6nlmetmaxbrandombc	NA	NA	NA
PL_6nlstmaxc	6.476876	0.594142	106796.5
PL_6nlmetmaxcrandomabc	NA	NA	NA
PL_6nlmetmaxcrandoma	7.449576	0.53319	80028.28
PL_6nlmetmaxcrandomb	NA	NA	NA
PL_6nlmetmaxcrandomc	NA	NA	NA
PL_6nlmetmaxcrandomab	NA	NA	NA
PL_6nlmetmaxcrandomac	10.25738	0.357246	79777.12
PL_6nlmetmaxcrandombc	NA	NA	NA
PL_7nls	7.602723	0.523594	108764.3
PL_7nlme	NA	NA	NA
PL_7nlmea	7.699632	0.517521	81245.22
PL_7nlmeb	7.644128	0.520999	81780.97
PL_7nlmec	7.729359	0.515659	81521.17
PL_7nlmeab	NA	NA	NA
PL_7nlmeac	8.483465	0.468404	80996.75
PL_7nlmebc	7.747669	0.514511	81012
PL_7nlstmax	6.498026	0.592817	106737.6
PL_7nlmetmaxrandomabc	NA	NA	NA
PL_7nlmetmaxrandoma	7.135325	0.552882	80455.39
PL_7nlmetmaxrandomb	7.101911	0.554976	80751.19
PL_7nlmetmaxrandomc	7.19477	0.549157	80759.52
PL_7nlmetmaxrandomab	NA	NA	NA
PL_7nlmetmaxrandomac	7.561618	0.52617	79941.06
PL_7nlmetmaxrandombc	7.213238	0.548	80036.38
PL_7nlstmaxa	6.419424	0.597742	106926.4
PL_7nlmetmaxarandomabc	NA	NA	NA
PL_7nlmetmaxarandoma	8.83707	0.446247	81174.04
PL_7nlmetmaxarandomb	7.346959	0.539621	80687.87
PL_7nlmetmaxarandomc	7.264382	0.544795	80624.99
PL_7nlmetmaxarandomab	7.256338	0.545299	79525.57
PL_7nlmetmaxarandomac	9.154699	0.426343	79715.31
PL_7nlmetmaxarandombc	NA	NA	NA
PL_7nlstmaxb	6.693647	0.580559	106568.7
PL_7nlmetmaxbrandomabc	NA	NA	NA
PL_7nlmetmaxbrandoma	8.323286	0.478442	81753.7
PL_7nlmetmaxbrandomb	7.920281	0.503695	80524.99

Model name	MSE	R^2	AIC
PL_7nlmetmaxbrandomc	7.737239	0.515165	84206.19
PL_7nlmetmaxbrandomab	8.016153	0.497687	79708.01
PL_7nlmetmaxbrandomac	9.568217	0.400431	79756.41
PL_7nlmetmaxbrandombc	8.12556	0.490832	80010.49
PL_7nlstmaxc	6.437839	0.596589	106782.3
PL_7nlmetmaxcrandomabc	9.541769	0.402088	79197.48
PL_7nlmetmaxcrandoma	7.235998	0.546574	80289.11
PL_7nlmetmaxcrandomb	7.493842	0.530417	84417.14
PL_7nlmetmaxcrandomc	7.13042	0.55319	80693.58
PL_7nlmetmaxcrandomab	7.29029	0.543172	79725.27
PL_7nlmetmaxcrandomac	8.584853	0.462051	79702.73
PL_7nlmetmaxcrandombc	7.252961	0.545511	80102.9

Table C.4a CMI added models selection criteria for species Black spruce

Model name	MSE	R^2	AIC
SB_1nls	4.146092	0.663549	29262.39
SB_1nlme	NA	NA	NA
SB_1nlmea	4.724229	0.616634	23498.07
SB_1nlmeb	4.910728	0.601499	23629.25
SB_1nlscmi	4.4228	0.641094	29008.79
SB_1nlmecmirandomab	NA	NA	NA
SB_1nlmecmirandoma	5.33714	0.566897	24595.87
SB_1nlmecmirandomb	6.547888	0.468646	23271.85
SB_1nlscmia	4.477855	0.636627	29020.98
SB_1nlmecmiarandomab	4.698586	0.618715	22959.91
SB_1nlmecmiarandoma	5.549057	0.5497	24621.95
SB_1nlmecmiarandomb	5.640179	0.542305	23235.49
SB_1nlscmib	4.469311	0.63732	29028.37
SB_1nlmecmibrandomab	NA	NA	NA
SB_1nlmecmibrandoma	5.401261	0.561693	23119.88
SB_1nlmecmibrandomb	5.668938	0.539971	23252.89
SB_2nls	3.853479	0.687294	29272.7
SB_2nlme	4.859814	0.605631	23255.95
SB_2nlmea	4.734411	0.615807	23628.64
SB_2nlmeb	4.507778	0.634198	24156.12
SB_2nlscmi	4.125834	0.665193	29019.09
SB_2nlmecmirandomab	6.356246	0.484197	23069.74
SB_2nlmecmirandoma	5.106397	0.585621	23391.81
SB_2nlmecmirandomb	5.724644	0.535451	24130.68
SB_2nlscmia	4.195693	0.659524	28993.75

Model name	MSE	R^2	AIC
SB_2nlmecmiarandomab	5.666471	0.540172	22793.12
SB_2nlmecmiarandoma	5.563537	0.548525	23191.14
SB_2nlmecmiarandomb	5.170256	0.580439	23715.44
SB_2nlscmib	4.112687	0.66626	29015.59
SB_2nlmecmibrandomab	5.443643	0.558254	22844.4
SB_2nlmecmibrandoma	5.340957	0.566587	23221.48
SB_2nlmecmibrandomb	5.013722	0.593142	23753.24
SB_3nls	3.896351	0.683815	29211.01
SB_3nlme	4.975237	0.596265	23282
SB_3nlmea	4.597035	0.626955	23581.42
SB_3nlmeb	5.02875	0.591922	23732.46
SB_3nlscmi	4.156708	0.662687	28955.6
SB_3nlmecmirandomab	NA	NA	NA
SB_3nlmecmirandoma	6.450292	0.476565	24042.13
SB_3nlmecmirandomb	7.095941	0.424172	23770.57
SB_3nlscmia	4.177219	0.661023	28949.69
SB_3nlmecmiarandomab	5.580634	0.547137	22870.69
SB_3nlmecmiarandoma	5.300368	0.569881	23375.35
SB_3nlmecmiarandomb	5.703871	0.537137	23770.57
SB_3nlscmib	4.236847	0.656184	28940.47
SB_3nlmecmibrandomab	5.470464	0.556077	22840.15
SB_3nlmecmibrandoma	5.420307	0.560148	23378.2
SB_3nlmecmibrandomb	5.446066	0.558057	23312.52
SB_4nls	3.848508	0.687698	29292.33
SB_4nlme	4.415724	0.641669	23385.69
SB_4nlmea	5.535713	0.550783	24548.36
SB_4nlmeb	4.435279	0.640082	23842.78
SB_4nlscmi	4.121921	0.66551	29040.62
SB_4nlmecmirandomab	5.009227	0.593506	23018.19
SB_4nlmecmirandoma	6.861183	0.443222	24171.64
SB_4nlmecmirandomb	5.705727	0.536986	24227.41
SB_4nlscmia	4.208856	0.658456	29010.31
SB_4nlmecmiarandomab	5.091898	0.586798	22954.29
SB_4nlmecmiarandoma	6.877267	0.441917	24283.33
SB_4nlmecmiarandomb	5.149831	0.582097	23805.59
SB_4nlscmib	4.105321	0.666857	29036.07
SB_4nlmecmibrandomab	4.919542	0.600784	22981.88
SB_4nlmecmibrandoma	6.441887	0.477247	24311.88
SB_4nlmecmibrandomb	4.987817	0.595244	23843.6
SB_5nls	3.972976	0.677597	29202.48

Model name	MSE	R^2	AIC
SB_5nlme	NA	NA	NA
SB_5nlmea	NA	NA	NA
SB_5nlmeb	NA	NA	NA
SB_5nlmec	NA	NA	NA
SB_5nlmeab	NA	NA	NA
SB_5nlmeac	NA	NA	NA
SB_5nlmebc	NA	NA	NA
SB_5nlscmi	4.237709	0.656114	28941.34
SB_5nlmecmirandomabc	NA	NA	NA
SB_5nlmecmirandoma	NA	NA	NA
SB_5nlmecmirandomb	NA	NA	NA
SB_5nlmecmirandomc	NA	NA	NA
SB_5nlmecmirandomab	NA	NA	NA
SB_5nlmecmirandomac	NA	NA	NA
SB_5nlmecmirandombc	NA	NA	NA
SB_5nlscmia	4.289821	0.651885	28932.44
SB_5nlmecmiarandomabc	NA	NA	NA
SB_5nlmecmiarandoma	6.048546	0.509167	24121.9
SB_5nlmecmiarandomb	NA	NA	NA
SB_5nlmecmiarandomc	NA	NA	NA
SB_5nlmecmiarandomab	NA	NA	NA
SB_5nlmecmiarandomac	NA	NA	NA
SB_5nlmecmiarandombc	NA	NA	NA
SB_5nlscmib	4.290448	0.651835	28936.09
SB_5nlmecmibrandomabc	NA	NA	NA
SB_5nlmecmibrandoma	NA	NA	NA
SB_5nlmecmibrandomb	NA	NA	NA
SB_5nlmecmibrandomc	NA	NA	NA
SB_5nlmecmibrandomab	NA	NA	NA
SB_5nlmecmibrandomac	NA	NA	NA
SB_5nlmecmibrandombc	NA	NA	NA
SB_5nlscmic	4.235459	0.656297	28958.69
SB_5nlmecmicrandomabc	NA	NA	NA
SB_5nlmecmicrandoma	NA	NA	NA
SB_5nlmecmicrandomb	NA	NA	NA
SB_5nlmecmicrandomc	NA	NA	NA
SB_5nlmecmicrandomab	NA	NA	NA
SB_5nlmecmicrandomac	NA	NA	NA
SB_5nlmecmicrandombc	NA	NA	NA
SB_6nls	3.977516	0.677229	29203.06

Model name	MSE	R^2	AIC
SB_6nlme	NA	NA	NA
SB_6nlmea	4.822349	0.608671	24394.84
SB_6nlmeb	NA	NA	NA
SB_6nlmec	NA	NA	NA
SB_6nlmeab	NA	NA	NA
SB_6nlmeac	4.739938	0.615359	23542.25
SB_6nlmebc	NA	NA	NA
SB_6nlscmi	4.241243	0.655827	28941.48
SB_6nlmecmirandomabc	NA	NA	NA
SB_6nlmecmirandoma	5.803545	0.529048	24025.32
SB_6nlmecmirandomb	NA	NA	NA
SB_6nlmecmirandomc	NA	NA	NA
SB_6nlmecmirandomab	NA	NA	NA
SB_6nlmecmirandomac	5.407427	0.561193	23175.99
SB_6nlmecmirandombc	NA	NA	NA
SB_6nlscmia	4.29394	0.651551	28933.57
SB_6nlmecmiarandomabc	NA	NA	NA
SB_6nlmecmiarandoma	5.274424	0.571986	23154.51
SB_6nlmecmiarandomb	NA	NA	NA
SB_6nlmecmiarandomc	NA	NA	NA
SB_6nlmecmiarandomab	NA	NA	NA
SB_6nlmecmiarandomac	5.427531	0.559561	23138.04
SB_6nlmecmiarandombc	NA	NA	NA
SB_6nlscmib	4.296418	0.65135	28936.85
SB_6nlmecmibrandomabc	NA	NA	NA
SB_6nlmecmibrandoma	NA	NA	NA
SB_6nlmecmibrandomb	NA	NA	NA
SB_6nlmecmibrandomc	NA	NA	NA
SB_6nlmecmibrandomab	NA	NA	NA
SB_6nlmecmibrandomac	5.445294	0.55812	23146.49
SB_6nlmecmibrandombc	NA	NA	NA
SB_6nlscmic	4.294165	0.651533	28939.03
SB_6nlmecmicrandomabc	NA	NA	NA
SB_6nlmecmicrandoma	NA	NA	NA
SB_6nlmecmicrandomb	NA	NA	NA
SB_6nlmecmicrandomc	NA	NA	NA
SB_6nlmecmicrandomab	NA	NA	NA
SB_6nlmecmicrandomac	5.468247	0.556257	23145.2
SB_6nlmecmicrandombc	NA	NA	NA
SB_7nls	3.976312	0.677326	29232.31

Model name	MSE	R^2	AIC
SB_7nlme	NA	NA	NA
SB_7nlmea	4.870933	0.604729	24380.98
SB_7nlmeb	NA	NA	NA
SB_7nlmec	NA	NA	NA
SB_7nlmeab	NA	NA	NA
SB_7nlmeac	4.085403	0.668474	23483.23
SB_7nlmebc	NA	NA	NA
SB_7nlscmi	4.238226	0.656072	28966.46
SB_7nlmecmirandomabc	NA	NA	NA
SB_7nlmecmirandoma	5.227379	0.575804	23120.52
SB_7nlmecmirandomb	NA	NA	NA
SB_7nlmecmirandomc	NA	NA	NA
SB_7nlmecmirandomab	NA	NA	NA
SB_7nlmecmirandomac	4.443369	0.639425	23107.27
SB_7nlmecmirandombc	NA	NA	NA
SB_7nlscmia	4.290579	0.651824	28956.68
SB_7nlmecmiarandomabc	NA	NA	NA
SB_7nlmecmiarandoma	5.99912	0.513178	24030.37
SB_7nlmecmiarandomb	NA	NA	NA
SB_7nlmecmiarandomc	NA	NA	NA
SB_7nlmecmiarandomab	NA	NA	NA
SB_7nlmecmiarandomac	NA	NA	NA
SB_7nlmecmiarandombc	NA	NA	NA
SB_7nlscmib	4.20814	0.658514	29000.4
SB_7nlmecmibrandomabc	NA	NA	NA
SB_7nlmecmibrandoma	5.153426	0.581805	24064.87
SB_7nlmecmibrandomb	NA	NA	NA
SB_7nlmecmibrandomc	NA	NA	NA
SB_7nlmecmibrandomab	NA	NA	NA
SB_7nlmecmibrandomac	4.431991	0.640348	22965.34
SB_7nlmecmibrandombc	NA	NA	NA
SB_7nlscmic	4.296898	0.651311	28967.01
SB_7nlmecmicrandomabc	NA	NA	NA
SB_7nlmecmicrandoma	NA	NA	NA
SB_7nlmecmicrandomb	NA	NA	NA
SB_7nlmecmicrandomc	NA	NA	NA
SB_7nlmecmicrandomab	NA	NA	NA
SB_7nlmecmicrandomac	4.523335	0.632936	22994.67
SB_7nlmecmicrandombc	NA	NA	NA

Table C.4b Tmax added models selection criteria for species Black spruce

Model name	MSE	R^2	AIC
SB_1nls	4.146092	0.663549	29262.39
SB_1nlme	NA	NA	NA
SB_1nlmea	4.724229	0.616634	23498.07
SB_1nlmeb	4.910728	0.601499	23629.25
SB_1nlstmax	4.1282	0.665001	29245.97
SB_1nlmetmaxrandomab	NA	NA	NA
SB_1nlmetmaxrandoma	4.67171	0.620896	23512.35
SB_1nlmetmaxrandomb	NA	NA	NA
SB_1nlstmaxa	4.108658	0.666587	29250.89
SB_1nlmetmaxarandomab	4.003115	0.675151	23253.38
SB_1nlmetmaxarandoma	4.667631	0.621226	24743.24
SB_1nlmetmaxarandomb	4.773679	0.612621	23530.47
SB_1nlstmaxb	4.116908	0.665917	29257.24
SB_1nlmetmaxbrandomab	3.972794	0.677612	23237.71
SB_1nlmetmaxbrandoma	4.662098	0.621676	24737.16
SB_1nlmetmaxbrandomb	4.789329	0.611351	23496.36
SB_2nls	3.853479	0.687294	29272.7
SB_2nlme	4.859814	0.605631	23255.95
SB_2nlmea	4.734411	0.615807	23628.64
SB_2nlmeb	4.507778	0.634198	24156.12
SB_2nlstmax	3.825167	0.689592	29257.58
SB_2nlmetmaxrandomab	NA	NA	NA
SB_2nlmetmaxrandoma	4.470348	0.637236	23619.92
SB_2nlmetmaxrandomb	4.385673	0.644107	23521.54
SB_2nlstmaxa	3.857844	0.68694	29274.4
SB_2nlmetmaxarandomab	4.738536	0.615473	23111.03
SB_2nlmetmaxarandoma	4.66661	0.621309	23476.08
SB_2nlmetmaxarandomb	4.333664	0.648328	24096.46
SB_2nlstmaxb	3.826519	0.689482	29261.04
SB_2nlmetmaxbrandomab	4.7046	0.618227	23151.29
SB_2nlmetmaxbrandoma	4.626019	0.624603	23534.23
SB_2nlmetmaxbrandomb	4.30869	0.650354	24038.6
SB_3nls	3.896351	0.683815	29211.01
SB_3nlme	4.975237	0.596265	23282
SB_3nlmea	4.597035	0.626955	23581.42
SB_3nlmeb	5.02875	0.591922	23732.46
SB_3nlstmax	3.87512	0.685538	29190.51
SB_3nlmetmaxrandomab	NA	NA	NA
SB_3nlmetmaxrandoma	4.54449	0.631219	23401.12

Model name	MSE	R^2	AIC
SB_3nlmetmaxrandomb	4.677017	0.620465	23683.87
SB_3nlstmaxa	3.869337	0.686007	29200.71
SB_3nlmetmaxarandomab	4.80554	0.610035	23164.84
SB_3nlmetmaxarandoma	4.523937	0.632887	23660.78
SB_3nlmetmaxarandomb	4.921441	0.60063	23683.87
SB_3nlstmaxb	3.903065	0.68327	29212.42
SB_3nlmetmaxbrandomab	4.841368	0.607128	23139.38
SB_3nlmetmaxbrandoma	4.540262	0.631562	23707.81
SB_3nlmetmaxbrandomb	4.968506	0.596811	23588.68
SB_4nls	3.848508	0.687698	29292.33
SB_4nlme	4.415724	0.641669	23385.69
SB_4nlmea	5.535713	0.550783	24548.36
SB_4nlmeb	4.435279	0.640082	23842.78
SB_4nlstmax	3.819869	0.690022	29277.63
SB_4nlmetmaxrandomab	NA	NA	NA
SB_4nlmetmaxrandoma	NA	NA	NA
SB_4nlmetmaxrandomb	4.381298	0.644462	23553.49
SB_4nlstmaxa	3.854601	0.687203	29293.69
SB_4nlmetmaxarandomab	4.312417	0.650052	23279.2
SB_4nlmetmaxarandoma	5.796619	0.52961	24483.12
SB_4nlmetmaxarandomb	4.328567	0.648741	24192
SB_4nlstmaxb	3.822496	0.689808	29281.36
SB_4nlmetmaxbrandomab	4.303289	0.650793	23288.01
SB_4nlmetmaxbrandoma	5.675249	0.539459	24506.4
SB_4nlmetmaxbrandomb	4.293315	0.651602	24125.48
SB_5nls	3.972976	0.677597	29202.48
SB_5nlme	NA	NA	NA
SB_5nlmea	NA	NA	NA
SB_5nlmeb	NA	NA	NA
SB_5nlmec	NA	NA	NA
SB_5nlmeab	NA	NA	NA
SB_5nlmeac	NA	NA	NA
SB_5nlmebc	NA	NA	NA
SB_5nlstmax	3.95064	0.67941	29185.1
SB_5nlmetmaxrandomabc	NA	NA	NA
SB_5nlmetmaxrandoma	NA	NA	NA
SB_5nlmetmaxrandomb	NA	NA	NA
SB_5nlmetmaxrandomc	NA	NA	NA
SB_5nlmetmaxrandomab	NA	NA	NA
SB_5nlmetmaxrandomac	NA	NA	NA

Model name	MSE	R^2	AIC
SB_5nlmetmaxrandombc	NA	NA	NA
SB_5nlstmaxa	3.963757	0.678345	29201
SB_5nlmetmaxarandomabc	NA	NA	NA
SB_5nlmetmaxarandoma	5.102416	0.585944	24382.7
SB_5nlmetmaxarandomb	NA	NA	NA
SB_5nlmetmaxarandomc	NA	NA	NA
SB_5nlmetmaxarandomab	NA	NA	NA
SB_5nlmetmaxarandomac	NA	NA	NA
SB_5nlmetmaxarandombc	NA	NA	NA
SB_5nlstmaxb	3.945016	0.679866	29193.22
SB_5nlmetmaxbrandomabc	NA	NA	NA
SB_5nlmetmaxbrandoma	4.845764	0.606771	24364.84
SB_5nlmetmaxbrandomb	NA	NA	NA
SB_5nlmetmaxbrandomc	NA	NA	NA
SB_5nlmetmaxbrandomab	NA	NA	NA
SB_5nlmetmaxbrandomac	NA	NA	NA
SB_5nlmetmaxbrandombc	NA	NA	NA
SB_5nlstmaxc	3.922769	0.681671	29172.73
SB_5nlmetmaxcrandomabc	NA	NA	NA
SB_5nlmetmaxcrandoma	4.839562	0.607275	24403.48
SB_5nlmetmaxcrandomb	NA	NA	NA
SB_5nlmetmaxcrandomc	NA	NA	NA
SB_5nlmetmaxcrandomab	NA	NA	NA
SB_5nlmetmaxcrandomac	NA	NA	NA
SB_5nlmetmaxcrandombc	NA	NA	NA
SB_6nls	3.977516	0.677229	29203.06
SB_6nlme	NA	NA	NA
SB_6nlmea	4.822349	0.608671	24394.84
SB_6nlmeb	NA	NA	NA
SB_6nlmec	NA	NA	NA
SB_6nlmeab	NA	NA	NA
SB_6nlmeac	4.739938	0.615359	23542.25
SB_6nlmebc	NA	NA	NA
SB_6nlstmax	3.956546	0.67893	29186.23
SB_6nlmetmaxrandomabc	NA	NA	NA
SB_6nlmetmaxrandoma	NA	NA	NA
SB_6nlmetmaxrandomb	NA	NA	NA
SB_6nlmetmaxrandomc	NA	NA	NA
SB_6nlmetmaxrandomab	NA	NA	NA
SB_6nlmetmaxrandomac	4.629773	0.624299	23487.63

Model name	MSE	R^2	AIC
SB_6nlmetmaxrandombc	NA	NA	NA
SB_6nlstmaxa	3.967731	0.678023	29201.42
SB_6nlmetmaxarandomabc	NA	NA	NA
SB_6nlmetmaxarandoma	NA	NA	NA
SB_6nlmetmaxarandomb	NA	NA	NA
SB_6nlmetmaxarandomc	NA	NA	NA
SB_6nlmetmaxarandomab	NA	NA	NA
SB_6nlmetmaxarandomac	4.522083	0.633038	23307.56
SB_6nlmetmaxarandombc	NA	NA	NA
SB_6nlstmaxb	3.949547	0.679498	29193.84
SB_6nlmetmaxbrandomabc	NA	NA	NA
SB_6nlmetmaxbrandoma	NA	NA	NA
SB_6nlmetmaxbrandomb	NA	NA	NA
SB_6nlmetmaxbrandomc	NA	NA	NA
SB_6nlmetmaxbrandomab	3.827783	0.689379	23306.4
SB_6nlmetmaxbrandomac	4.579939	0.628343	23433.41
SB_6nlmetmaxbrandombc	NA	NA	NA
SB_6nlstmaxc	3.958935	0.678736	29200.42
SB_6nlmetmaxcrandomabc	NA	NA	NA
SB_6nlmetmaxcrandoma	NA	NA	NA
SB_6nlmetmaxcrandomb	NA	NA	NA
SB_6nlmetmaxcrandomc	NA	NA	NA
SB_6nlmetmaxcrandomab	NA	NA	NA
SB_6nlmetmaxcrandomac	4.620508	0.62505	23414.31
SB_6nlmetmaxcrandombc	NA	NA	NA
SB_7nls	3.976312	0.677326	29232.31
SB_7nlme	NA	NA	NA
SB_7nlmea	4.870933	0.604729	24380.98
SB_7nlmeb	NA	NA	NA
SB_7nlmec	NA	NA	NA
SB_7nlmeab	NA	NA	NA
SB_7nlmeac	4.085403	0.668474	23483.23
SB_7nlmebc	NA	NA	NA
SB_7nlstmax	3.955948	0.678979	29216.13
SB_7nlmetmaxrandomabc	NA	NA	NA
SB_7nlmetmaxrandoma	4.532563	0.632187	23479.07
SB_7nlmetmaxrandomb	NA	NA	NA
SB_7nlmetmaxrandomc	NA	NA	NA
SB_7nlmetmaxrandomab	NA	NA	NA
SB_7nlmetmaxrandomac	4.067867	0.669897	23470.41

Model name	MSE	R^2	AIC
SB_7nlmetmaxrandombc	NA	NA	NA
SB_7nlstmaxa	3.968599	0.677952	29231.54
SB_7nlmetmaxarandomabc	NA	NA	NA
SB_7nlmetmaxarandoma	5.052397	0.590003	24290.23
SB_7nlmetmaxarandomb	NA	NA	NA
SB_7nlmetmaxarandomc	NA	NA	NA
SB_7nlmetmaxarandomab	4.426552	0.64079	23146.99
SB_7nlmetmaxarandomac	4.022434	0.673584	23363.21
SB_7nlmetmaxarandombc	NA	NA	NA
SB_7nlstmaxb	3.928706	0.68119	29187.11
SB_7nlmetmaxbrandomabc	NA	NA	NA
SB_7nlmetmaxbrandoma	4.527895	0.632566	23457.18
SB_7nlmetmaxbrandomb	NA	NA	NA
SB_7nlmetmaxbrandomc	NA	NA	NA
SB_7nlmetmaxbrandomab	NA	NA	NA
SB_7nlmetmaxbrandomac	4.014701	0.674211	23398.45
SB_7nlmetmaxbrandombc	NA	NA	NA
SB_7nlstmaxc	3.947177	0.679691	29221.06
SB_7nlmetmaxcrandomabc	NA	NA	NA
SB_7nlmetmaxcrandoma	NA	NA	NA
SB_7nlmetmaxcrandomb	NA	NA	NA
SB_7nlmetmaxcrandomc	NA	NA	NA
SB_7nlmetmaxcrandomab	4.44309	0.639448	23135.24
SB_7nlmetmaxcrandomac	4.050269	0.671325	23339.1
SB_7nlmetmaxcrandombc	NA	NA	NA

Table C.5a CMI added models selection criteria for species White spruce

Model name	MSE	R^2	AIC
SW_1nls	10.67265	0.699339	121033.1
SW_1nlme	NA	NA	NA
SW_1nlmea	NA	NA	NA
SW_1nlmeb	17.16202	0.516525	98609.25
SW_1nlscmi	9.221604	0.740216	118547.3
SW_1nlmecmirandomab	9.909771	0.72083	96192.59
SW_1nlmecmirandoma	13.65925	0.615202	97097.25
SW_1nlmecmirandomb	13.87109	0.609235	98483.53
SW_1nlscmia	9.309945	0.737728	118957.8
SW_1nlmecmiarandomab	9.969578	0.719145	96346.55
SW_1nlmecmiarandoma	14.11584	0.60234	97290.91
SW_1nlmecmiarandomb	15.98023	0.549818	98440.75

Model name	MSE	R^2	AIC
SW_1nlscmib	9.365393	0.736166	119054.3
SW_1nlmecmibrandomab	NA	NA	NA
SW_1nlmecmibrandoma	14.40908	0.594079	97330.11
SW_1nlmecmibrandomb	16.17005	0.54447	98483.42
SW_2nls	9.041206	0.745298	117125.3
SW_2nlme	13.04533	0.632497	94757.22
SW_2nlmea	13.77141	0.612043	96918.6
SW_2nlmeb	11.30974	0.681391	98702.95
SW_2nlscmi	7.966876	0.775563	114986.9
SW_2nlmecmirandomab	NA	NA	NA
SW_2nlmecmirandoma	11.45189	0.677386	95744.63
SW_2nlmecmirandomb	9.203253	0.740733	99353.78
SW_2nlscmia	7.975745	0.775314	115047.3
SW_2nlmecmiarandomab	12.5269	0.647102	94552.54
SW_2nlmecmiarandoma	12.43199	0.649776	96593.42
SW_2nlmecmiarandomb	10.0115	0.717964	98157.51
SW_2nlscmib	8.020779	0.774045	114942.4
SW_2nlmecmibrandomab	12.55531	0.646302	94542.43
SW_2nlmecmibrandoma	12.59606	0.645154	96639.89
SW_2nlmecmibrandomb	10.07011	0.716313	98354.24
SW_3nls	9.270053	0.738851	117497.2
SW_3nlme	13.35074	0.623894	94552.24
SW_3nlmea	12.89484	0.636737	96879.83
SW_3nlmeb	15.89412	0.552243	97660.3
SW_3nlscmi	8.071923	0.772604	115097.5
SW_3nlmecmirandomab	11.8242	0.666898	94274.52
SW_3nlmecmirandoma	11.19437	0.684641	95633.82
SW_3nlmecmirandomb	12.48515	0.648278	97822.69
SW_3nlscmia	8.15211	0.770345	115218.1
SW_3nlmecmiarandomab	12.92376	0.635922	94535.67
SW_3nlmecmiarandoma	11.57054	0.674044	96537.79
SW_3nlmecmiarandomb	14.42805	0.593544	97822.69
SW_3nlscmib	8.175231	0.769694	115472.8
SW_3nlmecmibrandomab	12.27189	0.654286	94302.29
SW_3nlmecmibrandoma	11.69836	0.670443	96471.23
SW_3nlmecmibrandomb	14.68357	0.586346	97446.98
SW_4nls	9.021831	0.745844	117130.3
SW_4nlme	12.4201	0.650111	94831.51
SW_4nlmea	14.97157	0.578233	97513.01
SW_4nlmeb	11.18933	0.684783	99023.02

Model name	MSE	R^2	AIC
SW_4nlscmi	7.966113	0.775585	115036.9
SW_4nlmecmirandomab	NA	NA	NA
SW_4nlmecmirandoma	12.79594	0.639523	97501.8
SW_4nlmecmirandomb	10.17374	0.713394	97248.62
SW_4nlscmia	7.947065	0.776122	115073.8
SW_4nlmecmiarandomab	11.16617	0.685435	94524.37
SW_4nlmecmiarandoma	13.50293	0.619606	97193.88
SW_4nlmecmiarandomb	9.96106	0.719385	96942.27
SW_4nlscmib	8.016178	0.774175	114968.8
SW_4nlmecmibrandomab	11.2888	0.681981	94535.25
SW_4nlmecmibrandoma	11.14305	0.686087	95793.53
SW_4nlmecmibrandomb	10.0202	0.717719	97082.25
SW_5nls	8.987987	0.746798	116961.5
SW_5nlme	NA	NA	NA
SW_5nlmea	13.79271	0.611443	97735.81
SW_5nlmeb	12.36614	0.651631	95576.38
SW_5nlmec	14.27197	0.597941	103250.8
SW_5nlmeab	NA	NA	NA
SW_5nlmeac	NA	NA	NA
SW_5nlmebc	NA	NA	NA
SW_5nlscmi	7.947551	0.776108	114771.4
SW_5nlmecmirandomabc	NA	NA	NA
SW_5nlmecmirandoma	12.00115	0.661913	97432.71
SW_5nlmecmirandomb	11.26858	0.682551	95347.19
SW_5nlmecmirandomc	12.27071	0.654319	103088.4
SW_5nlmecmirandomab	NA	NA	NA
SW_5nlmecmirandomac	NA	NA	NA
SW_5nlmecmirandombc	NA	NA	NA
SW_5nlscmia	7.936778	0.776411	114882.9
SW_5nlmecmiarandomabc	NA	NA	NA
SW_5nlmecmiarandoma	12.33922	0.652389	97428.67
SW_5nlmecmiarandomb	11.33876	0.680573	95297.48
SW_5nlmecmiarandomc	NA	NA	NA
SW_5nlmecmiarandomab	NA	NA	NA
SW_5nlmecmiarandomac	NA	NA	NA
SW_5nlmecmiarandombc	NA	NA	NA
SW_5nlscmib	7.917434	0.776956	114750.7
SW_5nlmecmibrandomabc	NA	NA	NA
SW_5nlmecmibrandoma	12.66499	0.643212	97358.69
SW_5nlmecmibrandomb	11.0975	0.68737	95305.8

Model name	MSE	R^2	AIC
SW_5nlmecmibrandomc	12.00593	0.661778	102907.5
SW_5nlmecmibrandomab	NA	NA	NA
SW_5nlmecmibrandomac	NA	NA	NA
SW_5nlmecmibrandombc	NA	NA	NA
SW_5nlscmic	8.146174	0.770512	114972.5
SW_5nlmecmicrandomabc	NA	NA	NA
SW_5nlmecmicrandoma	13.14184	0.629779	97503.87
SW_5nlmecmicrandomb	11.42854	0.678044	95396.41
SW_5nlmecmicrandomc	12.83173	0.638515	103112.8
SW_5nlmecmicrandomab	NA	NA	NA
SW_5nlmecmicrandomac	NA	NA	NA
SW_5nlmecmicrandombc	NA	NA	NA
SW_6nls	9.000459	0.746446	116957.7
SW_6nlme	NA	NA	NA
SW_6nlmea	12.99797	0.633832	101657.2
SW_6nlmeb	NA	NA	NA
SW_6nlmec	NA	NA	NA
SW_6nlmeab	NA	NA	NA
SW_6nlmeac	NA	NA	NA
SW_6nlmebc	NA	NA	NA
SW_6nlscmi	7.951037	0.77601	114753.5
SW_6nlmecmirandomabc	NA	NA	NA
SW_6nlmecmirandoma	11.83911	0.666478	97352.3
SW_6nlmecmirandomb	NA	NA	NA
SW_6nlmecmirandomc	NA	NA	NA
SW_6nlmecmirandomab	NA	NA	NA
SW_6nlmecmirandomac	NA	NA	NA
SW_6nlmecmirandombc	NA	NA	NA
SW_6nlscmia	7.948144	0.776091	114875.9
SW_6nlmecmiarandomabc	NA	NA	NA
SW_6nlmecmiarandoma	11.6098	0.672938	95352.14
SW_6nlmecmiarandomb	NA	NA	NA
SW_6nlmecmiarandomc	NA	NA	NA
SW_6nlmecmiarandomab	NA	NA	NA
SW_6nlmecmiarandomac	NA	NA	NA
SW_6nlmecmiarandombc	NA	NA	NA
SW_6nlscmib	7.912814	0.777086	114743.2
SW_6nlmecmibrandomabc	NA	NA	NA
SW_6nlmecmibrandoma	11.61617	0.672759	95303.62
SW_6nlmecmibrandomb	NA	NA	NA

Model name	MSE	R^2	AIC
SW_6nlmecmibrandomc	NA	NA	NA
SW_6nlmecmibrandomab	NA	NA	NA
SW_6nlmecmibrandomac	NA	NA	NA
SW_6nlmecmibrandombc	NA	NA	NA
SW_6nlscmic	7.920586	0.776868	114740.8
SW_6nlmecmicrandomabc	NA	NA	NA
SW_6nlmecmicrandoma	NA	NA	NA
SW_6nlmecmicrandomb	NA	NA	NA
SW_6nlmecmicrandomc	NA	NA	NA
SW_6nlmecmicrandomab	NA	NA	NA
SW_6nlmecmicrandomac	NA	NA	NA
SW_6nlmecmicrandombc	NA	NA	NA
SW_7nls	8.995317	0.746591	116972.7
SW_7nlme	NA	NA	NA
SW_7nlmea	13.69995	0.614056	97486.54
SW_7nlmeb	NA	NA	NA
SW_7nlmec	12.37625	0.651346	95765.38
SW_7nlmeab	12.45122	0.649234	94641.12
SW_7nlmeac	NA	NA	NA
SW_7nlmebc	NA	NA	NA
SW_7nlscmi	7.95363	0.775937	114754.2
SW_7nlmecmirandomabc	NA	NA	NA
SW_7nlmecmirandoma	11.8332	0.666645	97128.24
SW_7nlmecmirandomb	11.03563	0.689113	104181.5
SW_7nlmecmirandomc	11.22596	0.683751	95493.22
SW_7nlmecmirandomab	11.10127	0.687264	94348.02
SW_7nlmecmirandomac	NA	NA	NA
SW_7nlmecmirandombc	NA	NA	NA
SW_7nlscmia	7.95245	0.77597	114900.4
SW_7nlmecmiarandomabc	NA	NA	NA
SW_7nlmecmiarandoma	12.23943	0.6552	97193.86
SW_7nlmecmiarandomb	11.40541	0.678696	103982.9
SW_7nlmecmiarandomc	11.3705	0.679679	95505.49
SW_7nlmecmiarandomab	11.19681	0.684572	94347.86
SW_7nlmecmiarandomac	NA	NA	NA
SW_7nlmecmiarandombc	NA	NA	NA
SW_7nlscmib	8.200375	0.768986	115049.4
SW_7nlmecmibrandomabc	NA	NA	NA
SW_7nlmecmibrandoma	13.06127	0.632048	97265.72
SW_7nlmecmibrandomb	11.89946	0.664778	97298.95

Model name	MSE	R^2	AIC
SW_7nlmecmibrandomc	NA	NA	NA
SW_7nlmecmibrandomab	11.41059	0.67855	94393.75
SW_7nlmecmibrandomac	9.448082	0.733836	94469.65
SW_7nlmecmibrandombc	NA	NA	NA
SW_7nlscmic	7.925242	0.776736	114754.7
SW_7nlmecmicrandomabc	NA	NA	NA
SW_7nlmecmicrandoma	12.515	0.647437	97089.43
SW_7nlmecmicrandomb	10.82402	0.695074	103869.8
SW_7nlmecmicrandomc	NA	NA	NA
SW_7nlmecmicrandomab	11.19769	0.684548	94344.98
SW_7nlmecmicrandomac	9.150969	0.742206	94412.67
SW_7nlmecmicrandombc	11.08666	0.687675	94599.33

Table C.5b Tmax added models selection criteria for species White spruce

Model name	MSE	R^2	AIC
SW_1nls	10.67265	0.699339	121033.1
SW_1nlme	NA	NA	NA
SW_1nlmea	NA	NA	NA
SW_1nlmeb	17.16202	0.516525	98609.25
SW_1nlstmax	9.963713	0.71931	118770.1
SW_1nlmetmaxrandomab	10.84465	0.694493	96569.86
SW_1nlmetmaxrandoma	14.03373	0.604653	97371.22
SW_1nlmetmaxrandomb	NA	NA	NA
SW_1nlstmaxa	10.16511	0.713637	119766.8
SW_1nlmetmaxarandomab	12.08281	0.659613	96468.1
SW_1nlmetmaxarandoma	17.22158	0.514847	97401.72
SW_1nlmetmaxarandomb	17.95314	0.494238	98593.67
SW_1nlstmaxb	10.19841	0.712698	119955.5
SW_1nlmetmaxbrandomab	12.01047	0.661651	96402.54
SW_1nlmetmaxbrandoma	18.09593	0.490216	104180.1
SW_1nlmetmaxbrandomb	18.75797	0.471565	98538.02
SW_2nls	9.041206	0.745298	117125.3
SW_2nlme	13.04533	0.632497	94757.22
SW_2nlmea	13.77141	0.612043	96918.6
SW_2nlmeb	11.30974	0.681391	98702.95
SW_2nlstmax	8.746356	0.753605	115985.7
SW_2nlmetmaxrandomab	NA	NA	NA
SW_2nlmetmaxrandoma	NA	NA	NA
SW_2nlmetmaxrandomb	17.65395	0.502667	95942.42
SW_2nlstmaxa	8.844779	0.750832	116101.5

Model name	MSE	R^2	AIC
SW_2nlmetmaxarandomab	NA	NA	NA
SW_2nlmetmaxarandoma	16.55807	0.533539	96680.51
SW_2nlmetmaxarandomb	11.96016	0.663068	98646.33
SW_2nlstmaxb	8.738908	0.753814	115839.3
SW_2nlmetmaxbrandomab	15.93813	0.551004	94755.65
SW_2nlmetmaxbrandoma	14.53299	0.590588	96888.76
SW_2nlmetmaxbrandomb	13.73081	0.613186	98486.16
SW_3nls	9.270053	0.738851	117497.2
SW_3nlme	13.35074	0.623894	94552.24
SW_3nlmea	12.89484	0.636737	96879.83
SW_3nlmeb	15.89412	0.552243	97660.3
SW_3nlstmax	8.851537	0.750642	115933.9
SW_3nlmetmaxrandomab	13.96605	0.60656	94493.17
SW_3nlmetmaxrandoma	15.1431	0.5734	95450.66
SW_3nlmetmaxrandomb	NA	NA	NA
SW_3nlstmaxa	8.914436	0.74887	116149.1
SW_3nlmetmaxarandomab	16.42751	0.537217	94682.56
SW_3nlmetmaxarandoma	15.39272	0.566368	96655.45
SW_3nlmetmaxarandomb	15.62207	0.559908	95978.57
SW_3nlstmaxb	9.030447	0.745601	116538.4
SW_3nlmetmaxbrandomab	16.52227	0.534548	94601.48
SW_3nlmetmaxbrandoma	13.28764	0.625671	95686.47
SW_3nlmetmaxbrandomb	18.24424	0.486038	97496.84
SW_4nls	9.021831	0.745844	117130.3
SW_4nlme	12.4201	0.650111	94831.51
SW_4nlmea	14.97157	0.578233	97513.01
SW_4nlmeb	11.18933	0.684783	99023.02
SW_4nlstmax	8.742091	0.753725	116053.1
SW_4nlmetmaxrandomab	15.04683	0.576113	94432.79
SW_4nlmetmaxrandoma	13.73268	0.613134	95896.76
SW_4nlmetmaxrandomb	NA	NA	NA
SW_4nlstmaxa	8.846549	0.750782	116110.7
SW_4nlmetmaxarandomab	14.55151	0.590067	94649.42
SW_4nlmetmaxarandoma	14.30661	0.596965	95893.27
SW_4nlmetmaxarandomb	11.77627	0.668248	98973.72
SW_4nlstmaxb	8.729553	0.754078	115865.2
SW_4nlmetmaxbrandomab	13.95831	0.606778	94724.41
SW_4nlmetmaxbrandoma	15.99967	0.54927	97500.46
SW_4nlmetmaxbrandomb	NA	NA	NA
SW_5nls	8.987987	0.746798	116961.5

Model name	MSE	R^2	AIC
SW_5nlme	NA	NA	NA
SW_5nlmea	13.79271	0.611443	97735.81
SW_5nlmeb	12.36614	0.651631	95576.38
SW_5nlmec	14.27197	0.597941	103250.8
SW_5nlmeab	9.875498	0.721795	94515.75
SW_5nlmeac	12.55126	0.646416	94519.57
SW_5nlmebc	NA	NA	NA
SW_5nlstmax	8.766343	0.753042	115747.1
SW_5nlmetmaxrandomabc	NA	NA	NA
SW_5nlmetmaxrandoma	12.94179	0.635414	95602.88
SW_5nlmetmaxrandomb	13.09329	0.631146	95485.1
SW_5nlmetmaxrandomc	14.26589	0.598113	96694.74
SW_5nlmetmaxrandomab	11.51748	0.675539	94358.44
SW_5nlmetmaxrandomac	13.78917	0.611542	94389.31
SW_5nlmetmaxrandombc	NA	NA	NA
SW_5nlstmaxa	8.847673	0.75075	115962.1
SW_5nlmetmaxarandomabc	NA	NA	NA
SW_5nlmetmaxarandoma	17.54663	0.50569	97544.45
SW_5nlmetmaxarandomb	13.78399	0.611688	95433.83
SW_5nlmetmaxarandomc	16.41286	0.53763	96693.25
SW_5nlmetmaxarandomab	11.59853	0.673255	94323.56
SW_5nlmetmaxarandomac	14.63631	0.587677	94334.44
SW_5nlmetmaxarandombc	NA	NA	NA
SW_5nlstmaxb	8.75367	0.753399	115651.6
SW_5nlmetmaxbrandomabc	NA	NA	NA
SW_5nlmetmaxbrandoma	13.61219	0.616528	95566.84
SW_5nlmetmaxbrandomb	14.27017	0.597992	95471.17
SW_5nlmetmaxbrandomc	16.56757	0.533272	96666.65
SW_5nlmetmaxbrandomab	11.52306	0.675381	94402.92
SW_5nlmetmaxbrandomac	14.34449	0.595898	94413.87
SW_5nlmetmaxbrandombc	NA	NA	NA
SW_5nlstmaxc	8.665423	0.755885	115656.3
SW_5nlmetmaxcrandomabc	NA	NA	NA
SW_5nlmetmaxcrandoma	13.83538	0.610241	97724.49
SW_5nlmetmaxcrandomb	13.38955	0.6228	95522.78
SW_5nlmetmaxcrandomc	15.99633	0.549364	103215.2
SW_5nlmetmaxcrandomab	10.84113	0.694592	94454.63
SW_5nlmetmaxcrandomac	13.8208	0.610651	94455.76
SW_5nlmetmaxcrandombc	NA	NA	NA
SW_6nls	9.000459	0.746446	116957.7

Model name	MSE	R^2	AIC
SW_6nlme	NA	NA	NA
SW_6nlmea	12.99797	0.633832	101657.2
SW_6nlmeb	NA	NA	NA
SW_6nlmec	NA	NA	NA
SW_6nlmeab	9.762623	0.724975	94588.48
SW_6nlmeac	NA	NA	NA
SW_6nlmebc	NA	NA	NA
SW_6nlstmax	8.768014	0.752994	115733.8
SW_6nlmetmaxrandomabc	NA	NA	NA
SW_6nlmetmaxrandoma	12.33148	0.652607	97764.86
SW_6nlmetmaxrandomb	NA	NA	NA
SW_6nlmetmaxrandomc	13.25483	0.626595	95415.77
SW_6nlmetmaxrandomab	12.60057	0.645027	94605.61
SW_6nlmetmaxrandomac	11.34925	0.680278	94652.35
SW_6nlmetmaxrandombc	NA	NA	NA
SW_6nlstmaxa	8.863457	0.750306	115964
SW_6nlmetmaxarandomabc	NA	NA	NA
SW_6nlmetmaxarandoma	14.92436	0.579563	95450.15
SW_6nlmetmaxarandomb	13.0686	0.631842	95398.35
SW_6nlmetmaxarandomc	NA	NA	NA
SW_6nlmetmaxarandomab	11.4121	0.678507	94399.16
SW_6nlmetmaxarandomac	NA	NA	NA
SW_6nlmetmaxarandombc	10.11433	0.715067	94487.13
SW_6nlstmaxb	8.769653	0.752948	115648.2
SW_6nlmetmaxbrandomabc	NA	NA	NA
SW_6nlmetmaxbrandoma	NA	NA	NA
SW_6nlmetmaxbrandomb	NA	NA	NA
SW_6nlmetmaxbrandomc	NA	NA	NA
SW_6nlmetmaxbrandomab	11.29134	0.681909	94481.15
SW_6nlmetmaxbrandomac	12.02897	0.661129	94621.21
SW_6nlmetmaxbrandombc	10.19069	0.712916	94544.99
SW_6nlstmaxc	8.777196	0.752736	115742
SW_6nlmetmaxcrandomabc	NA	NA	NA
SW_6nlmetmaxcrandoma	NA	NA	NA
SW_6nlmetmaxcrandomb	NA	NA	NA
SW_6nlmetmaxcrandomc	NA	NA	NA
SW_6nlmetmaxcrandomab	11.32534	0.680951	94447.02
SW_6nlmetmaxcrandomac	NA	NA	NA
SW_6nlmetmaxcrandombc	10.40253	0.706948	94499.49
SW_7nls	8.995317	0.746591	116972.7

Model name	MSE	R^2	AIC
SW_7nlme	10.5573	0.702588	94468.43
SW_7nlmea	13.69995	0.614056	97486.54
SW_7nlmeb	NA	NA	NA
SW_7nlmec	NA	NA	NA
SW_7nlmeab	12.45122	0.649234	94641.12
SW_7nlmeac	NA	NA	NA
SW_7nlmebc	NA	NA	NA
SW_7nlstmax	8.787204	0.752454	115720.4
SW_7nlmetmaxrandomabc	11.37679	0.679502	94390.42
SW_7nlmetmaxrandoma	12.75587	0.640652	95855.76
SW_7nlmetmaxrandomb	NA	NA	NA
SW_7nlmetmaxrandomc	12.07481	0.659838	101872.4
SW_7nlmetmaxrandomab	13.552	0.618224	94536.03
SW_7nlmetmaxrandomac	NA	NA	NA
SW_7nlmetmaxrandombc	12.7768	0.640062	94830.88
SW_7nlstmaxa	8.871097	0.750091	115991.4
SW_7nlmetmaxarandomabc	NA	NA	NA
SW_7nlmetmaxarandoma	17.39261	0.510029	97302.36
SW_7nlmetmaxarandomb	13.38859	0.622827	97570.43
SW_7nlmetmaxarandomc	NA	NA	NA
SW_7nlmetmaxarandomab	NA	NA	NA
SW_7nlmetmaxarandomac	11.77257	0.668353	94436.07
SW_7nlmetmaxarandombc	NA	NA	NA
SW_7nlstmaxb	8.664732	0.755904	115658.4
SW_7nlmetmaxbrandomabc	11.5719	0.674006	94436.05
SW_7nlmetmaxbrandoma	13.60851	0.616632	97482.51
SW_7nlmetmaxbrandomb	14.89885	0.580281	97466.54
SW_7nlmetmaxbrandomc	NA	NA	NA
SW_7nlmetmaxbrandomab	13.46517	0.62067	94596.68
SW_7nlmetmaxbrandomac	10.67067	0.699394	94605.3
SW_7nlmetmaxbrandombc	13.43787	0.621439	94828.26
SW_7nlstmaxc	8.76663	0.753033	115667.2
SW_7nlmetmaxcrandomabc	12.60865	0.644799	94360.88
SW_7nlmetmaxcrandoma	14.15997	0.601097	97468.77
SW_7nlmetmaxcrandomb	12.37237	0.651455	104452
SW_7nlmetmaxcrandomc	NA	NA	NA
SW_7nlmetmaxcrandomab	13.94383	0.607185	94560.6
SW_7nlmetmaxcrandomac	11.80778	0.667361	94525.69
SW_7nlmetmaxcrandombc	14.49732	0.591593	94755.22

Appendix D: Minimum and maximum values of CMI and Tmax for the period of 1959-2009 for the study area

PlotID	Min of CMI	Max of CMI	Min of Tmax	Max of Tmax
1	-16.54	48.81	5.9	11.4
2	-16.44	49.02	5.9	11.4
3	-15.59	51.36	5.7	11.2
4	-14.37	54.11	5.6	11.2
5	-13.86	54.54	5.5	11.2
6	-12.86	55.92	5.4	10.7
7	-14.24	54.23	5.3	10.4
8	-17.68	54.20	5.3	10.4
9	-12.28	53.15	5.0	10.0
10	-12.50	53.86	5.1	10.0
11	-10.62	48.65	5.0	9.6
12	-10.70	48.45	5.0	9.6
13	-10.96	48.42	5.0	9.6
14	-16.33	49.25	5.4	10.0
15	-7.72	54.53	4.3	8.6
16	-6.05	56.81	4.0	8.4
17	-7.51	54.72	4.0	9.1
18	-8.29	52.58	4.1	9.2
19	-8.38	50.91	4.2	9.2
20	-9.90	49.00	4.4	9.4
21	-9.82	48.88	4.4	9.4
22	-9.24	52.61	4.7	9.6
23	-12.56	42.77	4.6	9.3
24	-11.38	43.05	4.5	9.2
25	-10.58	41.05	4.5	9.1
26	-12.38	39.50	4.9	9.3
27	-10.29	40.11	4.5	9.1
28	-12.72	39.68	5.0	9.4
29	-13.04	39.97	5.1	9.4
30	-15.28	37.40	5.6	10.1
31	-16.65	40.04	6.0	10.7
32	-16.35	39.50	6.0	10.6
33	-16.03	40.29	5.9	10.5
34	-15.65	41.82	5.8	10.4

PlotID	Min of CMI	Max of CMI	Min of Tmax	Max of Tmax
35	-15.17	43.16	5.7	10.3
36	-14.87	44.00	5.6	10.3
37	-13.23	48.65	5.4	10.1
38	-11.94	52.00	5.3	9.9
39	-12.86	51.89	5.3	10.0
40	-14.17	51.63	5.4	10.4
41	-14.58	50.78	5.4	10.1
42	-15.22	53.02	5.5	10.6
43	-12.70	55.55	5.4	10.6
44	-23.37	25.14	5.3	10.6
45	-23.55	27.34	5.5	10.7
46	-19.63	41.01	6.2	10.6
47	-20.49	40.49	6.2	10.6
48	-23.84	36.85	6.3	10.8
49	-22.37	37.42	6.3	10.7
50	-22.42	37.28	6.3	10.7
51	-22.31	38.63	6.1	10.6
52	-22.92	36.66	6.2	10.7
53	-22.83	36.21	6.2	10.7
54	-23.70	30.80	5.6	10.8
55	-18.73	44.56	5.6	10.3
56	-18.61	43.66	5.6	10.5
57	-18.42	44.61	5.5	10.2
58	-18.28	44.72	5.5	10.2
59	-18.10	43.96	5.5	10.4
60	-18.37	43.50	5.5	10.4
61	-17.85	44.02	5.4	10.3
62	-18.18	42.95	5.5	10.4
63	-18.02	43.19	5.4	10.3
64	-18.41	42.31	5.5	10.4
65	-19.11	41.19	5.6	10.5
66	-19.44	40.73	5.6	10.5
67	-19.58	40.32	5.7	10.5
68	-20.23	39.39	5.7	10.6
69	-20.46	39.03	5.8	10.7
70	-20.36	39.00	5.8	10.7
71	-21.81	41.93	6.3	11.0
72	-21.55	42.45	6.3	11.0

PlotID	Min of CMI	Max of CMI	Min of Tmax	Max of Tmax
73	-22.87	40.84	6.4	11.1
74	-21.42	43.28	6.3	11.0
75	-17.37	50.04	6.8	10.9
76	-17.54	50.75	6.7	10.8
77	-17.34	50.89	6.7	10.8
78	-18.57	50.17	6.6	10.7
79	-18.46	50.00	6.5	10.6
80	-18.80	49.45	6.5	10.6
81	-18.22	50.35	6.4	10.6
82	-17.78	51.70	6.4	10.5
83	-16.76	52.86	6.3	10.4
84	-25.32	38.39	7.4	11.3
85	-25.17	38.73	7.4	11.0
86	-24.78	40.13	7.3	10.9
87	-25.03	40.17	7.3	10.9
88	-24.96	40.74	7.3	10.9
89	-24.66	42.36	7.2	10.8
90	-24.55	44.09	7.1	10.9
91	-12.36	49.67	7.0	11.8
92	-12.25	49.78	7.0	11.8
93	-10.61	50.71	6.9	11.7
94	-10.61	50.71	6.9	11.7
95	-10.82	50.90	6.9	11.8
96	-10.41	50.86	6.9	11.7
97	-9.74	53.20	6.9	11.7
98	-10.48	50.39	6.9	11.6
99	-11.85	49.41	7.0	11.7
100	-12.47	48.43	7.1	11.8
101	-5.88	61.94	5.0	9.0
102	-5.53	59.53	4.9	8.9
103	-6.20	58.68	5.0	9.1
104	-6.86	56.87	5.1	9.2
105	-8.31	54.65	5.5	9.6
106	-7.95	54.79	5.4	9.6
107	-7.70	55.09	5.4	9.5
108	-9.53	51.08	5.6	9.8
109	-8.21	51.47	5.3	9.5
110	-7.62	52.10	5.2	9.4

PlotID	Min of CMI	Max of CMI	Min of Tmax	Max of Tmax
111	-7.40	50.45	5.7	10.0
112	-8.56	48.51	5.6	10.0
113	-8.64	48.26	5.6	10.0
114	-8.40	48.66	5.5	9.9
115	-8.49	50.78	5.6	10.0
116	-17.85	29.89	6.4	10.8
117	-13.54	43.13	6.2	10.8
118	-13.58	43.47	6.3	10.8
119	-11.77	51.35	6.2	10.8
120	-11.64	51.73	6.2	10.8
121	-10.75	52.70	6.1	10.7
122	-7.69	53.22	5.6	10.1
123	-6.79	53.00	5.4	9.9
124	-8.98	52.06	5.8	10.3
125	-9.94	52.43	5.9	10.5
126	-11.19	50.19	6.0	10.6
127	-11.59	46.19	6.1	10.6
128	-7.48	44.79	6.0	10.5
129	-12.96	50.04	7.4	11.4
130	-12.12	48.15	7.3	11.5
131	-12.14	48.13	7.3	11.5
132	-11.05	50.47	7.3	11.5
133	-10.98	50.61	7.3	11.5
134	-9.06	52.23	6.9	11.3
135	-9.12	52.60	7.0	11.3
136	-9.35	49.87	6.9	11.2
137	-8.94	50.75	6.8	11.2
138	-4.11	54.90	5.9	10.4
139	-4.06	55.13	5.9	10.5
140	-6.16	54.19	6.2	10.9
141	-2.53	51.96	4.6	9.3
142	-1.70	53.35	4.5	9.2
143	-1.63	51.87	4.8	9.5
144	-2.17	52.03	4.7	9.5
145	-3.08	49.95	4.9	9.7
146	-5.43	52.28	5.0	9.6
147	-10.84	48.35	6.9	11.7
148	-8.62	49.76	6.7	11.3

PlotID	Min of CMI	Max of CMI	Min of Tmax	Max of Tmax
149	-8.86	49.55	6.8	11.3
150	-3.89	60.55	6.4	10.8
151	-2.58	65.49	5.4	10.5
152	-0.90	61.71	5.2	10.3
153	0.97	62.65	5.4	10.1
154	0.76	62.84	5.4	10.0
155	-7.92	54.26	6.6	11.0
156	-7.53	54.50	6.6	10.9
157	-6.79	55.14	6.5	10.8
158	-7.14	54.69	6.7	10.8
159	-5.69	56.14	6.4	10.5
160	-5.93	55.92	6.4	10.6
161	-6.05	55.76	6.4	10.6
162	1.04	59.30	5.4	9.7
163	-12.28	51.59	6.9	11.5
164	-11.92	59.41	6.6	11.1
165	-7.42	53.43	6.3	10.7
166	-7.50	53.38	6.3	10.7
167	-10.10	50.68	6.8	11.1
168	-9.78	51.07	6.7	11.0
169	-12.45	50.53	6.5	11.4
170	-13.22	46.91	7.2	11.5
171	-9.32	52.74	6.5	10.9
172	-10.65	51.75	6.7	11.2
173	-10.15	49.43	6.7	11.2
174	-15.68	47.22	6.8	11.6
175	-18.42	48.59	7.0	12.0
176	-18.02	47.63	6.9	11.4
177	-19.42	40.07	7.0	11.9
178	-16.69	42.18	6.6	11.5
179	-16.53	44.44	6.6	11.6
180	-15.56	42.80	6.5	11.4
181	-11.07	49.61	6.1	10.9
182	-17.68	47.91	6.3	11.2
183	-17.75	47.78	6.3	11.1
184	-17.66	47.54	6.3	11.1
185	-12.93	44.75	6.4	11.2
186	-12.98	44.64	6.4	11.2

PlotID	Min of CMI	Max of CMI	Min of Tmax	Max of Tmax
187	-14.62	44.24	6.4	11.2
188	-12.09	45.27	6.1	11.0
189	-13.33	44.26	6.3	11.1
190	-17.54	47.30	6.2	11.2
191	-17.73	47.24	6.2	11.8
192	-12.43	41.99	6.2	11.2
193	-17.84	47.04	6.2	11.8
194	-14.49	41.68	6.3	11.3
195	-15.44	41.37	6.4	11.3
196	-16.05	40.72	6.6	11.5
197	-15.48	37.76	6.6	11.7
198	-15.64	37.57	6.5	11.6
199	-15.58	37.55	6.5	11.6
200	-15.66	37.58	6.5	11.6
201	-13.63	43.35	6.3	11.2
202	-13.42	43.46	6.2	11.1
203	-13.72	43.87	6.2	11.2
204	-12.29	43.64	6.2	11.1
205	-13.50	40.37	6.3	11.4
206	-14.28	41.83	6.4	11.2
207	-13.85	40.32	6.3	11.4
208	-12.04	43.15	6.2	11.1
209	-13.56	40.27	6.4	11.4
210	-13.77	40.00	6.5	11.4
211	-22.03	34.09	4.5	9.4
212	-21.61	34.70	4.5	9.3
213	-19.08	39.64	4.3	9.1
214	-15.23	48.90	3.9	8.8
215	-14.10	45.87	4.5	9.5
216	-14.12	45.92	4.5	9.5
217	-14.31	45.09	4.6	9.5
218	-14.11	41.93	4.9	9.4
219	-14.01	42.11	4.8	9.4
220	-14.74	43.81	4.6	9.4
221	-15.10	43.09	4.6	9.4
222	-14.74	43.81	4.6	9.4
223	-14.80	43.66	4.6	9.4
224	-15.51	42.20	4.7	9.4

PlotID	Min of CMI	Max of CMI	Min of Tmax	Max of Tmax
225	-15.71	41.88	4.7	9.4
226	-12.88	52.14	4.3	9.4
227	-15.63	48.74	4.5	9.7
228	-18.63	50.24	4.7	9.9
229	-12.22	48.75	4.4	9.0
230	-12.55	47.73	4.5	9.6
231	-13.19	46.61	4.6	9.7
232	-14.37	47.27	4.6	9.8
233	-15.34	45.71	4.6	9.9
234	-18.40	46.26	4.7	9.9
235	-18.46	46.35	4.7	9.9
236	-18.43	46.67	4.7	9.9
237	-19.61	51.96	4.8	10.0
238	-14.09	52.55	6.0	11.7
239	-12.72	45.15	6.0	11.7
240	-11.18	46.23	5.8	11.5
241	-12.64	44.89	6.0	11.7
242	-9.41	45.12	5.8	11.4
243	-8.31	45.24	5.7	11.3
244	-3.22	44.50	5.5	11.1
245	-2.72	47.48	5.5	11.0
246	-2.85	47.92	5.5	11.0
247	-2.90	48.20	5.5	11.0
248	-3.40	49.48	5.5	11.0
249	-3.89	50.31	5.5	11.0
250	-8.62	46.94	5.8	11.3
251	-8.32	47.31	6.2	10.9
252	-16.79	49.18	5.9	11.4
253	-17.57	42.36	5.8	11.3
254	-17.90	40.64	6.7	10.8
255	-16.54	43.15	5.9	11.4
256	-16.30	43.22	5.9	11.4
257	-15.72	43.09	6.0	11.4
258	-15.25	43.10	5.9	11.4
259	-25.17	32.76	6.4	11.0
260	-23.24	37.86	6.4	11.0
261	-27.54	35.19	6.6	11.2
262	-19.89	37.83	6.0	11.0

PlotID	Min of CMI	Max of CMI	Min of Tmax	Max of Tmax
263	-16.39	40.28	5.7	10.9
264	-23.99	36.56	6.6	11.1
265	-26.28	36.28	6.6	11.3
266	-19.06	38.54	6.1	11.1
267	-17.06	40.85	5.9	11.0
268	-13.55	41.95	6.1	11.0
269	-13.62	41.97	6.2	11.0
270	-13.66	42.01	6.1	11.0
271	-12.59	40.35	6.2	11.0
272	-16.54	40.93	6.2	11.0
273	-16.45	41.04	6.2	10.9
274	-16.03	41.61	6.1	10.9
275	-15.66	41.77	6.1	10.9
276	-16.09	41.41	6.1	10.9
277	-16.15	41.42	6.2	10.9
278	-20.44	36.28	2.7	8.1
279	-20.64	28.73	3.2	8.2
280	-20.83	30.58	3.2	8.2
281	-21.29	32.33	3.0	8.2
282	-21.32	32.95	3.0	8.2
283	-21.22	33.31	3.0	8.2
284	-20.19	36.33	2.7	8.1
285	-20.35	37.15	2.7	8.1
286	-20.89	33.11	3.1	8.3
287	-20.59	33.50	3.0	8.2
288	-20.45	33.49	3.0	8.2
289	-20.56	33.61	3.0	8.2
290	-16.00	32.97	3.0	8.3
291	-16.62	23.21	3.8	8.5
292	-21.52	24.26	3.6	8.4
293	-13.00	25.96	3.4	8.1
294	-20.86	28.81	3.8	8.7
295	-20.81	26.24	3.7	8.6
296	-18.97	28.50	3.2	8.3
297	-19.22	28.23	3.3	8.3
298	-19.80	30.02	3.5	8.5
299	-18.65	31.46	3.2	8.4
300	-18.41	31.58	3.1	8.3

PlotID	Min of CMI	Max of CMI	Min of Tmax	Max of Tmax
301	-15.29	35.39	2.4	7.9
302	-15.12	35.53	2.4	7.8
303	-16.53	32.43	3.1	8.3
304	-26.06	22.52	2.9	7.3
305	-26.21	21.58	3.0	7.4
306	-25.83	24.09	2.9	7.3
307	-24.95	26.15	2.7	7.1
308	-20.38	37.60	1.6	6.6
309	-21.98	34.34	2.1	6.7
310	-22.41	32.85	2.2	6.8
311	-21.89	35.01	2.0	6.7
312	-21.90	37.14	2.0	6.8
313	-22.25	35.88	2.1	6.8
314	-20.90	39.96	1.7	6.7
315	-25.06	24.77	0.3	7.2
316	-25.50	25.10	1.3	7.2
317	-26.34	21.24	3.0	7.4
318	-25.44	24.91	1.4	7.2
319	-25.48	25.04	1.4	7.2
320	-26.22	22.60	3.0	7.4
321	-25.62	25.21	2.1	7.2
322	-25.09	24.52	0.6	7.2
323	-24.83	22.91	0.1	7.2
324	-24.84	22.65	0.1	7.2
325	-24.76	21.83	0.1	7.2
326	-25.13	20.00	0.2	7.2
327	-25.16	25.19	0.5	7.3
328	-21.22	18.48	0.7	7.0
329	-21.47	18.64	0.5	7.0
330	-20.75	18.29	0.8	7.0
331	-19.79	18.28	-0.1	6.8
332	-19.80	18.16	-0.1	6.8
333	-19.19	18.33	-0.1	6.6
334	-27.09	19.61	3.4	7.7
335	-27.11	19.66	3.4	7.7
336	-24.23	31.38	2.6	7.2
337	-26.00	25.18	3.2	7.4
338	-19.01	41.05	3.5	8.3

PlotID	Min of CMI	Max of CMI	Min of Tmax	Max of Tmax
339	-17.72	40.56	3.6	8.3
340	-17.77	40.65	3.6	8.3
341	-17.83	40.98	3.6	8.3
342	-17.65	40.14	3.6	8.3
343	-17.58	39.97	3.6	8.3
344	-17.93	41.12	3.6	8.3
345	-17.77	40.73	3.6	8.3
346	-17.59	42.79	3.3	8.3
347	-17.42	42.91	3.3	8.2
348	-19.51	32.32	3.0	8.7
349	-20.08	31.71	3.1	8.7
350	-20.38	30.55	3.2	8.9
351	-21.67	29.63	3.4	9.0
365	-12.72	45.23	6.0	11.6
366	-14.23	51.08	5.4	10.1
367	-25.16	21.98	4.0	9.7
368	-25.13	24.51	4.9	9.9
369	-25.21	27.92	4.0	9.7
370	-25.81	27.12	4.0	9.2
371	-25.61	27.76	3.9	9.5
372	-26.10	27.65	3.9	9.1
373	-16.21	41.64	4.8	9.5
374	-22.96	31.64	5.2	10.1
375	-21.13	30.50	5.0	9.8
376	-20.03	30.18	4.9	9.8
377	-20.55	30.58	4.9	9.8
378	-19.08	42.99	4.5	9.7
379	-19.36	41.97	4.5	9.7
380	-16.70	40.69	4.3	9.7
381	-15.38	44.33	4.5	9.3
382	-13.69	47.18	4.5	9.1
383	-19.51	36.08	5.0	10.1
384	-19.38	36.17	5.0	10.0
385	-17.31	39.98	4.4	9.7
386	-17.31	40.01	4.4	9.7
387	-17.75	38.29	4.4	9.7
400	-22.20	29.82	5.0	9.8
401	-22.07	31.59	5.0	9.8

PlotID	Min of CMI	Max of CMI	Min of Tmax	Max of Tmax
402	-18.32	40.62	4.0	8.9
403	-17.55	36.66	4.1	9.2
404	-23.71	24.34	4.2	9.5
405	-21.17	26.16	3.9	9.3
407	-21.48	27.84	3.9	9.3
408	-16.96	31.17	3.5	8.8
409	-21.35	28.19	3.9	9.3
410	-21.42	28.05	3.9	9.3
411	-21.52	37.56	4.3	9.2
412	-21.15	26.20	3.9	9.3
413	-17.70	18.34	3.9	8.9
414	-21.42	28.15	3.9	9.3
415	-20.18	37.03	4.9	9.2
416	-19.80	38.10	4.8	9.1
417	-20.34	36.54	5.0	9.3
418	-18.44	44.21	4.9	9.1
419	-19.68	38.14	4.8	9.1
420	-18.34	44.13	4.9	9.1
421	-18.21	44.27	4.9	9.1
422	-17.14	44.77	4.8	9.0
430	-16.10	36.43	4.9	10.2
431	-13.76	40.71	4.7	9.9
432	-18.96	36.80	4.8	9.9
433	-20.26	36.17	5.0	10.0
434	-14.86	34.51	4.7	10.0
435	-16.61	35.54	5.0	10.2
436	-16.81	35.09	5.0	10.2
437	-24.07	26.66	4.6	9.4
438	-24.22	26.33	4.6	9.5
439	-24.22	29.29	4.0	9.8
440	-25.01	21.01	4.1	9.8
441	-25.93	26.44	4.0	9.3
442	-25.33	34.67	3.6	8.8
443	-25.80	37.29	3.6	8.8
444	-24.10	29.47	4.0	9.8
445	-16.96	43.94	3.0	8.5
446	-25.03	28.53	4.1	9.9
447	-22.30	27.16	4.9	9.8

PlotID	Min of CMI	Max of CMI	Min of Tmax	Max of Tmax
448	-18.28	40.86	4.0	8.9
449	-18.04	38.69	4.0	8.9
450	-16.16	41.35	4.6	9.4
451	-16.39	42.54	4.4	8.9
452	-18.76	39.25	4.2	9.1
453	-20.52	34.80	4.5	9.3
454	-18.88	34.66	5.1	9.2
455	-19.86	44.86	4.4	9.4
456	-22.23	40.94	4.5	9.4
457	-21.79	32.25	5.1	9.6
458	-22.19	28.97	5.2	9.7
459	-19.12	40.25	4.2	9.1
462	-11.59	37.90	6.0	10.6
463	-10.79	40.55	5.8	10.4
464	-11.03	39.71	5.8	10.4
466	-25.74	25.70	3.5	9.2
471	-25.80	25.41	3.5	9.2
473	-26.96	25.51	3.7	9.3
474	-26.82	25.41	3.7	9.3
475	-14.07	46.43	6.8	11.0
476	-12.90	49.30	6.3	10.7
477	-15.88	43.74	7.1	11.3
479	-13.54	47.74	6.7	10.8
481	-13.95	47.73	6.6	11.0
482	-14.03	48.23	6.6	10.9
483	-23.35	39.32	7.2	11.4
484	-1.13	65.73	5.6	9.4
485	-2.33	62.84	5.8	9.6
486	-8.55	60.48	6.8	10.4
487	-8.27	62.30	6.8	10.4
488	-7.62	66.30	6.7	10.3
489	-4.42	74.81	6.3	10.6
490	7.69	118.06	4.7	9.2
491	-11.47	51.96	6.5	10.6
492	-11.56	52.11	6.5	10.6
493	-7.60	59.40	7.4	11.9
494	-26.81	25.44	3.7	9.3
499	-27.61	38.35	7.3	11.5

PlotID	Min of CMI	Max of CMI	Min of Tmax	Max of Tmax
500	-4.70	85.56	6.2	9.8
501	-4.25	86.24	6.1	9.7
502	-5.27	80.48	6.4	10.1
503	-23.02	63.00	7.6	11.7
504	11.47	122.00	3.6	7.5
505	-6.77	68.95	6.6	10.2
506	-5.49	86.17	6.5	10.0
507	-13.92	41.64	6.7	10.9
508	-0.01	80.17	5.6	9.5
509	0.09	95.83	5.5	9.2
510	-14.14	41.30	6.7	10.9
511	-7.36	72.38	6.8	10.5
512	-2.96	79.21	5.9	10.2
513	8.89	56.04	4.5	8.6
514	-9.39	44.88	6.4	10.6
515	-10.56	42.50	6.3	10.6
516	3.27	59.96	3.9	9.0
517	5.52	63.98	3.6	8.6
518	-0.14	59.56	5.3	9.0
519	6.55	91.58	2.2	7.4
520	15.84	101.48	1.7	6.7
521	7.31	95.62	2.1	7.3
522	14.60	97.96	2.0	7.2
523	14.31	96.62	2.1	7.3
524	20.76	108.10	1.2	6.4
525	7.58	71.25	3.2	8.2
526	20.60	109.30	1.2	6.5
527	7.23	87.65	2.4	7.5
528	8.92	74.85	2.9	8.3
529	7.04	87.27	2.4	7.6
530	-8.53	86.90	1.0	6.3
531	2.47	59.34	4.2	9.2
532	10.67	71.70	3.4	8.2
533	8.41	81.35	3.1	8.0
534	8.71	84.97	2.9	8.0
535	8.90	99.17	2.5	7.6
536	8.91	89.08	2.8	7.9
537	9.02	90.60	2.8	7.9

PlotID	Min of CMI	Max of CMI	Min of Tmax	Max of Tmax
538	9.38	63.53	3.7	8.7
539	-15.65	41.28	6.8	11.0
540	-10.17	43.15	6.3	10.6
541	-10.12	42.88	6.3	10.6
542	-12.06	40.70	6.5	10.8
543	-10.30	41.98	6.3	10.6
544	-14.12	41.52	6.7	10.9
549	-14.34	37.75	7.0	11.4
550	-22.81	28.36	7.3	11.4
551	-17.98	29.86	7.1	11.3
556	-10.11	50.14	6.7	11.1
557	-7.98	52.85	6.3	10.7
558	-6.35	49.55	6.2	10.3
560	-6.23	49.62	6.1	10.2
569	-18.56	48.72	7.4	11.5
570	-16.01	52.55	7.2	11.3
571	-24.13	44.22	7.5	11.7
572	-26.58	24.91	3.5	8.6
574	-21.16	35.43	2.2	7.4
575	-21.87	30.78	2.8	8.3
576	-26.32	25.29	3.7	8.5
578	-26.71	22.14	3.5	7.9
579	-26.71	22.04	3.5	7.9
580	-24.78	21.31	0.1	7.2
581	-26.40	24.89	3.6	8.2
582	-26.69	22.06	3.5	7.9
583	-19.74	18.44	0.8	6.8
584	-12.75	55.51	5.4	10.6
585	-15.13	53.15	5.5	10.6
588	-3.95	53.74	7.1	11.3
590	-18.87	31.78	2.5	8.1
592	-18.55	32.49	2.4	8.0
593	-19.97	30.85	2.7	8.2
594	-21.08	31.02	2.6	8.2
595	-20.01	30.45	2.7	8.3
596	-23.19	30.82	2.6	8.4
598	-26.35	22.52	3.6	8.1
600	-16.55	31.10	4.0	9.1

PlotID	Min of CMI	Max of CMI	Min of Tmax	Max of Tmax
601	-4.22	58.86	4.8	8.7
603	-18.93	34.19	7.2	12.4
604	-8.57	55.99	6.4	11.0
605	-8.61	56.20	6.3	10.9
606	-9.24	55.41	6.4	11.0
607	-14.57	48.24	6.3	11.4
608	-14.00	49.10	6.4	11.3
609	-20.21	43.62	6.3	10.8
610	-20.65	42.02	6.4	10.8
611	-19.84	43.45	6.3	10.8
614	-13.47	54.03	6.9	11.3
615	-21.37	40.56	6.5	10.9
617	-19.43	37.26	6.2	10.9
618	-21.31	39.86	6.2	10.8
619	-21.21	39.87	6.6	11.1
620	-22.69	38.99	6.5	11.0
621	-18.24	42.18	6.4	11.3
634	-7.60	41.19	4.7	9.9
636	-14.13	49.53	5.3	10.0
639	-16.76	45.44	4.4	8.8
645	-19.24	33.92	4.2	9.6
646	-20.20	32.50	4.4	9.7
647	-20.25	32.47	4.4	9.8
648	-21.23	31.67	4.5	9.9
664	-13.49	48.07	7.1	11.5
700	-20.33	28.44	5.3	9.8